PACIFIC EARTHQUAKE ENGINEERING RESEARCH CENTER

Numerical Models for Analysis and Performance-Based Design of Shallow Foundations Subjected to Seismic Loading

Sivapalan Gajan
North Dakota State University

Tara C. Hutchinson
University of California, San Diego

Bruce L. Kutter
University of California, Davis

Prishati Raychowdhury
University of California, San Diego

José A. Ugalde
Fugro West Inc., Oakland, California

Jonathan P. Stewart
University of California, Los Angeles

PEER 2007/04
MAY 2008

Numerical Models for Analysis and Performance-Based Design of Shallow Foundations Subjected to Seismic Loading

Sivapalan Gajan
North Dakota State University

Tara C. Hutchinson
University of California, San Diego

Bruce L. Kutter
University of California, Davis

Prishati Raychowdhury
University of California, San Diego

José A. Ugalde
Fugro West Inc., Oakland, California

Jonathan P. Stewart
University of California, Los Angeles

PEER Report 2007/04
Pacific Earthquake Engineering Research Center
College of Engineering
University of California, Berkeley

May 2008

ABSTRACT

For stiff structural systems, such as shear walls and braced frames, deformations that occur at the soil-foundation interface can represent a significant component of the overall soil-foundation-structure system flexibility. Practical guidelines have been available for many years to characterize these soil-structure interaction (SSI) effects when structural analyses are performed using simplified pseudo-static force-based or pushover-type procedures. Those guidelines are typically based in large part on representing the soil-foundation interaction in terms of elastic impedance functions that describe stiffness and damping characteristics. Such approaches are not able to capture the nonlinear behavior at the foundation level, which may involve formation of a temporary gap between the footing and soil, the settlement of the foundation, sliding, or energy dissipation from the hysteretic effects.

Due to the importance of these effects, reliable characterization of structural system response within a performance-based design framework requires improved tools for modeling of the soil-foundation interaction. In this work, two such tools have been developed. The first, referred to as the beam-on-nonlinear-Winkler-foundation (BNWF) model, consists of a system of closely spaced independent nonlinear inelastic springs that are capable of capturing gapping and radiation damping. Vertical springs distributed along the base of the footing are used to capture the rocking, uplift, and settlement, while horizontal springs attached to the sides of the footing capture the resistance to sliding. The second tool is referred to as the contact interface model (CIM). The CIM provides nonlinear constitutive relations between cyclic loads and displacements at the footing-soil interface of a shallow rigid foundation that is subjected to combined moment, shear, and axial loading.

The major distinguishing characteristics of the two models are that (1) the BNWF model directly captures the behavior of structural footing elements with user-specified levels of stiffness and strength, whereas the CIM assumes a rigid footing and (2) the BNWF model does not couple foundation response in the vertical direction (in response to vertical loads and moments) with horizontal response, whereas the CIM does couple these responses. Accordingly, the BNWF model is preferred when simulation results are to be used to design footing elements and for complex foundation systems consisting of variable-stiffness elements (such as wall footings and columns footings). Conversely, the CIM is preferred when moment and shear

response are highly coupled. Some applications may involve a combination of CIM elements beneath wall footings and BNWF elements beneath other foundation components of a given structure.

Both models are described by a series of parameters that are categorized as being user-defined or hard-wired. User-defined parameters include those that are directly defined by foundation geometry or by conventional material properties such as shear strength and soil stiffness. Hard-wired parameters describe details of the cyclic or monotonic response and are coded into the computer codes. Both sets of parameters are fully described in this report and a consistent set of parameter selection protocols is provided. These protocols are intended to facilitate straightforward application of these codes in OpenSees.

The models are applied with the parameter selection protocols to a hypothetical shear wall building resting on clayey foundation soils and to shear wall and column systems supported on clean, dry, sand foundation soils tested in the centrifuge. Both models are shown to capture relatively complex moment-rotation behavior that occurs coincident with shear-sliding and settlement. Moment-rotation behavior predicted by the two models is generally consistent with each other and the available experimental data. Shear-sliding behavior can deviate depending on the degree of foundation uplift with coincident loss of foundation shear capacity. This can significantly affect isolated footings for shear walls or braced frames, but is less significant for multi-component, interconnected foundation systems such as are commonly used in buildings. Settlement response of footings tends to increase with the overall level of nonlinearity. Accordingly, in the absence of significant sliding, settlement responses tend to be consistent between the two models and with experimental data. However, conditions leading to sliding cause different settlement responses. For conditions giving rise to significant coupling between moment and shear responses (resulting in shear-sliding), CIM elements provide improved comparisons to data and their use is preferred.

This work has advanced the BNWF model and CIM from research tools used principally by the Ph.D. students that wrote the codes to working OpenSees models with well-defined (and at least partially validated) parameter selection protocols. We recognize that further validation against full-scale field performance data would be valuable to gain additional insights and confidence in the models. In the meantime, we encourage the application of these models, in parallel with more conventional methods of analysis, with the recognition that the simulation results from both established and new procedures should be interpreted with appropriate engineering judgment as part of the design process.

At present, many building engineers are reluctant to allow significant rocking rotations and soil nonlinearity at the soil-foundation interface. It is hoped that the availability of procedures that are able to reliably predict displacements caused by cyclic moment, shear, and axial loading will empower engineers to consider rocking of shallow foundations as an acceptable mechanism of yielding and energy dissipation in a soil-foundation-structure system. In some cases, the allowance of foundation nonlinearity may lead to economies in construction and improvements in performance.

ACKNOWLEDGMENTS

This work was supported by the Pacific Earthquake Engineering Research (PEER) Center Program of the National Science Foundation under award number EEC-9701568 and PEER project number 2262001. Any opinions, findings, conclusions or recommendations expressed in this report are those of the authors and do not necessarily reflect those of the NSF.

We would like to thank Professor Helmut Krawinkler of Stanford University for having the vision for this collaborative project and Professor Geoff Martin of USC for identifying and spearheading the importance of the topic of shallow foundation rocking. We also thank Christine Goulet of UCLA for her assistance in getting the project started with foundation design and for facilitating information exchange via a web portal that she designed. Helpful suggestions regarding the BNWF modeling by Professor Ross Boulanger are greatly appreciated. The authors would like to thank graduate students Key Rosebrook, Justin Phalen, and Jeremy Thomas and the entire staff at the Center for Geotechnical Modeling at the University of California, Davis, for their support and assistance during centrifuge experiments.

CONTENTS

LIST OF FIGURES

LIST OF TABLES

1 Introduction

1.1 PROBLEM STATEMENT

The vast majority of structural design in United States practice is performed under the assumption that the structural elements are fixed at the foundation level against translation, settlement, and in some cases, rotation. Structures excited by earthquake ground shaking develop inertial forces, which in turn, introduce base shear and moment to the foundation system. Unless the foundation system and supporting soil are rigid, these base shears and moments will introduce foundation displacements and rotations. For highly flexible structural systems, foundation displacements and rotations may be inconsequentially small relative to those in the building and can be safely neglected. However, for stiff structural systems such as shear walls and braced frames, foundation deformations can represent a significant component of system flexibility. Ignoring foundation deformations in such cases results in mischaracterization of dynamic properties such as the fundamental mode frequency and the damping ratio (e.g., Veletsos and Nair 1975; Stewart et al., 1999), which biases the engineering characterization of seismic demand. Moreover, Comartin et al. (2000) showed how ignoring foundation compliance could cause an engineer to mischaracterize seismic structural performance to such an extent that the wrong portion of a building would be retrofit.

Although not widely used in practice, engineering guidelines exist for simple characterization of soil-structure-interaction (SSI) effects. One set of guidelines is intended for use with force-based characterization of seismic design, as is commonly used for new building construction. These procedures were introduced by ATC (1978) and an updated version is currently published in the *NEHRP Recommended Provisions for Seismic Regulations for New Buildings and Other Structures* (BSSC 2004). The ATC and NEHRP procedures modify the fixed-base building period and damping ratio for the effects of foundation compliance. The modified vibration properties (termed "flexible-base") are used with the site design response spectrum to obtain the base shear for seismic design. The foundation-soil characterization inherent to these procedures consists of foundation springs for translational and rotational deformation modes that depend on a strain-compatible soil shear modulus. The soil behavior is modeled as visco-elastic with no limiting shear stress. Further information on this approach and its implementation in the NEHRP Provisions is available in Stewart et al. (2003).

The second set of guidelines is intended for use with nonlinear static methods for structural performance assessment, as commonly used for building retrofit design (ATC-40, FEMA-356, FEMA-440, ASCE-41). In this approach, the structural performance is characterized by a nonlinear static pushover curve. The shape of the pushover curve, as well as the distribution of member shears and moments, can be sensitive to foundation modeling. Accordingly, the aforementioned documents provide recommendations for modeling the foundation-soil system as elastic-perfectly-plastic elements positioned at each footing. The elastic portion is based on the real part of well-known impedance functions for foundation lateral translation, vertical translation, and rocking. The plastic portion of the foundation springs is based on limiting soil pressures associated with bearing capacity failure (in the vertical direction) and sliding/passive failure (in the lateral direction).

A large fraction of the earthquake engineering profession remains poorly educated about these simple engineering tools and their proper use. Recent short courses and workshops organized by EERI and others have attempted to fill this gap. Nonetheless, relatively sophisticated earthquake engineers that have successfully used these procedures have noted several shortcomings. First, the procedures are intended for relatively simply calculations of base shear or pushover curves, and are not immediately amenable for use in the relatively sophisticated nonlinear response history analyses that are becoming increasingly common for major projects. Second, while the procedures implicitly account for soil nonlinearity through the use of an equivalent-linear shear modulus, such springs inadequately represent the nonlinear response of foundations, which may include relatively complex gapping and energy-dissipation mechanisms. Accordingly, there is a recognized need in industry (advanced by a small but influential contingent of design professionals) for the development of relatively sophisticated engineering tools for characterizing the nonlinear, time-dependent behavior of the foundation-soil interface. The work presented in this report represents a major step forward towards meeting that objective, and will bring foundation modeling on a par with the nonlinear modeling of key structural components of buildings.

1.2 PROJECT ORGANIZATION AND GOALS

This project was organized within the Pacific Earthquake Engineering Research center as a highly collaborative effort of researchers from multiple institutions. Prior to this project, the PEER center had funded a series of centrifuge experiments of structural-footing systems at UC Davis and the nearly coincident development of preliminary engineering models. Recognizing that the full potential of those models might not be realized without proper coordination and oversight, Professor Helmut Krawinkler called upon the model development teams (led by Professor Kutter at UC Davis and Professor Hutchinson at UC San Diego) to work in a coordinated fashion to ensure that model performances were reasonable and that the models would be useful to others upon the termination of the NSF-funded phase of PEER research. Professor Stewart was asked to coordinate this activity.

The work has had three major phases. The first phase involved the identification of all major input parameters to the models. Some of these parameters have a clear physical basis and can be readily understood (e.g., bearing capacity). Other parameters are highly specific to the respective models and cannot be obtained from the information typically gathered during geotechnical site characterization. The centrifuge model tests and other tests were used to constrain the values of these parameters. After much iteration and discussion, a set of parameter selection protocols was developed along recommended values of additional parameters hard-wired into the codes for the respective models. The results of this work are presented principally in Chapters 2 and 3.

The second phase, which overlapped with the first, involved applying the models and their parameter selection protocols for a realistic building. Many "bugs" in the codes were identified through this process. The codes were made significantly more robust through this work. Insight was also gained into the variation of model performance and positive and negative attributes of each model. This work is presented in Chapter 4.

The third phase involved verifying the model performance against centrifuge test data for the specified parameter selection protocols. This work provided further insights into the capabilities of the models, some of their common features, and some of their relative strengths and weaknesses. That work is presented in Chapter 5. The report is concluded in Chapter 6 with a summative statement of project scope, high-level accomplishments, guidelines for users, and recommendations for future research.

2 Beam-on-Nonlinear-Winkler-Foundation Model

2.1 DESCRIPTION OF BNWF (BEAM-ON-NONLINEAR WINKLER FOUNDATION) MODEL

The beam-on-nonlinear Winkler foundation (BNWF) shallow footing model is constructed using a mesh generated of elastic beam-column elements to capture the structural footing behavior and zero-length soil elements to model the soil-footing behavior. In this work, the BNWF model is developed for a two-dimensional analysis; therefore, the one-dimensional elastic beam-column elements have three degrees-of-freedom per node (horizontal, vertical, rotation). Individual one-dimensional zero-length springs are independent of each other, with nonlinear inelastic behavior modeled using modified versions of the Qzsimple1, PySimple1 and TzSimple1 material models implemented in OpenSees by Boulanger (2000). As illustrated in Figure 2.1, those elements simulate vertical load-displacement behavior, horizontal passive load-displacement behavior against the side of a footing, and horizontal shear-sliding behavior at the base of a footing, respectively. Implicitly, via the distribution of vertical springs placed along the footing length, moment-rotation behavior is captured. The parameters that describe the backbone curves for these elements were calibrated against shallow footing load tests (Raychowdhury and Hutchinson 2008). Note that the element material models that were previously implemented in OpenSees are based on calibration against pile load tests. Therefore, their axes nomenclature follows the convention typically adopted for loaded piles. For example, for frictional resistance, a modified t-z material model was used, where z is the vertical direction along the length of the pile. However, for a shallow foundation, although a modified t-z material model (TzSimple1) is used, the sliding direction is along the x-axis (i.e., t-x).

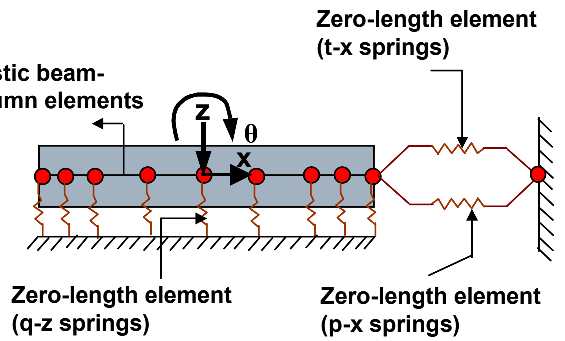

Axis	Force	Displacement
x	H	U
z	Q	S
θ	M	Θ

Fig. 2.1 BNWF schematic.

2.1.1 Attributes of BNWF Model

The shallow footing BNWF model has the following attributes:

- The model can account for behavior of the soil-foundation system due to nonlinear, inelastic[1] soil behavior and geometric (uplifting) nonlinearity. As illustrated in Figure 2.2, nonlinearity can be manifested in moment-rotation, shear-sliding, or axial-vertical displacement modes. Inelastic behavior is realized by development of gaps during cyclic loading. As a result, the model can capture rocking, sliding, and permanent settlement of the footing. It also captures hysteretic energy dissipation through these modes and can account for radiation damping at the foundation base.
- A variable stiffness distribution along the length of the foundation can be provided in this model to account for the larger reaction that can develop at the ends of stiff footings subjected to vertical loads. The BNWF model has the capability to provide larger stiffness and finer vertical spring spacing at the end regions of the footing such that the rotational stiffness is accounted for.
- In the application of this model, the following numerical parameters worked well to assure numerical stability: (i) the transformation method for solution constraint and (ii) the modified Newton-Raphson algorithm with a maximum of 40 iterations to a convergence tolerance ranging between 1e-8 and 1e-5 for solving the nonlinear equilibrium equations. The transformation method transforms the stiffness matrix by

[1] A distinction is made herein between material nonlinear and inelastic behavior. While a material can follow a nonlinear load-displacement path, it may not return along the same path (e.g., attain plastic deformation, thus responding inelastically). The materials used in this work are both nonlinear and inelastic.

condensing out the constrained degrees of freedom. This method reduces the size of the system for multi-point constraints (OpenSees 2008).

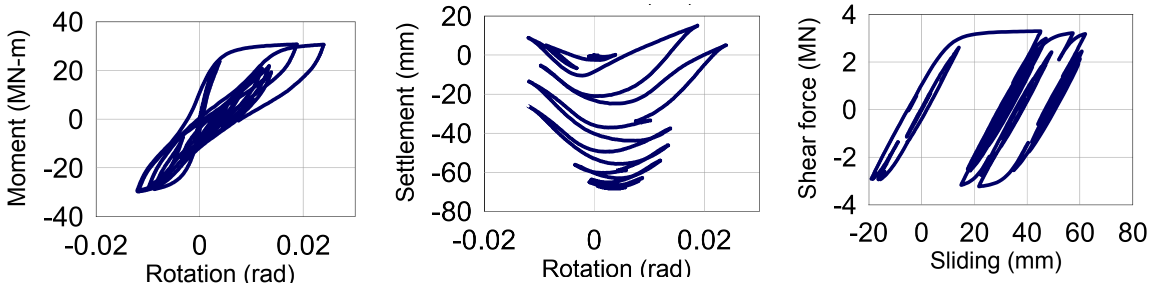

Fig. 2.2 Illustration of model capabilities in moment-rotation, settlement-rotation, and shear-sliding response.

2.1.2 Backbone and Cyclic Response of Mechanistic Springs

In general, the three springs are characterized by a nonlinear backbone resembling a bilinear behavior, with a linear region and a nonlinear region with gradually decreasing stiffness as displacement increases (Fig. 2.3). An ultimate load is defined for both the compression and tension regions of the PySimple1 and TzSimple1 materials, while the Qzsimple1 material has a reduced strength in tension to account for soil's limited capacity to carry tension loads. PySimple1 and QzSimple1 have the capability to account for soil-foundation separation via gap elements added in series with the elastic and plastic components. The elastic material captures the "far-field" behavior, while the plastic component captures the "near-field" permanent displacements as illustrated in Figure 2.4. The materials were originally implemented by Boulanger et al. (1999) for modeling the behavior of laterally loaded piles.

The expressions describing the behavior of the three springs are similar and the QzSimple1 expressions are provided here. In the elastic portion of the backbone, the load q is linearly related to the displacement z via the initial elastic (tangent) stiffness k_{in}, i.e.,

$$q = k_{in} z \tag{2.1}$$

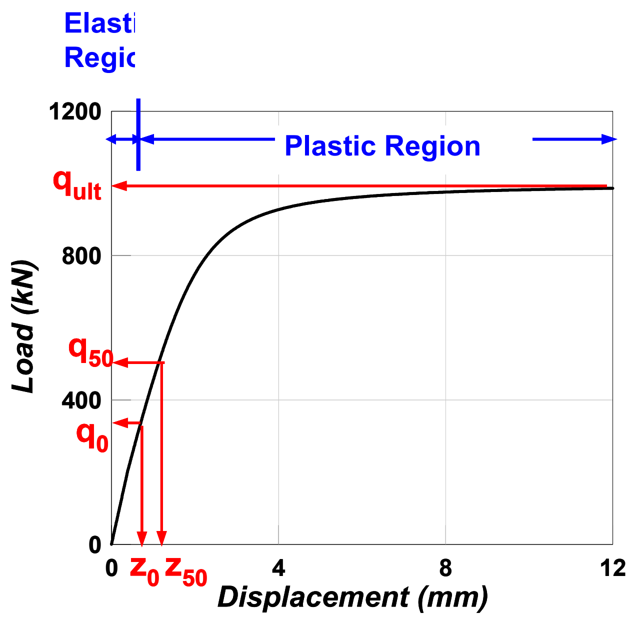

Fig. 2.3 Nonlinear backbone curve for QzSimple1 material.

The elastic region range is defined by relating the ultimate load q_{ult} to the load at the yield point q_0, through a parameter C_r, i.e.,

$$q_0 = C_r q_{ult} \tag{2.2}$$

In the nonlinear (post-yield) portion, the backbone is described by:

$$q = q_{ult} - (q_{ult} - q_0)\left[\frac{cz_{50}}{cz_{50} + \left|z - z_{0p}\right|}\right]^n \tag{2.3}$$

where z_{50} = displacement at which 50% of the ultimate load is mobilized, z_0 = displacement at the yield point, c and n = constitutive parameters controlling the shape of the post-yield portion of the backbone curve. The gap component of the spring is a parallel combination of a closure and drag spring. The closure component is a bilinear elastic spring which is relatively rigid in compression and very flexible in tension. Although the expressions governing both PySimple1 and TzSimple1 are quite similar, the constants, which control the general shape of the curve (c, n and C_r), are different.

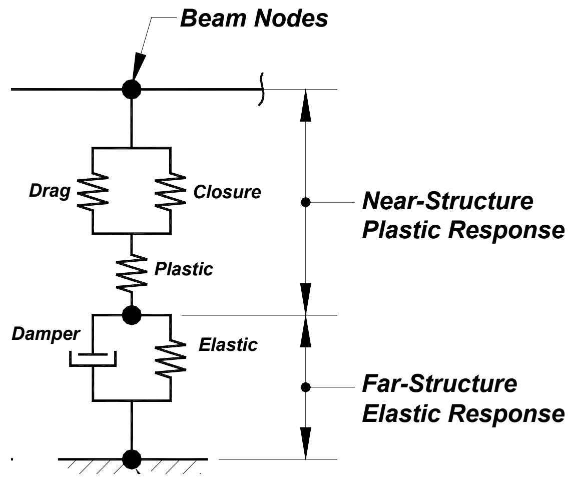

Fig. 2.4 Typical zero-length spring.

The PySimple1 material was originally intended to model horizontal (passive) soil resistance against piles. This model is used here to simulate passive resistance and potential gapping at the front and back sides of embedded footings. Boulanger (2000) fit the constants c, n, and C_r (Eqs. 2.1–2.3) to the backbone curves of Matlock (1970) and API (1987) and found c = 10, n = 5, and C_r = 0.35 for soft clay and c = 0.5, n = 2, and C_r = 0.2 for drained sand. P-y springs are generally placed in multiple locations along the length of a pile to allow the variation of pile deflections with depth to be calculated and also to capture depth-varying soil properties. However, for the shallow foundation modeling discussed here, the footing is assumed to be rigid with respect to shear and flexural deformations over its height; therefore a single spring is used.

The TzSimple1 material was originally intended to capture the frictional resistance along the length of a pile. It is used here to represent frictional resistance along the base of the footings. Its functional form is similar to that shown in Equations 2.1–2.3.

The cyclic response of the material models when subjected to a sinusoidal displacement is demonstrated in Figure 2.5. These figures demonstrate the salient properties described above, such as the gapping capabilities of the QzSimple1 and PySimple1 materials, the reduced strength in tension and corresponding asymmetric behavior of QzSimple1, the symmetric behavior of PySimple1 and TzSimple1 and the broad hysteresis of the sliding resistance (without gapping) provided by TzSimple1.

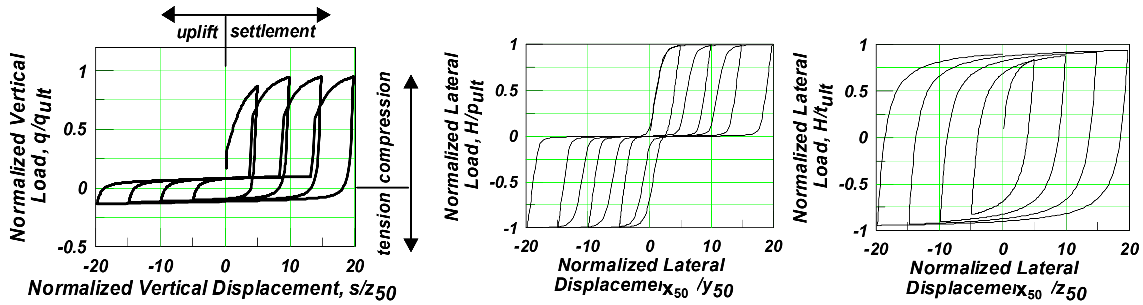

Fig. 2.5 Cyclic response of uni-directional zero-length spring models: (a) axial-displacement response (QzSimple1 material), (b) lateral passive response (PySimple1 material), and (c) lateral sliding response (TzSimple1 material).

2.2 IDENTIFICATION OF PARAMETERS

Input parameters for this model are divided into two groups: (1) user-defined parameters and (2) non-user-defined parameters. Non-user-defined parameters are internally "hard-wired" into the code.

2.2.1 User-Defined Input Parameters and Selection Protocol

Soil type: The user must specify whether the material is sand (Type 1) or clay (Type 2). Sand is assumed to respond under drained conditions, and strengths are defined using effective stress strength parameters ($c' = 0$, ϕ'). Clay is assumed to respond under undrained conditions and strengths are described using total stress strength parameters (c, $\phi = 0$). Based on the input soil type, backbone curves are described using effective or total stress strength parameters, as described above. In addition, corresponding hard-wired (non-user-specified) parameters (C_r, c, n) are used to complete the definition of the backbone curve. As described below, when shear strength parameters are specified, they are used with foundation dimensions to calculate ultimate load capacity. Note that currently, c-ϕ (or c'-ϕ') material backbone curves are not available. However, the OpenSees code can accept as input an externally calculated bearing capacity for a c-ϕ soil, which can be specified along with the Type 1 or 2 designations that corresponds best to the expected material response.

Load capacity (vertical and lateral): The user has the option to have either ultimate load capacity calculated by the mesh generator, or provide these values explicitly (Q_{ult}, P_{ult}, T_{ult} = ultimate load capacity for vertical bearing, horizontal passive, and horizontal sliding, respectively). If the mesh generator is calculating load capacity, the user specifies the footing dimensions (B = breadth, L = length, H = thickness), embedment (D_f), soil unit weight (γ), cohesion (c), angle of internal friction (ϕ'), and load inclination angle (β). Note that β defaults to zero (i.e., vertical load) absent input from the user. Once input or calculated, the total ultimate load capacity is then subdivided by the code internally and applied to the individual springs according to their tributary area (in the case of the vertical springs). P_{ult} and T_{ult} are directly applied to the horizontal springs. When calculated internally, ultimate bearing capacity is based on Terzaghi's bearing capacity theory (1943), in this case using the general bearing capacity equation that includes depth, shape, and load inclination factors of Meyerhof (1963):

$$q_{ult} = cN_c F_{cs} F_{cd} F_{ci} + \gamma D_f N_q F_{qs} F_{qd} F_{qi} + 0.5\gamma B N_\gamma F_{\gamma s} F_{\gamma d} F_{\gamma i} \qquad (2.4)$$

where q_{ult} = ultimate bearing capacity per unit area of footing, N_c, N_q, N_γ = bearing capacity factors, F_{cs}, F_{qs}, $F_{\gamma s}$ = shape factors, F_{cd}, F_{qd}, $F_{\gamma d}$ = depth factors and F_{ci}, F_{qi}, $F_{\gamma i}$ = inclination factors. Note that load inclination factors are generally neglected in this study, although the application is earthquake loading. This is to avoid the complication of time-dependence of the foundation bearing capacity. The equations for each of the above factors can be found in foundation engineering textbooks (e.g., Das 2006; Salgado 2006).

For the PySimple1 material, the ultimate lateral load capacity is determined as the total passive resisting force acting on the front side of the embedded footing. For homogeneous backfill against the footing, the passive resisting force can be calculated using a linearly varying pressure distribution resulting in the following expression:

$$p_{ult} = 0.5\gamma D_f^{\,2} K_p \qquad (2.5)$$

where p_{ult} = passive earth pressure per unit length of footing, K_p = passive earth pressure coefficient that may be calculated using Coulomb (1776), Rankine (1847), or logspiral theories (such as Caquot and Kerisel 1948). In this work, Coulomb's expressions are used. However, recall that the user may input P_{ult} directly if alternate earth pressure coefficients are desired.

For the TzSimple1 material, the lateral load capacity is the total sliding (frictional) resistance. The frictional resistance can be taken as the shear strength between the soil and footing, considering the friction angle between the footing base and soil material and the cohesion at the base:

$$t_{ult} = W_g \tan\delta + A_b c \tag{2.6}$$

where, t_{ult} = frictional resistance per unit area of foundation, $W_g =$ vertical force acting at the base of the foundation, δ = angle of friction between the foundation and soil (typically varying from 1/3ϕ to 2/3 ϕ) and A_b = the area of the base of footing in contact with the soil (=L x B).

Vertical and lateral stiffness: The user has the option to either have vertical and lateral stiffness calculated by the mesh generator or to provide these values explicitly (K_z and K_x = vertical and horizontal stiffness, respectively). If the mesh generator is calculating K_z and K_x, the user specifies the shear modulus G and Poisson's ratio ν, which are used with the footing dimensions to calculate foundation stiffnesses using the expressions by Gazetas (1991). The rotational stiffness of the foundation is accounted for implicitly from the differential movement of the vertical springs. Therefore, it is a function of the distribution of the vertical springs along the length of the footing (see input parameter 6). Note that uncertainly in soil shear modulus can greatly affect the stiffness of the springs and footing response; the use of shear moduli derived from measured seismic wave velocities are preferred. In addition, the shear modulus is expected to reduce with the level of shaking and can be accounted for using modulus reduction factors tabulated in design codes (e.g., FEMA-356, Chapter 4). The magnitude of reduction will be larger for softer soils. Table 2.1 summarizes the equations to calculate footing stiffness for the vertical, lateral, and rotational modes for cases with and without embeddment. In Table 2.1, K_i = uncoupled total surface stiffness for a rigid plate on a semi-infinite homogeneous elastic half-space and e_i = stiffness embedment factor for a rigid plate on a semi-infinite homogeneous elastic half-space.

Radiation damping (C_{rad}): The value for radiation damping is provided by the user. Radiation damping is accounted for through a dashpot placed within the far-field elastic component of each spring. The viscous force is proportional to the velocity that develops in the far-field elastic component of the material. If the user does not specify a radiation damping value, then 0% is the default. Gazetas (1991) provides expressions for radiation damping that can account for soil stiffness, footing shape, aspect ratio, and embedment.

Tension capacity (TP): For the QzSimple1 material, a tension capacity is specified by the user. Tension capacity is the maximum amount of suction force that can be taken by the soil in the vertical direction. It is input as a fraction of the ultimate vertical bearing capacity, ranging from 0–0.10. If the user provides a tension capacity greater than 0.10, OpenSees will default to 0.10. Absent an input from the user, a default of zero is used. The tension capacities of the PySimple1 and TzSimple1 materials are the same as the compressive capacity, and thus are not input by the user.

Distribution and magnitude of vertical stiffness: As illustrated in Figure 2.6, two parameters are input to account for the distribution and magnitude of the vertical stiffness along the footing length: (1) the stiffness intensity ratio, R_k (where, $R_k=K_{end}/K_{mid}$) and (2) the end length ratio, R_e (where, $R_e=L_{end}/L$). A variable stiffness distribution along the length of the foundation is used in the model to distribute vertical stiffness such that rotational stiffness equates to that of Gazetas (1991). Harden et al. (2005) developed an analytical equation for the end stiffness ratio, the results of which are shown in Figure 2.6 along with the recommendations of ATC-40 (1996). Note that ATC-40 suggests a constant value of R_k = 9.3. In this work, the recommendation of Harden et al. (2005) shown in Figure 2.6b are used.

Table 2.1 Gazetas equations for shallow foundation stiffness (after ATC-40, 1996).

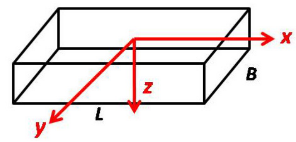

Stiffness	Equation
	Surface Stiffness
Vertical Translation	$K_Z' = \frac{GL}{1-\nu}\left[0.73 + 1.54\left(\frac{B}{L}\right)^{0.75}\right]$
Horizontal Translation (toward long side)	$K_Y' = \frac{GL}{2-\nu}\left[2 + 2.5\left(\frac{B}{L}\right)^{0.85}\right]$
Horizontal Translation (toward short side)	$K_X' = \frac{GL}{2-\nu}\left[2 + 2.5\left(\frac{B}{L}\right)^{0.85}\right] + \frac{GL}{0.75-\nu}\left[0.1\left(1-\frac{B}{L}\right)\right]$
Rotation about x-axis	$K_{\theta x}' = \frac{G}{1-\nu} I_X^{\ 0.75}\left(\frac{L}{B}\right)^{0.25}\left(2.4 + 0.5\frac{B}{L}\right)$
Rotation about y-axis	$K_{\theta y}' = \frac{G}{1-\nu} I_Y^{\ 0.75}\left[3\left(\frac{L}{B}\right)^{0.15}\right]$
	Stiffness Embedment Factors
Embedment Factor, Vertical Translation	$e_Z = \left[1 + 0.095\frac{D_f}{B}\left(1 + 1.3\frac{B}{L}\right)\right]\left[1 + 0.2\left(\frac{2L+2B}{LB}H\right)^{0.67}\right]$
Embedment Factor, Horizontal Translation (toward long side)	$e_Y = \left[1 + 0.15\left(\frac{2D_f}{B}\right)^{0.5}\right]\left\{1 + 0.52\left[\frac{\left(D_f - \frac{H}{2}\right)16(L+B)H}{BL^2}\right]^{0.4}\right\}$
Embedment Factor, Horizontal Translation (toward short side)	$e_X = \left[1 + 0.15\left(\frac{2D_f}{L}\right)^{0.5}\right]\left\{1 + 0.52\left[\frac{\left(D_f - \frac{H}{2}\right)16(L+B)H}{LB^2}\right]^{0.4}\right\}$
Embedment Factor, Rotation about x axis	$e_{\theta X} = 1 + 2.52\frac{H}{B}\left(1 + \frac{2H}{B}\left(\frac{d}{D_f}\right)^{-0.2}\left(\frac{B}{L}\right)^{0.5}\right)$
Embedment Factor, Rotation about y axis	$e_{\theta Y} = 1 + 0.92\left(\frac{2H}{L}\right)^{0.60}\left(1.5 + \left(\frac{2H}{L}\right)^{1.9}\left(\frac{H}{D_f}\right)^{-0.60}\right)$

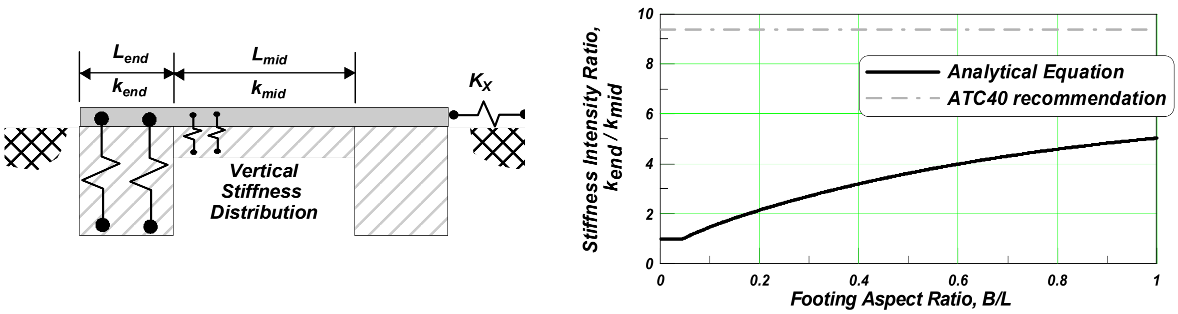

(a) (b)

Fig. 2.6 Increased end stiffness (a) spring distribution and (b) stiffness intensity ratio versus footing aspect ratio (Harden et al. 2005 and ATC-40 1996).

The end region L_{end} is defined as the length of the edge region over which the stiffness is increased. ATC-40 suggests L_{end} = B/6 from each end of the footing. Note that L_{end} is independent of the footing aspect ratio. As shown in Figure 2.7, Harden et al. (2005) showed that the end length ratio is a function of footing aspect ratio. For a square footing (aspect ratio=1), the end length ratio converges with that of ATC-40, with a value of about 16%.

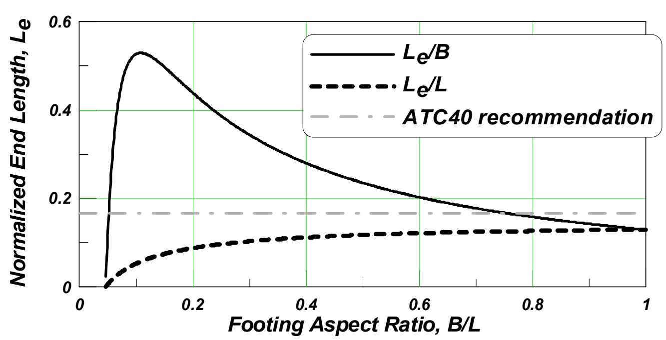

Fig. 2.7 End length ratio versus footing aspect ratio (Harden et al. 2005).

Spring spacing (s): The spring spacing is input by the user as a fraction of the footing length L (s = l_e/L), where l_e = length of the footing element. In this model, the minimum number of springs that can be provided is seven, resulting in six beam (footing) elements and s = 17% L (input as 0.17). The footing response (in terms of settlement, moment, rotation, and rotational stiffness) tends to converge once a certain minimal number of springs are provided. A minimum value of 25 springs (i.e., footing element length = 4% of total footing length) along the footing length is suggested to provide numerical stability and reasonable accuracy.

2.2.2 Non-User-Defined Parameters

In this sub-section, we discuss parameters that are not defined by users but are hard-coded into OpenSees. These parameters may not be directly obtained from physical tests, such as is the case for others defined in the previous section (e.g., shear strength or stiffness). Because the selection of these parameters is non-intuitive, guidelines for their selection are developed from sensitivity studies and calibration against laboratory and field test data.

These parameters influence the shape of the backbone curve by defining the limit of the elastic range, the nonlinear tangent stiffness and the unloading stiffness. Table 2.2 shows the recommended values of the hard-wired parameters prior to this study along with the current recommendations. Tests used in calibrating these factors are those of Rosebrook and Kutter (2001), Briaud and Gibbens (1994), Gadre and Dobry (1998), Duncan and Mokwa (2001), and Rollins and Cole (2006). Details of the calibration are provided in Raychowdhury and Hutchinson (2008).

Elastic range: As shown in Equation 2.2, the parameter C_r controls the range of the elastic region for the QzSimple1, PySimple1, and TzSimple1 materials. It is defined as the ratio of the load at which the material initiates nonlinear behavior to the ultimate capacity.

Nonlinear region of backbone curves: Rearranging Equation 2.3, the nonlinear tangent stiffness k_p, which describes the load-displacement relation within the nonlinear region of the backbone curves, may be expressed as:

$$k_p = n(q_{ult} - q_0)\left[\frac{(cz_{50})^n}{(cz_{50} - z_0 + z)^{n+1}}\right] \tag{2.7}$$

Note that the shape and instantaneous tangent stiffness of the nonlinear portion of the backbone curve is a function of the parameters c and n. Both of these parameters, which are correlated, are hard-wired within the OpenSees code (Table 2.2). It should be noted that the initial unloading stiffness is equal to the initial loading stiffness.

Table 2.2 Non-user-defined parameters (Raychowdhury and Hutchinson 2008).

Material Type	Soil Type	OpenSees recommended value (calibrated from pile tests)			References	Values used in the current study (calibrated from shallow footing tests if available)		
		C_r	n	c		C_r	N	c
QzSimple1	clay	0.2	1.2	0.35	*Reese & O'Neill (1988)*	0.22	1.2	0.5
	sand	0.3	5.5	12.3	*Vijayvergiya (1977)*	0.36	5.5	9.29
PySimple1	clay	0.35	5	10	*Matlock (1970)*	0.35	5	10
	sand	0.2	2	0.5	*API (1993)*	0.33	2	1.1
TzSimple1	clay	0.5	1.5	0.5	*Reese & O'Neill (1988)*	0.5	1.5	0.5
	sand	0.5	0.85	0.6	*Mosher (1984)*	0.48	0.85	0.26

2.3 SENSITIVITY OF SIMULATION RESULTS TO VARIATIONS IN HARD-WIRED BNWF PARAMETERS

In this section, we report the results of simulations performed using a number of values for the user input parameters. The objective is to demonstrate the effect of these parameters on the computed footing response.

Stiffness intensity ratio, R_k: Figure 2.8 shows the impact of varying R_k on the moment-rotation and rotation-settlement responses of a 5m-sq footing subjected to a quasi-static rotational displacement. Although R_k does not have a significant effect on the maximum moment or rotational stiffness, it does affect the permanent settlement, and thus should be chosen with care. The R_k values of 5 and 9 for this case are chosen based on recommendations of ATC-40 (1996) and Harden et al. (2005) for a square footing (as per Fig. 2.6). Validation exercises presented in Chapter 5 indicate that recommendations by Harden et al. (2005) for this parameter provide more reasonable comparison with experimental results.

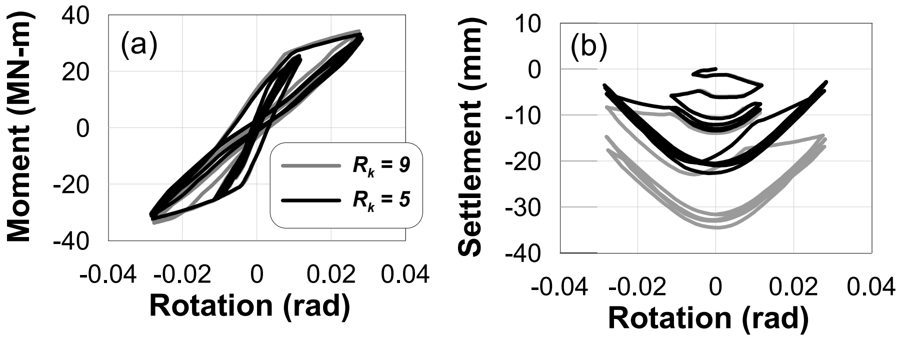

Fig. 2.8 Effect of varying stiffness ratio on footing response.

End length ratio, R_e: Simulation results considering a square footing subjected to sinusoidal loading indicate that changing the end length from 16% to only 0% of the total length does not have much of an effect on the peak developed moment (Fig. 2.9). However, it does have a modest effect on the shape of the settlement-rotation and moment-rotation curve and also nominally on total settlement.

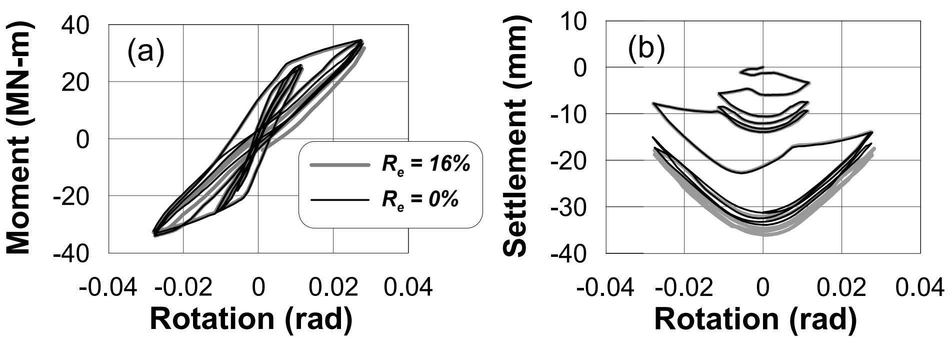

Fig. 2.9 Effect of varying end length ratio on footing response (for 5m-sq footing subjected to sinusoidal rotational motion).

Spring spacing, s: Figure 2.10 shows the variation of response with spring spacing. A smoother footing response occurs when a greater number of springs are used (plots on left). Figure 2.11 shows the sensitivity of total settlement to spring spacing. The total settlement obtained using s = 0.17 is 67mm, more than twice the total settlement obtained when s = 0.06 or less. The variation of settlement with spring spacing is also sensitive to the stiffness of the footing relative to the soil. A footing with a larger EI will result in less variability in settlement estimates when the spring spacing is varied.

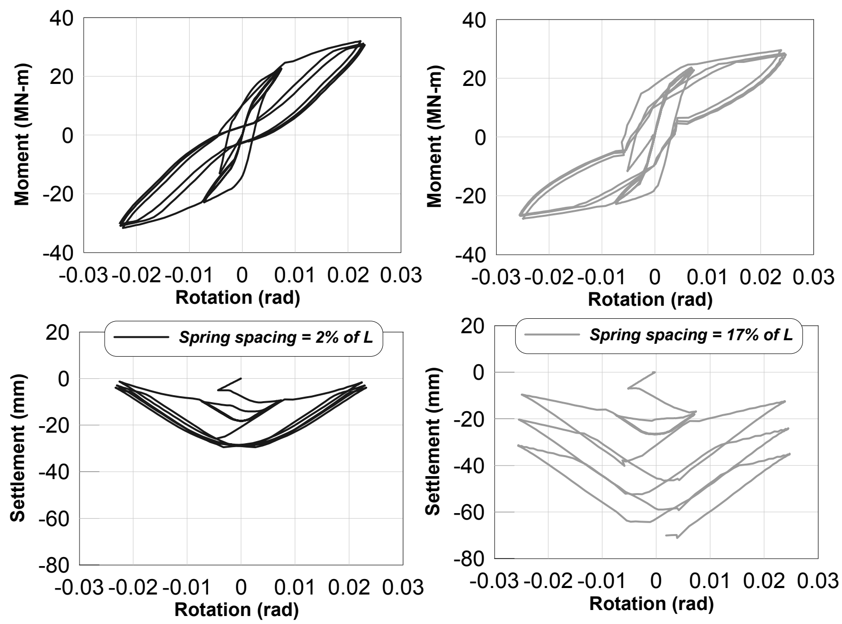

Fig. 2.10 Effect of varying spring spacing on overall footing response (for 5m-sq footing subjected to sinusoidal rotational motion).

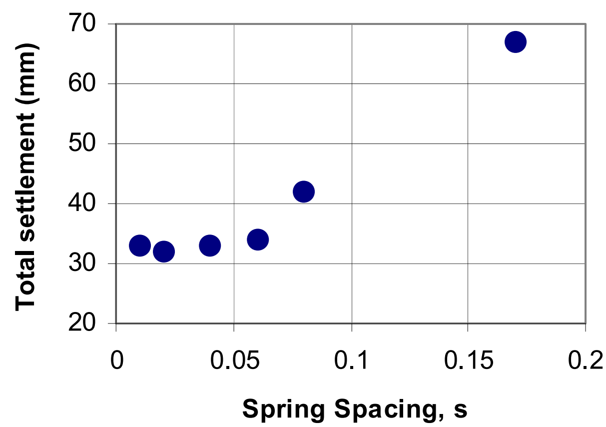

Fig. 2.11 Effect of varying spring spacing on total settlement (for 5m-sq footing subjected to sinusoidal rotational motion).

Elastic range, C_r: Figure 2.12 shows backbone curves with different limits on the elastic range of the spring response. The range of C_r is chosen based on the calibration described above. Figures 2.13–2.14 show the effect of varying C_r on the footing response. A larger C_r extends the elastic region, which reduces the total settlement for a given load. Conversely, a smaller C_r increases the total settlement.

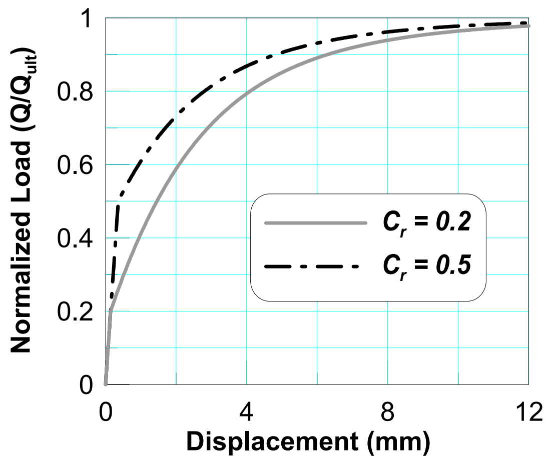

Fig. 2.12 Effect of varying C_r on single spring response.

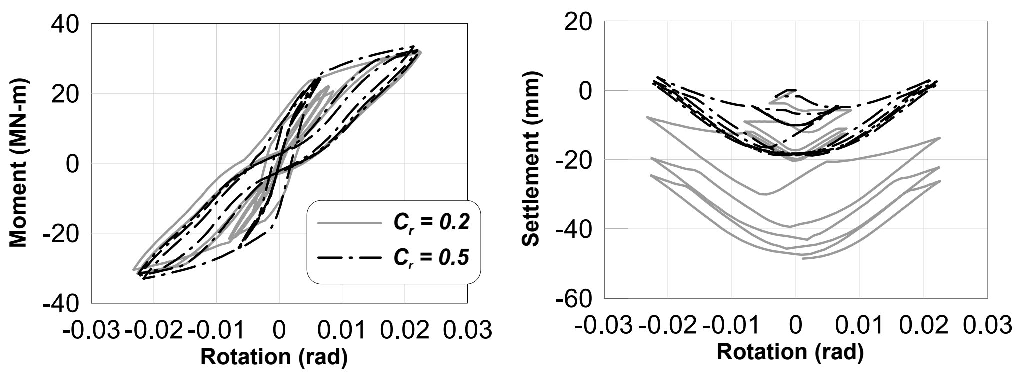

Fig. 2.13 Effect of varying C_r on footing response (for 5m-sq footing subjected to sinusoidal rotational motion).

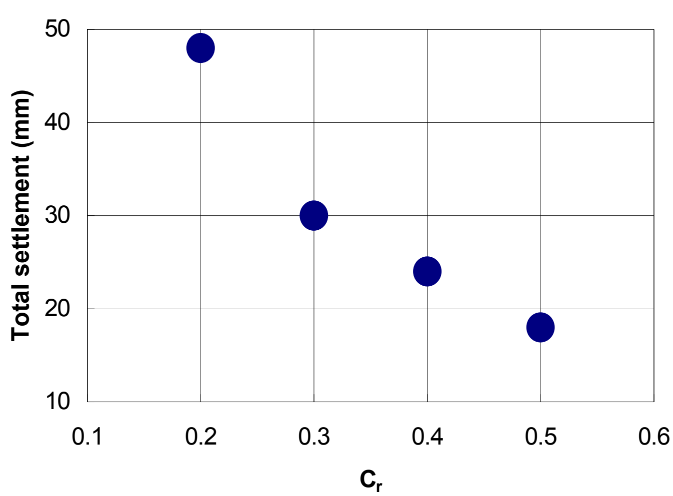

Fig. 2.14 Effect of varying C_r on total settlement.

Nonlinear region of backbone curves: To demonstrate the effect of varying the parameter c on the shallow footing response, the default value of 12.3 for the QzSimple1 sand material model (listed in Table 2.2) is varied up and down by a factor of four. The effect of these variations on the response of a single spring are shown in Figure 2.15. The stiffness in the nonlinear region is expressed as a fraction of the initial stiffness by introducing a variable α_{80}. The parameter α_{80} is the ratio of the stiffness at 80% of q_{ult} to the initial elastic stiffness. Figure 2.16 demonstrates that varying c has the most pronounced effect on rotational stiffness (nonlinear portion) and settlement (total settlement is increased by 75%, assuming a three-fold increase in c).

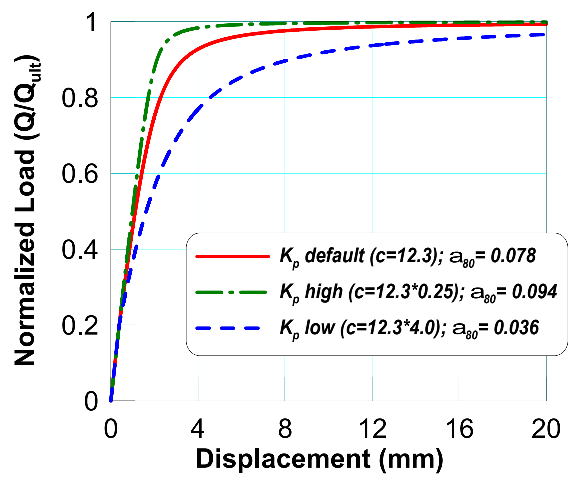

Fig. 2.15 Effect of varying k_p on single spring response.

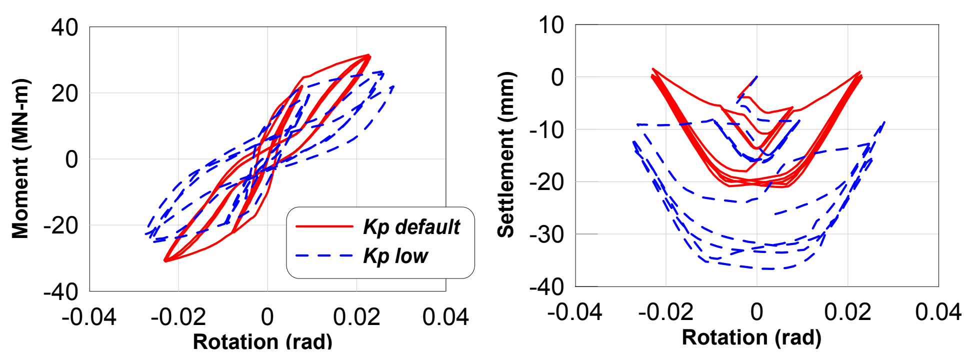

Fig. 2.16 Effect of varying k_p on overall footing response (for 5m-sq footing subjected to sinusoidal rotational motion).

Unloading stiffness, K_{unl}: During cyclic loading, the unloading stiffness may affect the cumulative permanent settlement. Figures 2.17–2.18 show the effect of varying the unloading stiffness on a single spring and an entire footing, respectively. Reducing the unloading stiffness to 20% of the loading stiffness only increases the settlement by 6%, while other response parameters remain similar. Thus the effect of unloading stiffness on the footing response is relatively insignificant. As noted previously, by default the unloading load-displacement curve is identical in shape to the loading curve.

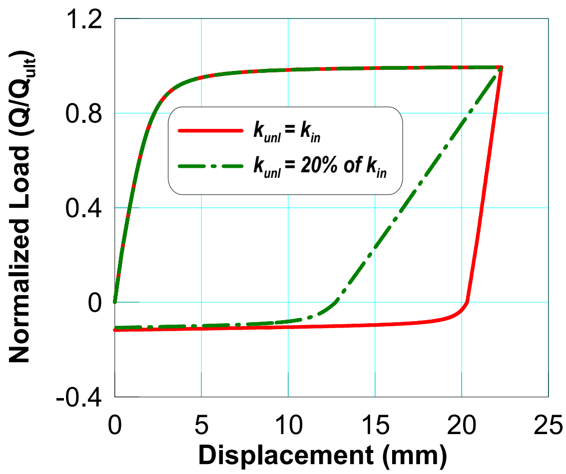

Fig. 2.17 Unloading stiffness of an individual spring.

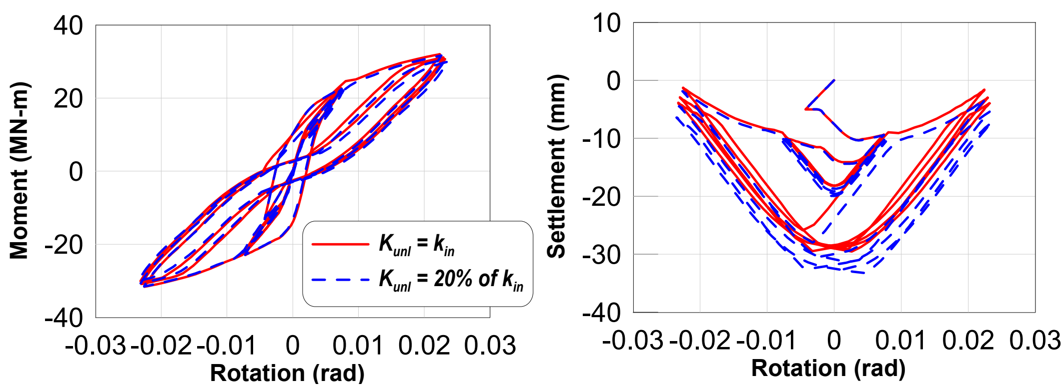

Fig. 2.18 Effect of varying unloading stiffness on footing response.

2.4 LIMITATIONS OF MODEL

The limitations of the BNWF model are as follows:

- Vertical and lateral capacities of the foundation are not coupled in this model. Therefore, if the vertical or moment capacity is increased or decreased, it will not affect the shear capacity. This might occur, for example, as a result of footing uplift, which decreases the shear capacity due to reduced foundation-soil contact area. Similarly, any change in the lateral capacity and the stiffness will not affect the axial and moment capacity.

- Individual springs along the base of the footing are uncoupled, as is common for any Winkler-based modeling procedure. This means that the response of one spring will not be influenced by the responses of its neighboring springs.

3 Contact Interface Model

3.1 DESCRIPTION OF CONTACT INTERFACE MODEL

This section presents a “contact interface model” (CIM) that has been developed to provide nonlinear constitutive relations between cyclic loads and displacements of the footing-soil system during combined cyclic loading (vertical, shear, and moment). The rigid footing and the soil beneath the footing in the zone of influence, considered as a macro-element, were modeled by keeping track of the geometry of the soil surface beneath the footing as well as the kinematics of the footing-soil system including moving contact areas and gaps.

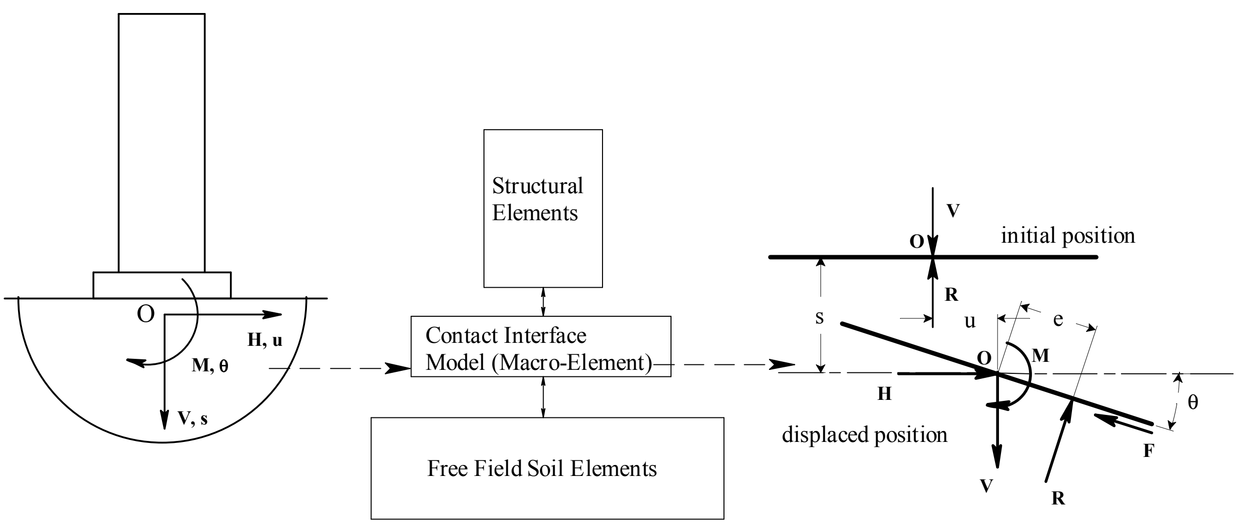

Fig. 3.1 Concept of macro-element contact interface model and forces and displacements at footing-soil interface during combined loading (Gajan and Kutter 2007).

From the numerical modeling point of view, the CIM is placed at the footing-soil interface, replacing the rigid foundation and surrounding soil in the zone of influence as indicated in Figure 3.1. When incremental displacements are given to the macro-element model as input, it returns the corresponding incremental loads and vice versa (Gajan 2006 and Gajan and Kutter 2007). The notation used for forces and displacements is indicated in Figure 3.1.

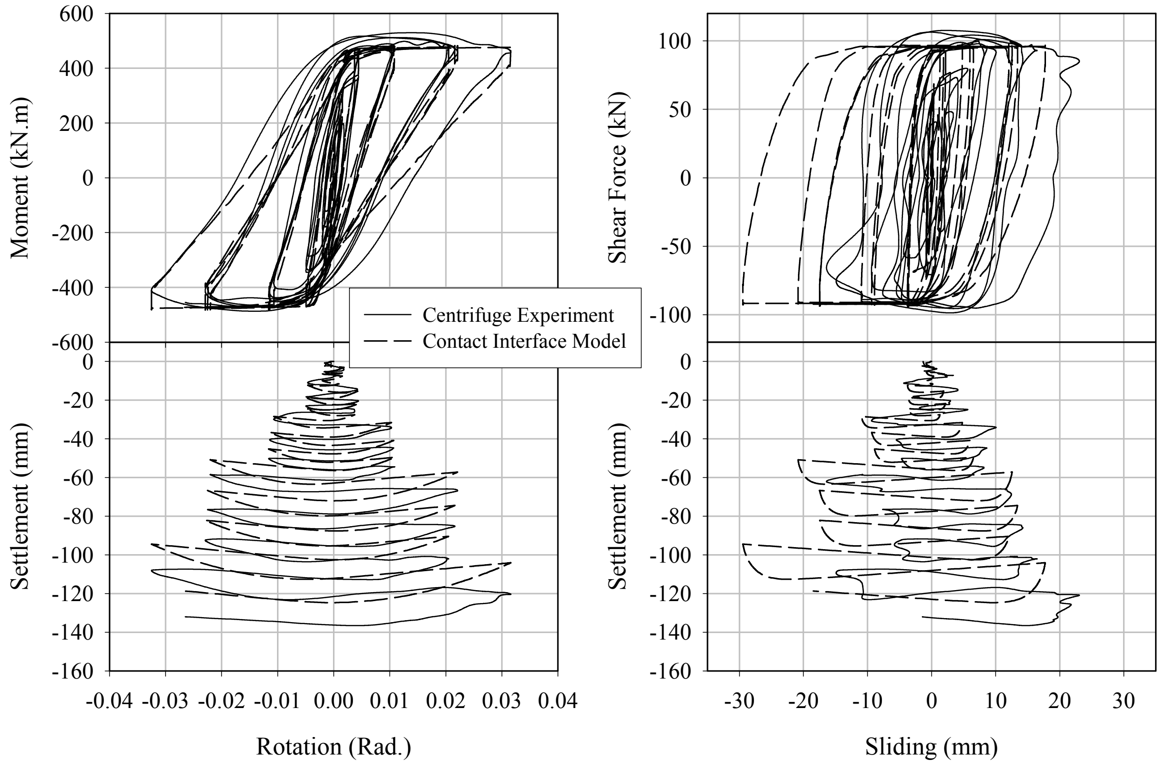

Fig. 3.2 Load-displacement results at base center point of footing for slow lateral cyclic test: Sand, Dr = 80%, L = 2.8 m, B = 0.65 m, D = 0.0 m, FSV = 2.6, M/(H.L) = 1.75.

Other researchers have used macro-element concepts to model the load-displacement behavior of structural elements and shallow foundations (Nova and Montrasio 1991; Cremer et al. 2001; Houlsby and Cassidy 2002). Most of the previous attempts with macro-element models for shallow foundations describe the constitutive relations based on yield surfaces, potential surfaces, and tracking the load path history in the generalized load space. The macro-element contact interface model presented in this paper differs in the sense that the constitutive relations are obtained by tracking the geometry of gaps and the contacts of the soil-footing interface. The contact interface model, with seven user-defined input parameters, is intended to capture the essential features (load capacities, stiffness degradation, energy dissipation, and permanent deformations) of the cyclic load-deformation behavior of shallow foundations. Figure 3.2

illustrates the ability to capture these important features for a centrifuge model of a strip footing with a static factor of safety of 2.6 on a dense sand foundation.

3.1.1 Parameterization of Footing-Soil Interface Contact Area

A key feature of the CIM is its ability to capture the gap formation between the footing and underlying soil as well as the effect of the gap on the vertical and lateral foundation capacities. Foundation-soil contact is tracked using a parameter called the critical contact area ratio A/Ac; where A is the area of the footing and Ac is the area of the footing required to have contact with soil to support the vertical and shear loads. A/Ac can be considered to be an alternate definition of the factor of safety with respect to bearing capacity. For a two-dimensional shear wall structure loaded in the plane of the wall, area ratio A/Ac equals the footing length ratio L/Lc, which is illustrated in Figure 3.3. As rotation increases, the contact length of the footing approaches its minimum value, Lc, and assuming that the pressure distribution is uniform within this critical area, the resultant soil reaction occurs at a maximum eccentricity, $e_{max} = (L – Lc)/2$. For small rotation angles, θ ($Cos(\theta) \approx 1$), the moment capacity may be calculated as $M_{ult} = V(L – Lc)/2$, where V is the vertical load on the interface.

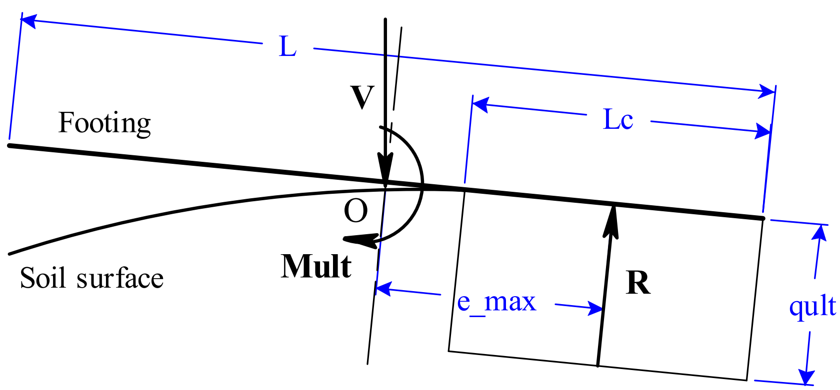

Fig. 3.3 Critical contact length and ultimate moment (Gajan 2006).

3.1.2 Curved Soil Surfaces and Rebound

Figure 3.3 illustrates the CIM showing the contact of the rigid footing with the rounded soil surface beneath the footing and the forces acting at the interface. As shown in Figure 3.4, soil_min and soil_max represent two different rounded soil surfaces beneath the footing. Soil_max represents the lowest position of the soil surface (hence the maximum instantaneous local settlement). Soil_min represents the partially rebounded soil surface that exists after gap formation as the footing rocks. The difference between soil_max and soil_min is conceptually attributed to the elastic rebound and the bulging of soil into the gap associated with plastic compression in neighboring loaded areas.

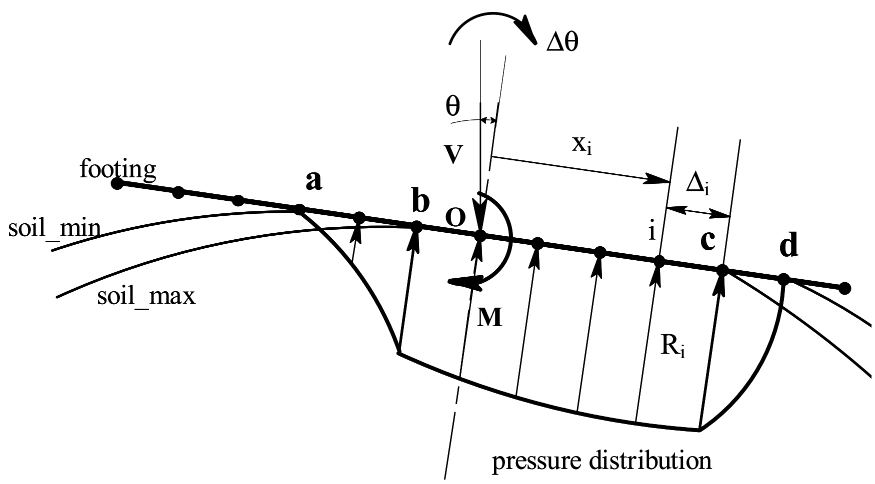

Fig. 3.4 Contact interface model for cyclic moment loading (Gajan and Kutter 2007).

3.1.3 Coupling between Shear, Moment, and Vertical Loads and Displacements

One advantage of the CIM over the BNWF model is that the moment, shear, and vertical load capacities are coupled. The coupling between the vertical and moment capacities results from gap formation. That is, the moment capacity typically occurs after a gap has formed, causing the vertical capacity to drop. The coupling between shear and the moment capacity is accounted for using the interaction diagram in Figure 3.5.

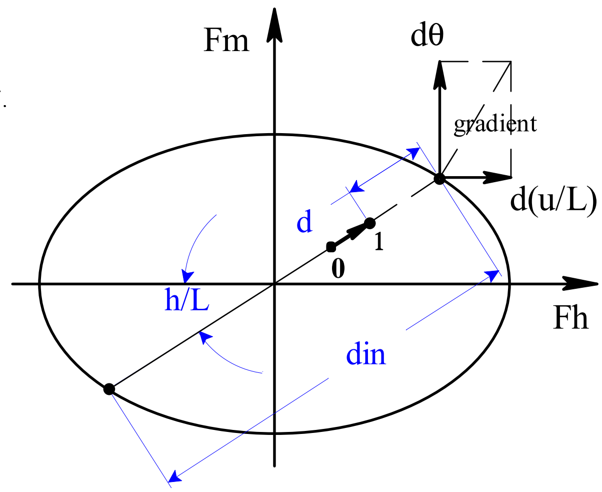

Fig 3.5 Cross section of bounding surface in normalized M-H plane and geometrical parameters used in interface model (Gajan 2006).

The sliding resistance and hence the magnitude of the sliding displacement for a given applied horizontal load, depends on the proximity to the bounding surface, which is quantified by the ratio d/din. The strain-compatible shear stiffness of the footing is a function of (d/din), which determines the shape of the nonlinear transition from the initial stiffness to capacity. The bounding surface in Figure 3.5 not only describes the interaction between the moment and shear capacities but also relates the incremental rotations to the incremental sliding by assuming associative flow. The procedures for calculating load capacities and displacements are detailed in Gajan (2006).

3.2 IDENTIFICATION OF PARAMETERS

The description of model parameters is organized according to user-defined input parameters and non-user-defined parameters.

3.2.1 User-Defined Input Parameters and Parameter Selection Protocols

The input parameters for CIM are the ultimate vertical load (V_{ULT}), the length of footing (L), the initial vertical stiffness (Kv), the initial horizontal stiffness (Kh), the elastic rotation limit ($\theta_{elastic}$), the rebound ratio (Rv), and the internal node spacing (D_l). Note that the initial rotation stiffness is calculated by CIM based on the given vertical stiffness and footing geometry.

Guidelines for the selection of these user-defined parameters are given below. Additional details are provided in Gajan and Kutter (2008).

Ultimate vertical load (V_{ULT}): The maximum vertical load that can be applied to the footing, which occurs with full footing-soil contact. V_{ULT} is calculated in units of force for vertical loading applied to the footing through its centroid using general bearing capacity theory (e.g., Salgado 2006).

Length of footing (L): The linear dimension of the footing in the plane of rocking.

Initial vertical stiffness (Kv): The initial (elastic) vertical stiffness of the footing in full contact with soil for pure vertical loading. This may be taken as the elastic vertical stiffness of the entire footing in units of force/displacement from elastic solutions for rigid footings (Gazetas 1991).

Initial horizontal stiffness (Kh): The elastic shear stiffness of the footing in full contact with the soil for pure shear loading. This may be taken as the elastic horizontal stiffness of the entire footing in units of force/displacement from elastic solutions for rigid footings (Gazetas 1991).

Elastic rotation limit ($\theta_{elastic}$): The maximum amplitude of rotation for which no settlements occur. This elastic range was introduced subsequent to Gajan et al. (2005) and Gajan (2006). This may be taken as 0.001 radians, as this has shown to match centrifuge experiments reasonably well. If $\theta_{elastic}$ is too small the model tends to predict an unreasonable amount of settlement during the small amplitude shaking at the beginning and end of an earthquake. Figure 3.6 illustrates the observed behavior in physical model tests that is simulated by the introduction of the parameter $\theta_{elastic}$.

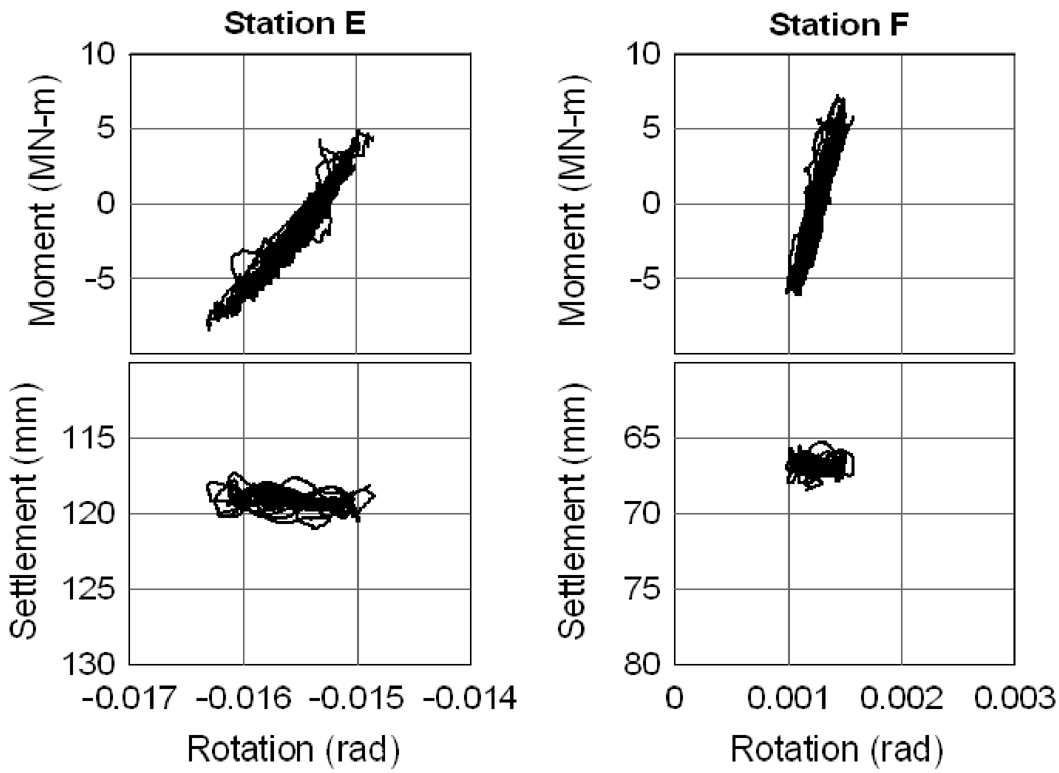

Fig. 3.6 Elastic range for two identical structures on different sized footings.

Rebound ratio (Rv): Rv is an empirical factor to account for the elastic rebound and bulging of soil into the gap associated with the plastic compression in neighboring loaded areas described in Section 3.1.2. The model assumes that the amount of rebound is proportional to the total settlement computed by the element. For example, if Rv is 0.1, any gap between the uplifting footing and soil surface smaller than 10% of the previous settlement would be filled by rebounding soil and the distance between soil_max and soil_min is at any point is 10% of the settlement of that point.

A default value of 0.1 has been used for many simulations, as it reasonably fits the current data from centrifuge model tests for rectangular and square footings on sand and clay. An increase in Rv will slightly reduce calculated settlements. In cases where convergence is a problem, especially with footings with a large vertical factor of safety and a large number of load cycles, increasing Rv can increase the length of the transition zone between soil_max and soil_min shown in Figure 3.4, which stabilizes numerical convergence. The use of Rv as a parameter to control numerical stability is shown in Figure 3.7. It should be noted that increasing

Rv does not always make the model more stable. Increasing Rv will stiffen the load-deformation response which can make the model less stable in some situations.

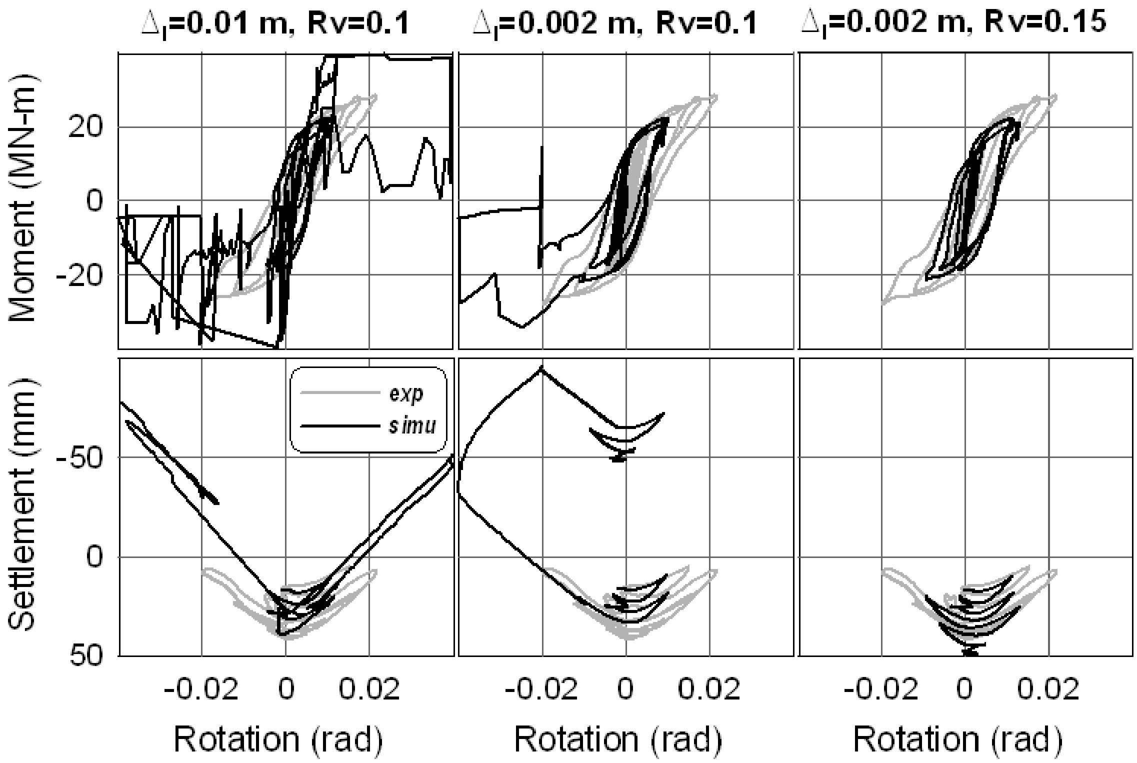

Fig. 3.7 Effect of D_l and Rv on moment-rotation and settlement-rotation of footing.

Footing node spacing (D_l): D_l specifies the distance between the footing nodes internally created in the model (Fig. 3.4). This user-defined parameter affects numerical stability and accuracy as well as the computation time. Node spacings should be selected in consideration of model properties. As the critical contact length (Lc) decreases (or as FSv increases), D_l should be small enough to define the pressure distribution along the soil-footing contact length depicted in Figure 3.4. For a large range of L and FSv, D_l of 0.01m is a reasonable choice. The number of internally created footing nodes necessary for numerical stability and accuracy will range from a few hundred nodes for FSv below 10 to a few thousand for FSv of 50. For example, a footing length of 5m with a D_l of 0.01m will have 501 internally created footing nodes. Computation time is sensitive to this input parameter.

3.2.2 Summary of Non-User-Defined Parameters

In this section we describe parameters that are hard-wired into the code. More detailed information can be found in Gajan (2006) and in the source code (/SRC/material/section/yieldsurface/soilfootingsection2D). These parameters are as follows:

- n_load = 0.5, n_unload = 2: describe the limiting shape of the parabolic pressure distribution on at the edges of the contact length between points a and b and c and d in Figure 3.5. When the loading direction is reversed, there is a smooth transition in the shape (from n = 0.5 to n = 2) given by the following equations:

$$n\_load = 1.5 \cdot \left(\frac{\theta - \theta_{elastic}}{2 \cdot \theta_{elastic}} \right) + 0.5 \tag{3.1}$$

$$n\_unload = 1.5 \cdot \left(\frac{\theta_{elastic} - \theta}{2 \cdot \theta_{elastic}} \right) + 0.5 \tag{3.2}$$

- a = 0.32, b = 0.37, c = 0.25, d= 55, e = 0.8 and f = 0.8: define the bounding surface in normalized moment-shear-vertical load space (Cremer et al. 2001). The bounding surface is defined by the following three equations:

$$\frac{{F_H}^2}{A^2} + \frac{{F_M}^2}{B^2} = 1 \tag{3.3}$$

$$A = a \cdot {F_V}^c \cdot (1 - F_V)^d \tag{3.4}$$

$$B = b \cdot {F_V}^e \cdot (1 - F_V)^f \tag{3.5}$$

where F_H, F_M, and F_V are the normalized shear, moment, and vertical capacities of the foundation-soil interface. ($F_V = V/V_{ULT}$, $F_H = H/V_{ULT}$ and $F_M = M/(V_{ULT}\,L)$, and V_{ULT} is failure load for pure vertical loading). This bounding surface was verified with centrifuge tests shown in Figure 3.5.

- $c = 1$, $n = 2$: coefficient and exponent describing the sharpness of the transition between elastic and plastic behavior for shear-sliding. These parameters were selected by comparing to a variety of data and were not found to be critical parameters.

4 Comparison of Model Predictions for Typical Structures

4.1 DESCRIPTION OF CASE STUDY BUILDINGS AND INPUT MOTIONS

OpenSees simulations were carried out for typical shear wall structures supported by shallow foundations using both the beam on nonlinear Winkler foundation (BNWF) approach and the macro-element modeling approach (contact interface model, CIM). Three benchmark shear wall configurations were developed for the OpenSees simulations. Figure 4.1 shows the plan view common to all buildings, whereas Figure 4.2 shows individual profiles for each building. The footing was designed for a combination of gravity lateral seismic forces as prescribed in the 1997 UBC.

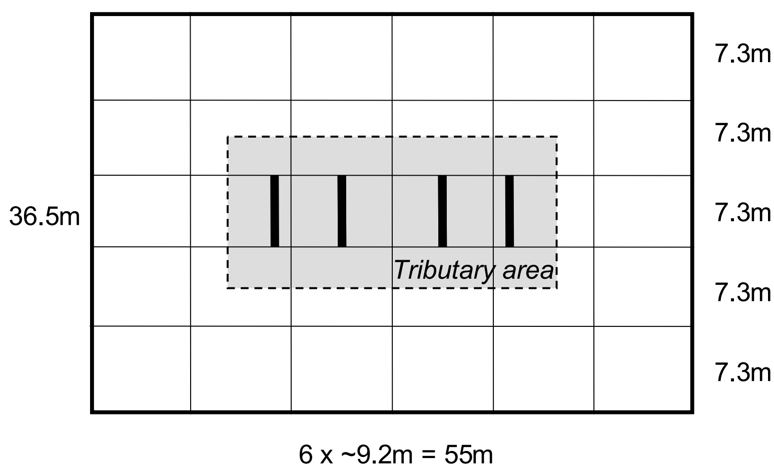

Fig. 4.1 Plan view of benchmark structure with shear walls considered in OpenSees simulations. Tributary area for vertical loads carried by wall footings is shown in gray.

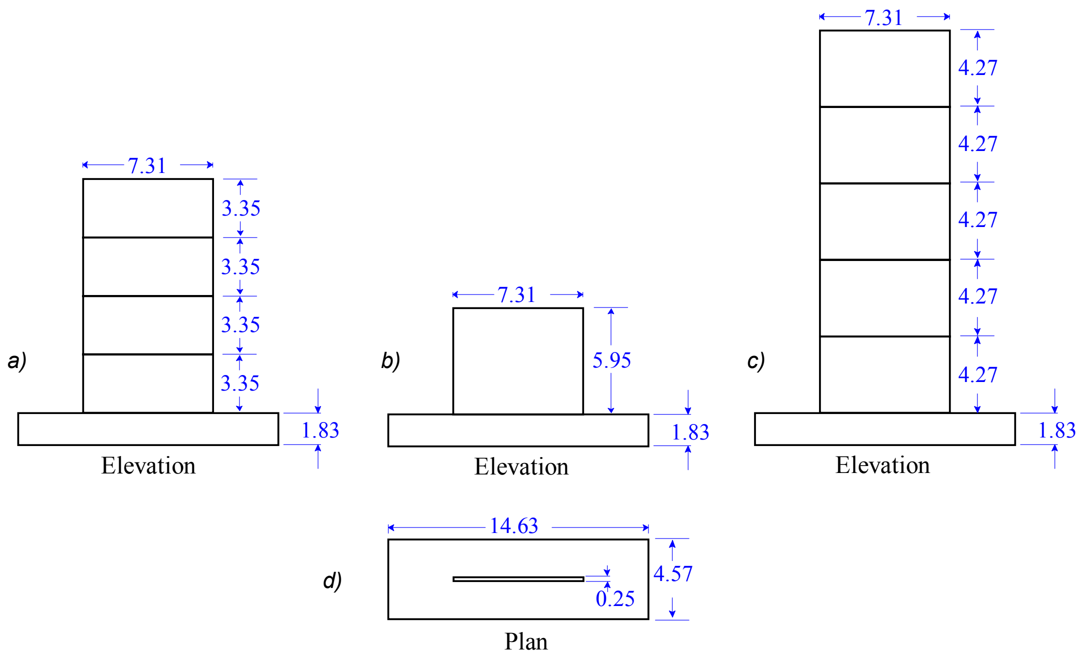

Fig. 4.2 Geometry and dimensions of three benchmark structures (dimensions in meters).

4.1.1 Sizing of Footings for Bearing Capacity

The four-story model was developed first (Fig. 4.2a) and includes a core consisting of four concrete shear walls to carry all lateral loads and vertical loads within the tributary area (Fig. 4.1). The core shear walls are supported by shallow strip foundations. The foundation dimensions shown in Figure 4.2(d) were determined using conventional foundation design techniques (e.g., Coduto 2001). The foundation bearing capacity was calculated using a depth-invariant undrained shear strength (i.e., total stress cohesion) of 50 kPa. The foundation bearing demand was calculating considering vertical forces and a pseudo-static horizontal force to represent the effects of earthquake shaking. The vertical forces were calculated using the wall weights and effective floor loads (acting within the tributary area from Fig. 4.1) given in Table 4.1. The pseudo-static horizontal load was calculated per UBC (1997) using a representative spectral acceleration S_{ds} = 1.0g and response modification factor R = 6, providing a seismic coefficient of 0.17. Since all horizontal loads are carried by the shear walls, the full footprint area was used with the floor load and the UBC seismic coefficient to calculate the horizontal force. The vertical force and moment on the footing were converted to a trapezoidal distribution of vertical stress containing a uniform (rectangular) component from gravity loads and a triangular distribution due to overturning moment. The footing dimensions given in Figure 4.2 were obtained by matching the bearing capacity to two thirds of the maximum stress (q_{max}), as depicted in Figure 4.3. Note that this allows a zero stress (uplift) zone beneath portions of the footing. All footings are assumed to rest on the ground surface (no embedment).

For the other building configurations (one- and five-story buildings), the same vertical load was assumed to act on the footings, despite the varying heights. We recognize that those vertical loads may not be realistic. However, this was done so that the ensuing sensitivity studies would apply for a constant vertical factor of safety against foundation bearing failure, the only variable from case-to-case being wall height and the corresponding applied seismic moment. Accordingly, the footing dimensions given in Figure 4.2 apply to all three cases. Table 4.1 and Figure 4.2 summarize loads and footing dimensions for these other building configurations.

Given the shear strength of the foundation soil and the foundation dimensions shown in Figure 4.2, the vertical ultimate bearing load is Q_{ult} = 18.1 MN and the lateral ultimate load is T_{ult} = 3.3 MN. Larger lateral capacities are also considered by coupling footings, which is described further below. Factors of safety against vertical bearing failure in the absence of lateral loads (FSv) are indicated in Table 4.1.

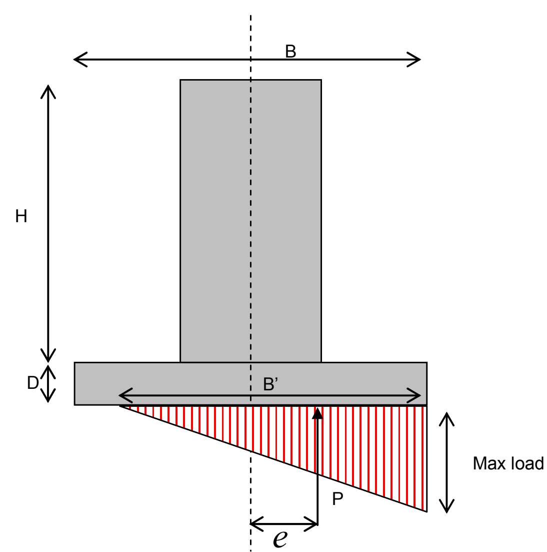

Fig. 4.3 Schematic geometry and parameters used for design.

Table 4.1 Load and other parameters used for footing design.

Model	Aspect ratio	Eccentricity e (m)	Load on one wall (kN)	Weight of one wall (kN)	Vertical FS (FSv)
4-story	0.69	5.4	741.9	29.7	3.1
1-story	0.35	6.1	320.4	13.0	4.8
5-story	1.06	5.2	674.4	47.2	2.6

4.1.2 Foundation Stiffness

As described in Stewart et al. (2004) and FEMA-440, a critical consideration in the evaluation of foundation stiffness for building systems such as depicted in Figure 4.1 is the coupling of deformations between footings. Fully coupled foundations are slaved to have identical displacements/rotations, whereas uncoupled foundations are independent. We assume rotations and vertical displacements of wall footings to be uncoupled. Both coupled and uncoupled conditions are considered for lateral displacements. The uncoupled case would correspond to independent (non-connected) spread footings beneath wall footings and other footings for other load-bearing elements in the building. This is rarely the case in modern buildings in seismically active regions. More commonly, footing elements are interconnected with grade beams or slabs, which couples horizontal displacements. If these connecting elements are sufficiently stiff, rotations would also be coupled, but that is not considered here.

The small-strain shear modulus of the foundations clays is taken as G_{max} = 26 MPa and the Poisson's ratio as ν = 0.5. These parameters are used with the foundation dimensions shown in Figure 4.2 to calculate elastic foundation stiffnesses of K_v = 814 MN/m, K_θ= 14520 MNm/rad, K_x=750 MN/m (uncoupled), and K_x=1800 MN/m (coupled, using full foundation dimensions).

4.1.3 Loads Applied in OpenSees Simulations

OpenSees models of the wall-foundation systems described above were subjected to three types of lateral loads to characterize the system response. For all types of analysis, gravity loads are applied first in 10 equal load steps. The three types of lateral loading are:

Pushover analysis: Static horizontal loading is applied to characterize the nonlinear backbone response, particularly the yield and post-yield characteristics of the footing-wall structures. During this incremental static analysis, the structures are pushed to a maximum of five times the yield displacement.

Slow cyclic analysis: A ramped sinusoidal horizontal displacement is applied to the top of the structure and the lateral force required to produce the displacement is calculated. The prescribed displacement history is shown in Figure 4.4. The loading is "slow" in the sense that no inertial loads develop during cycling.

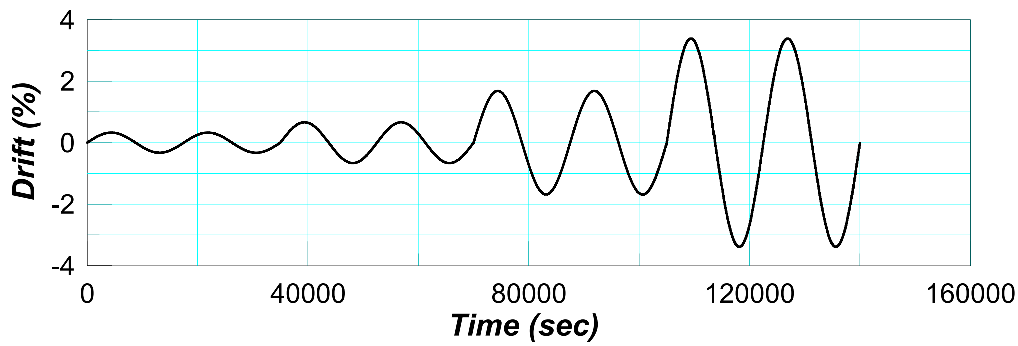

Fig. 4.4 Top of wall displacement history used for slow cyclic loading.

Earthquake ground motion analysis: Nonlinear response history analyses are conducted using the Saratoga W. Valley College motion recorded at a site-source distance of 13 km during the M_w 6.9 1989 Loma Prieta earthquake. The WVC270 component used for the present application is shown without scaling in Figure 4.5. This motion is then amplitude scaled at the first mode period of each model to different target values of spectral acceleration. The target spectral accelerations were developed using probabilistic seismic hazard analyses for a site in Los Angeles, with details given in Goulet et al. (2007). The target spectral accelerations are taken at hazard levels of 50% probability of exceedance in 50 years, 10% in 50 years, and 2% in 50 years. Figure 4.6 shows the elastic pseudo-acceleration response spectra at 5% damping after scaling to these target amplitudes.

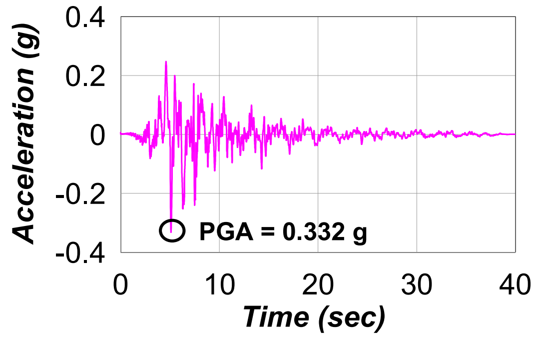

Fig. 4.5 Acceleration history of Sarasota recording of Loma Prieta earthquake used for response history analyses.

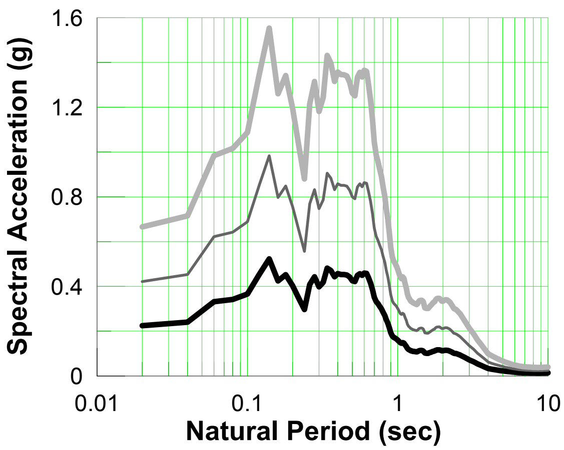

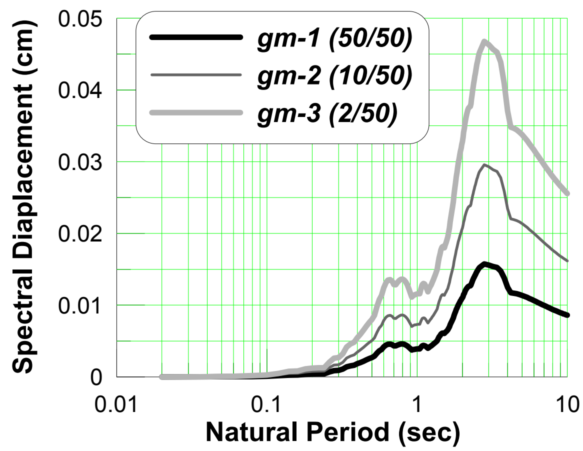

Fig. 4.6 Elastic 5% damped: (a) acceleration response spectra and (b) displacement response spectra for scaled motions.

4.2 NUMERICAL MODELS AND INPUT PARAMETERS

4.2.1 Details of OpenSees Meshes

(a) BNWF Model

The shear wall and footing system is represented in OpenSees as a two-dimensional lumped-mass model with nodes at each floor level and elastic beam-column elements joining the nodes. As shown in Figure 4.7, in the BNWF model, strip footings are modeled using elastic beam-column elements connected to zero length soil springs. A total of 60 elastic beam-column elements (i.e., spacing of 2% of the total length) are used to model the footing. As described in Chapter 2, inelastic q-z springs are used for vertical and moment resistance and t-x springs represent base sliding resistance. There are no p-x springs because the footings are not embedded. Vertical springs are distributed at a spacing of 2% of total length ($l_e/L=0.02$), which produces 61 vertical springs. The end region is assumed to extend across 15% of the footing length measured inward from the edges. Foundation stiffness is increased by a factor of three in this region for the reasons described in Section 2.2.1.

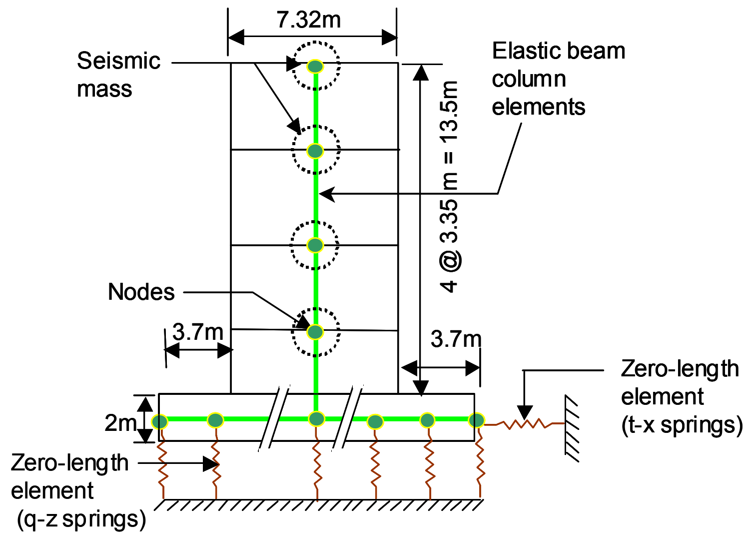

Fig. 4.7 OpenSees BNWF model with benchmark building (Model 1, 4-story building).

(b) Contact Interface Model (CIM)

Figure 4.8 shows the finite element mesh for the OpenSees simulations using the CIM. The shear wall and structural footing were modeled exactly the same way as in the BNWF model analysis; i.e., a two-dimensional three-degrees-of-freedom model, with point mass attached to each node, connected by elastic beam-column elements. The contact interface model, implemented as a material model (SoilFootingSection2d) in OpenSees, is connected at the footing-soil interface. Nodes 1 and 2, representing the footing-soil interface, were connected by a zero length section. For all analyses, node 1 was fixed and node 2 was allowed to settle, slide, and rotate.

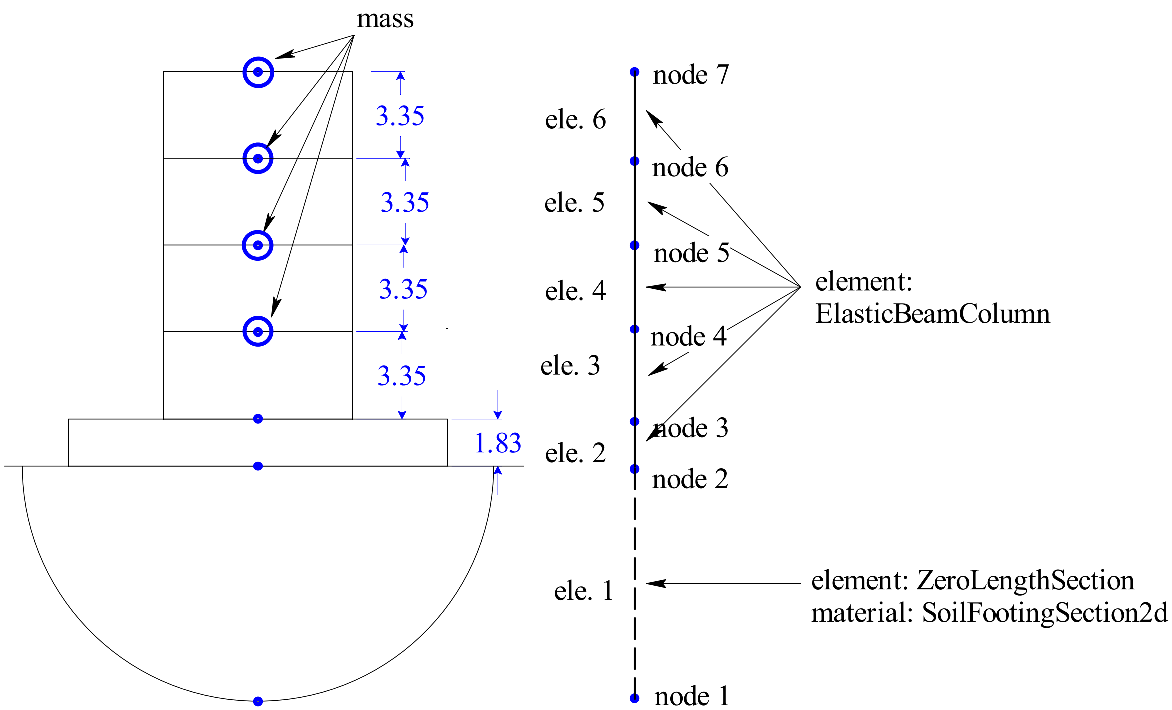

Fig. 4.8 OpenSEES mesh for CIM analysis (Model 1, 4-story building).

4.2.2 Model Input Parameters

(a) Elastic Beam-Column Elements

The shear wall is modeled using elastic beam-column elements with section modulus EI=2.1e^{10} N-m^2. The elastic beam-column element of the footing (used for the BNWF model but not the CIM model) has EI=2.45e^{12} N-m^2.

(b) BNWF Model

Vertical loads and factors of safety against bearing failure are as described above in Section 4.1.1. Tension capacity is taken as 10% of $q_{ult.}$ Radiation damping is taken as 5%. The elastic foundation stiffnesses are as given in Section 4.1.2. Five percent Rayleigh damping has been assumed for the structure vibrating in its first two modes. To solve the nonlinear equilibrium equations, the modified Newton-Raphson algorithm is used with a maximum of 40 iterations to a convergence tolerance of 1e-8. The transformation method (OpenSees 2008), which transforms the stiffness matrix by condensing out the constrained degrees of freedom, is used in the analysis as a constraint handler.

(b) Contact Interface Model (CIM)

The model parameters for CIM are described in Section 3.2.1. The vertical load capacity, foundation dimensions, and initial stiffness are as described in Sections 4.1.1–4.1.2. The elastic rotational range was selected as $\theta_{elastic}$=0.001 radian, while the rebounding ratio used was taken as Rv=0.1. The internal node spacing was taken as D_l=0.01 m. These are default values for these parameters as explained in Section 3.2.1.

4.3 RESULTS

4.3.1 Eigenvalue Analysis

Eigenvalue analysis is performed to determine the fixed- and flexible-base periods of the models. Table 4.2 summarizes the results from these analyses for both the BNWF and CIM models. The fixed-base periods are identical for the BNWF and CIM models. Flexible-base periods account for elastic stiffnesses in translation and rocking at the foundation level. Because the stiffness of vertical springs was selected to match target stiffnesses for vertical vibrations, the match for rocking is imperfect and varies between the BNWF and CIM models. Note that for practical application it is generally preferred to select vertical spring stiffnesses to match the target rotational stiffness. Had that been done for the present analysis, no differences would be expected in the flexible-base periods.

The flexible-base period is also calculated using the following expression, originally derived by Veletsos and Meek (1974):

$$\frac{\tilde{T}}{T} = \sqrt{1 + \frac{k}{k_u} + \frac{kh^2}{k_\theta}} \tag{4.1}$$

where, $\tilde{T}$ = flexible-base period of a surface foundation, T = fixed-base period, k, m = stiffness and mass of the structure, h = effective height of the structure, k_u and k_θ are the horizontal and the rotational stiffness of the foundation, respectively, on an elastic half-space.

As noted above, the misfit of the BNWF and CIF results relative to the Veletsos and Meek (1974) solution is because the vertical springs in the OpenSees models were not specified to reproduce the rotational stiffness, k_θ.

Table 4.2 Eigenvalue analysis results (first mode period).

Model	Fixed-base period (sec)	Flexible-base period (sec)			Flexible-base period (increased k_u and H_u) (sec)		
		BNWF model	CIM model	Veletsos & Meek (1974)	BNWF model	CIM model	Veletsos & Meek (1974)
4-story	0.45	0.87	0.90	0.82	0.85	0.88	0.80
1-story	0.21	0.46	0.48	0.41	0.43	0.44	0.39
5-story	0.76	1.42	1.46	1.25	1.38	1.43	1.24

4.3.2 Pushover Analysis

Nonlinear static pushover analyses were conducted to assess the lateral capacity of the footing-structure system. Figure 4.9 shows that the BNWF model of the wall-footing system exhibits nearly elastic-plastic behavior, with only nominal post-yield hardening. Yielding of the model only occurs at the footing interface. Defining yield at the drift level at which the first base spring exceeds 90% of its capacity, the yield drift ratio is determined as: 0.12% (four story), 0.38% (one story), and 0.1% (five story). The peak strengths are 0.23 (four story), 0.45 (one story), and 0.15 (five story) times the structure weight.

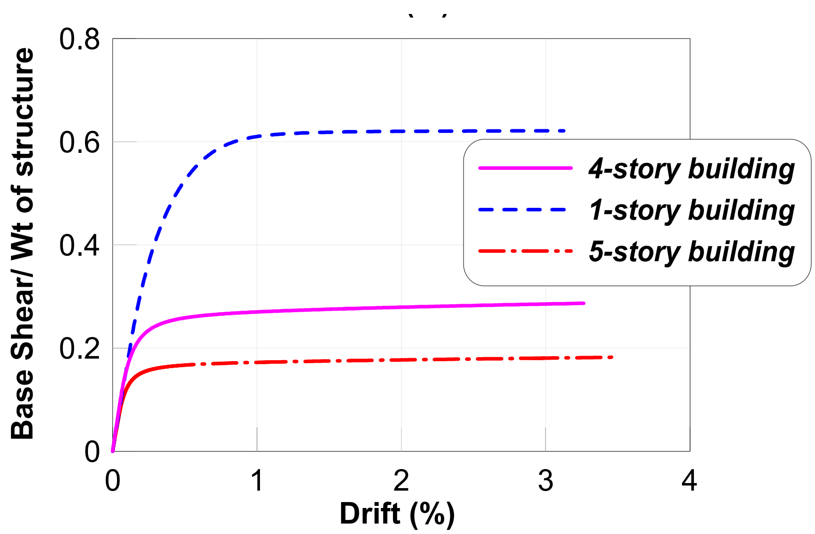

Fig 4.9 Nonlinear pushover analysis results for BNWF model.

4.3.3 Slow Cyclic Analysis

In this section we present the results of slow cyclic analysis in which the roof displacement history shown in Figure 4.4 is applied to the OpenSees models. Computed response quantities are relationships between moment-rotation, shear-sliding, settlement-rotation, and settlement-sliding at the base center point of the footing. The results for the BNWF and CIM models are plotted separately at different scales in Figure 4.10 and are plotted together in Figure 4.11.

For the four-story structure, the BNWF model reaches its design moment capacity (29 MN-m) but responds linearly in the shear mode. Therefore, very little sliding displacement (~3 mm) is calculated by the BNWF model. The CIM model also reaches its moment capacity of about 25 MN-m. However, the sliding capacity is exceeded in this case, resulting in elasto-plastic shear sliding behavior. The moment and shear capacities are reached simultaneously in the CIM model, since both are associated with peak levels of gap formation at peak drift. This is consistent with the moment-shear interaction concepts discussed in Section 3.1.3.

The different moment capacities in the two models result from the shear-moment capacity coupling in the CIM that is neglected in the BNWF. More permanent settlement (about 320 mm) is predicted by the CIM model than the BNWF model. We attribute this in part with the greater degree of foundation-soil nonlinearity in the CIM analysis associated with sliding.

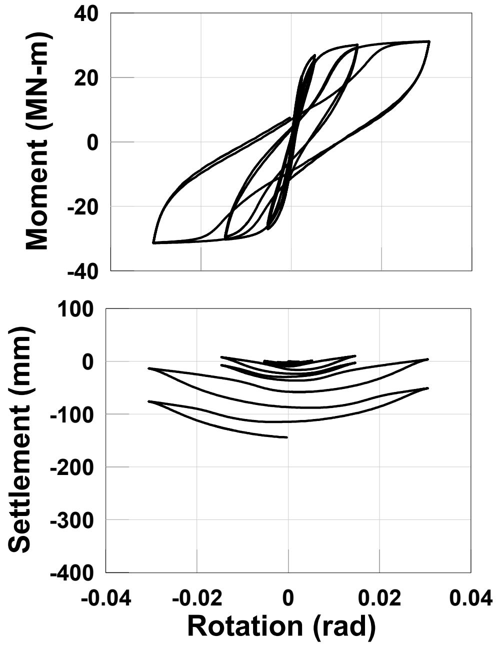

(a) BNWF model

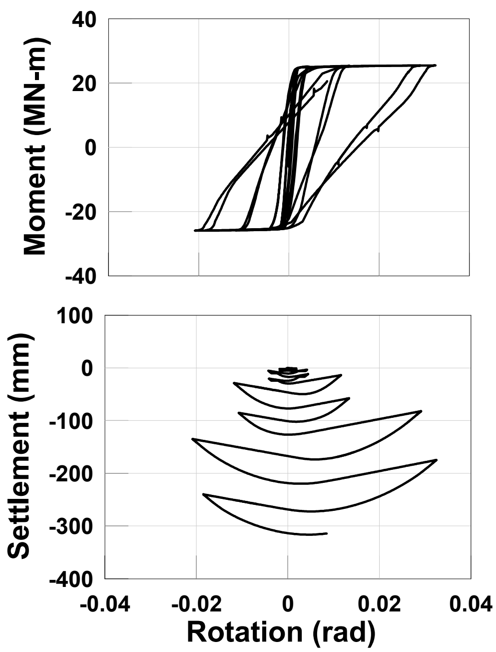

(b) CIM model

Fig 4.10 Footing response for 4-story building: (a) BNWF model (b) CIM model.

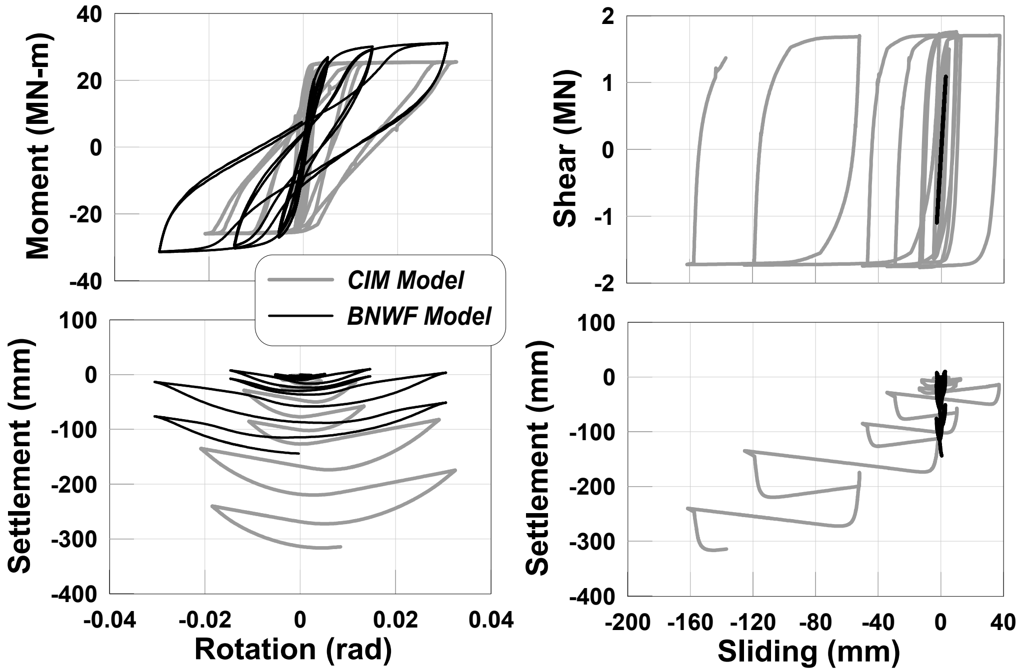

Fig 4.11 Footing response for 4-story building.

4.3.4 Ground Motion Analysis for Models with Uncoupled Footings

Ground motion analyses are performed for the two assumptions of foundation coupling described in Section 4.1.2. The first assumption (presented in this section) is for independent spread footings having the dimensions shown in Figure 4.2. This matches the configuration used elsewhere in this chapter. The following section considers the case in which horizontal displacements of all footings are coupled as a result of interconnection with grade beams or slabs.

Nonlinear response history analysis is conducted using the acceleration history input described in Section 4.1.3. Figures 4.12–4.14 summarize the footing response for the three wall-footing structures computed by the BNWF and CIM models.

The taller structures (four story and five story) are relatively moment-critical, as shown by significant nonlinear behavior (yield, hysteretic damping). The shorter structure (one story) is relatively shear-critical, as shown by a more significant nonlinear shear-sliding response. These results are qualitatively similar for the BNWF and CIM models. As expected, the degree of nonlinearity scales with ground motion amplitude.

As was found in the analyses using the slow cyclic input motion, the CIM model predicts significant permanent sliding due to the reduced shear capacity associated with foundation uplift. The sliding is much less in the BNWF model due to the lack of lateral capacity coupling with uplift. The BNWF and CIM models also exhibit different settlement-rotation relations; CIM has relatively flat within-cycle regions (especially for small excitation levels), whereas BNWF has a smoother "banana" shaped settlement-rotation response. The flat region in the CIM response results from the elastic rotation range for which no settlement occurs. As with the slow cyclic loading, CIM settlements exceed BNWF settlements due to the greater degree of foundation soil nonlinearity.

Numerical instabilities were not encountered in the BNWF analyses. For the CIM simulations, spikes appear in the shear-sliding response that exceed the shear capacity. These spikes are a result of numerical instability.

Figures 4.15–4.17 summarize the response histories of roof acceleration and total drift ratio. Total drift ratio is calculated as the relative roof displacement (i.e., roof lateral translation minus foundation lateral translation) divided by the building height. The peak acceleration demands and the shapes of the acceleration histories are qualitatively similar for the BNWF and CIM models. However, the transient and residual drift ratios differ with CIM predicting permanent drift associated with residual rotation at the footing-soil interface. This residual rotation is not predicted by the BNWF model.

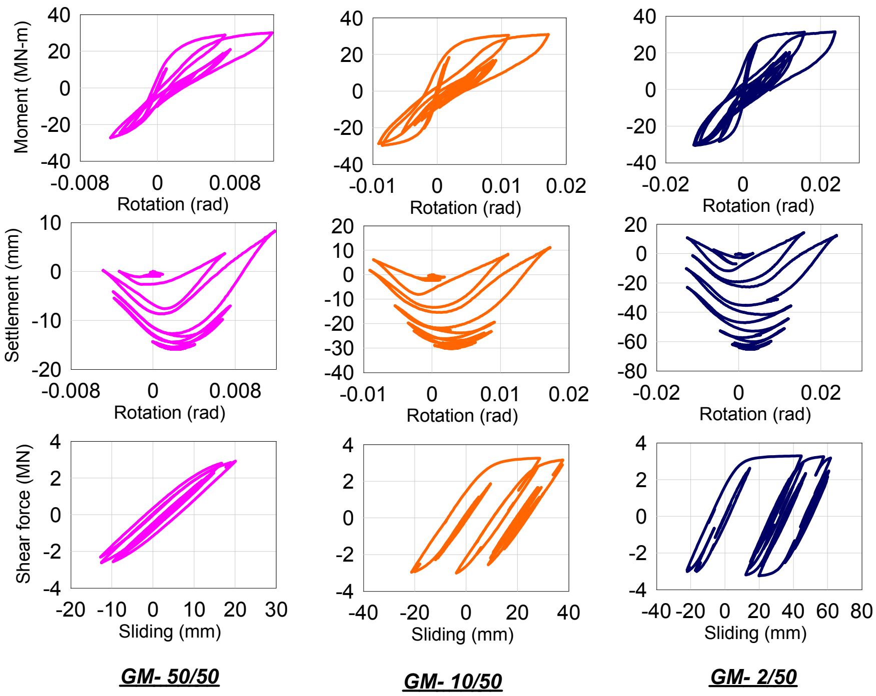

(a) BNWF model

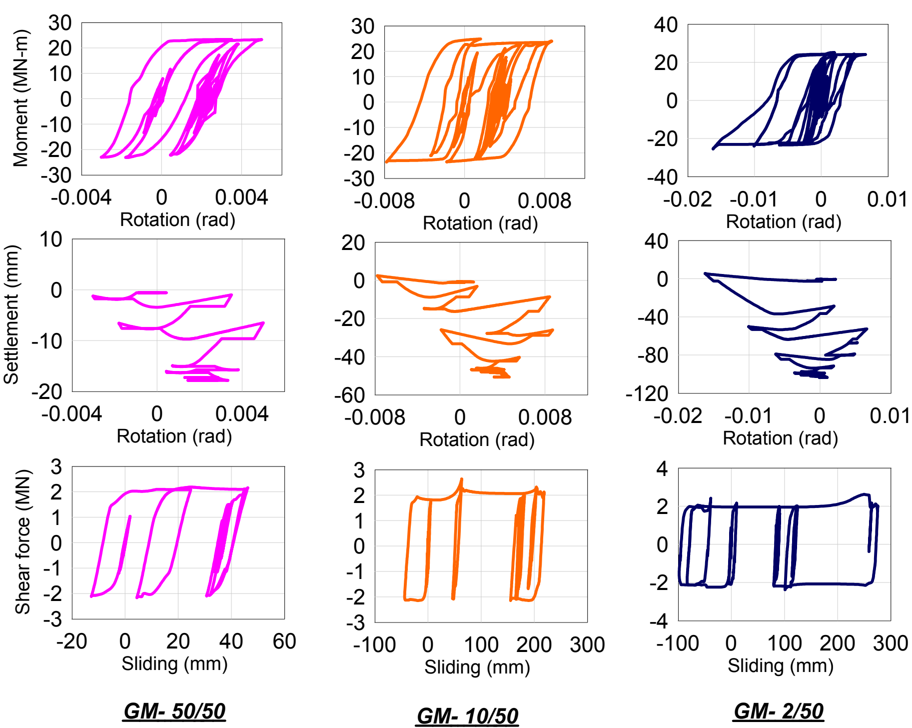

(b) CIM model

Fig 4.12 Footing response for 4-story building: (a) BNWF model (b) CIM model. Note scale differences.

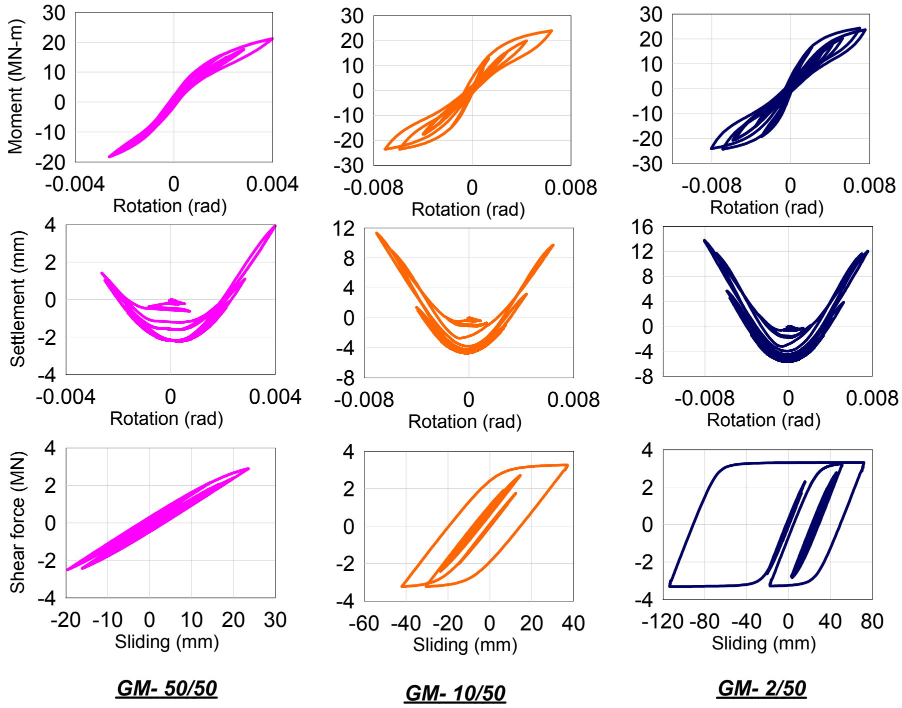

(a) BNWF model

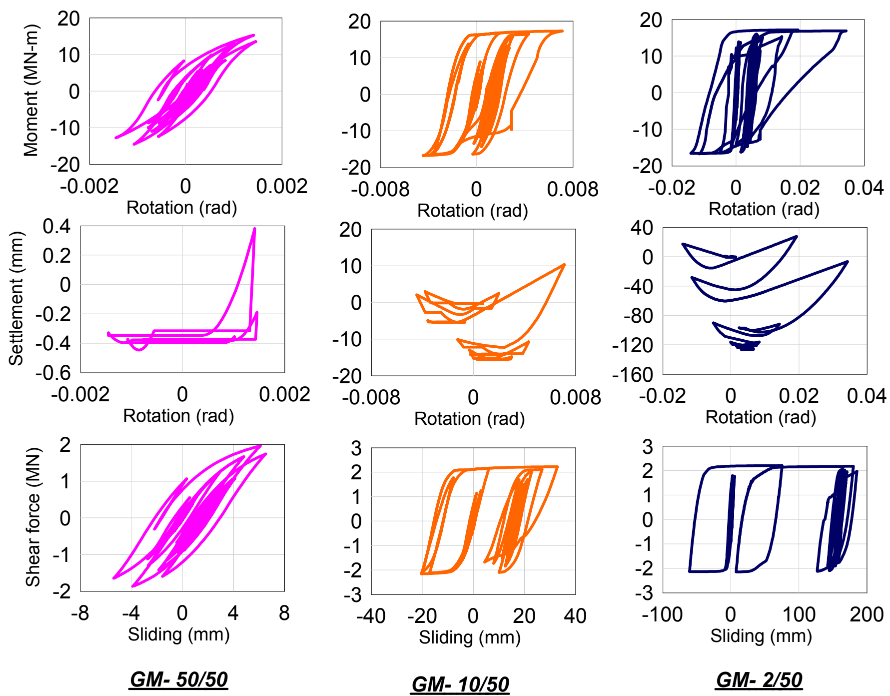

(b) CIM model

Fig 4.13 Footing response for 1-story building: (a) BNWF model (b) CIM model.

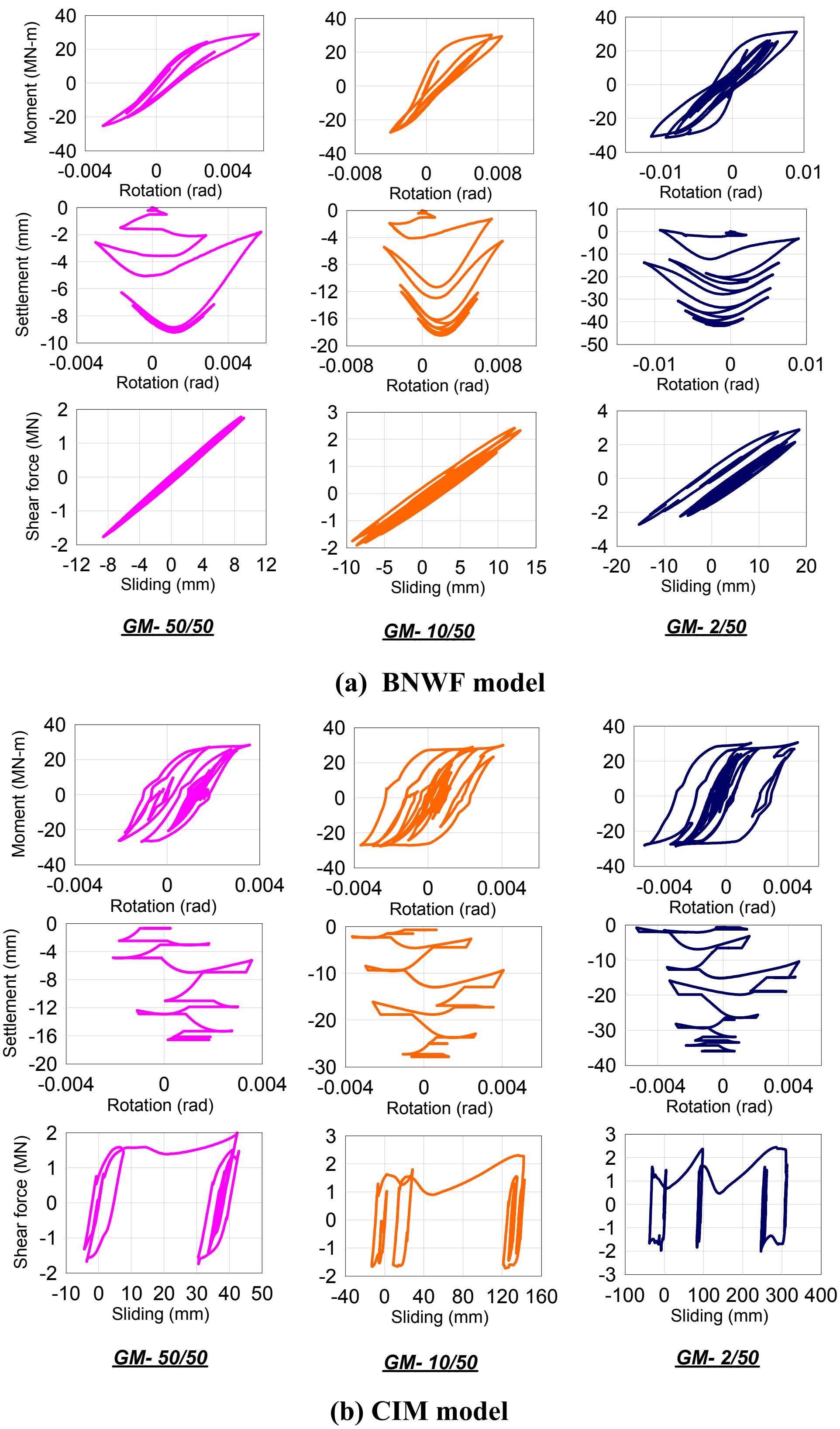

Fig 4.14 Footing response for 5-story building: (a) BNWF model (b) CIM model.

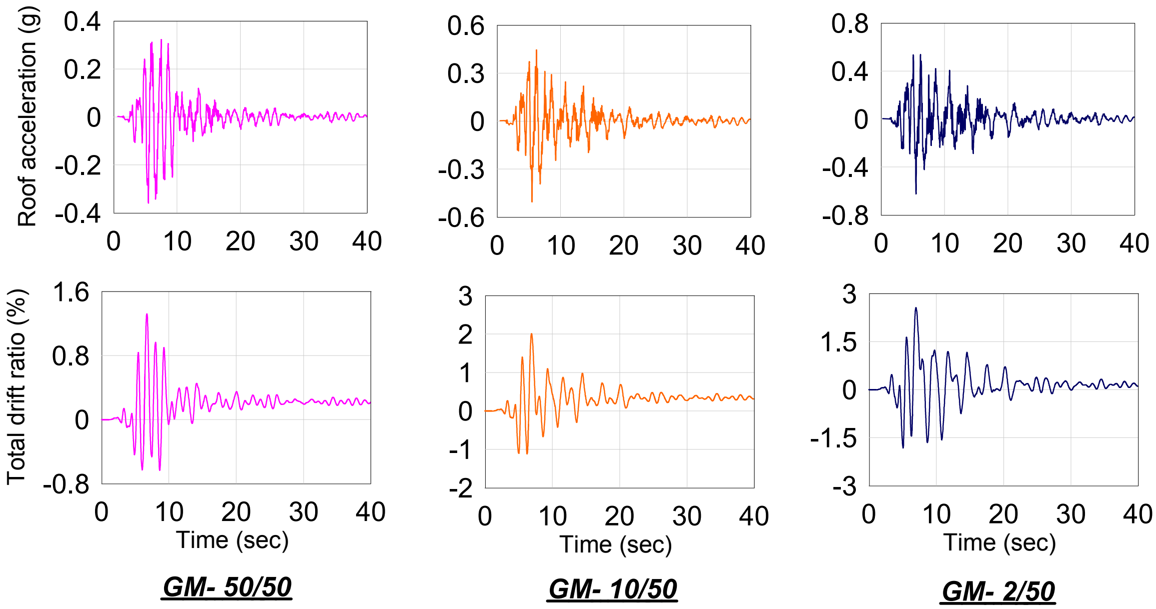

(a) BNWF model

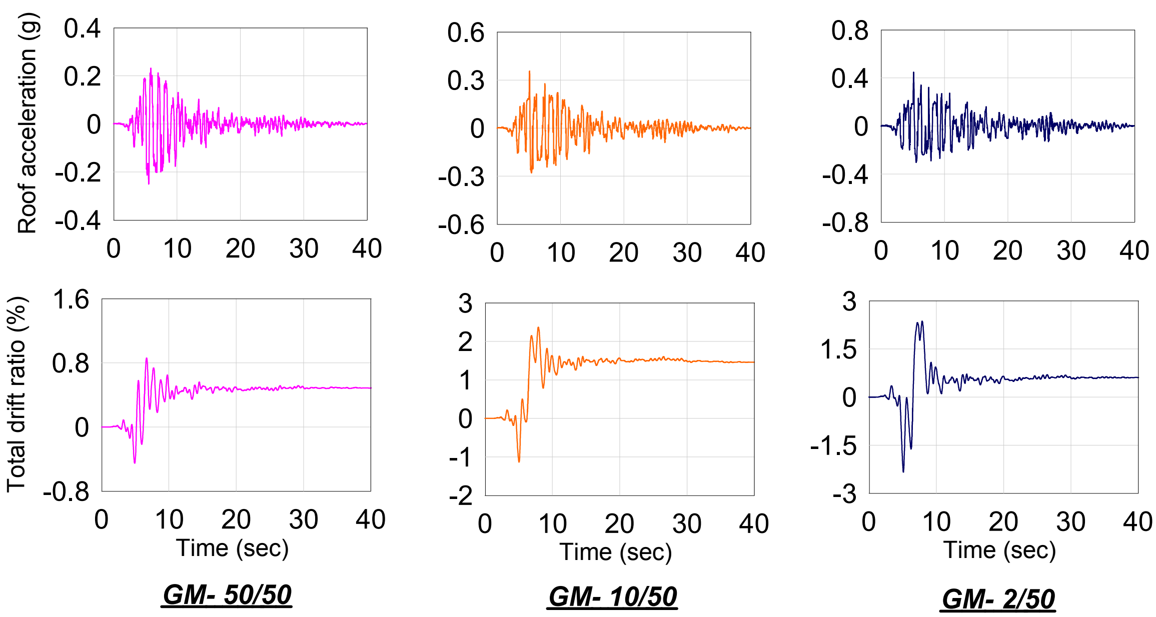

(b) CIM model

Fig 4.15 Structural response for 4-story building: (a) BNWF model (b) CIM model.

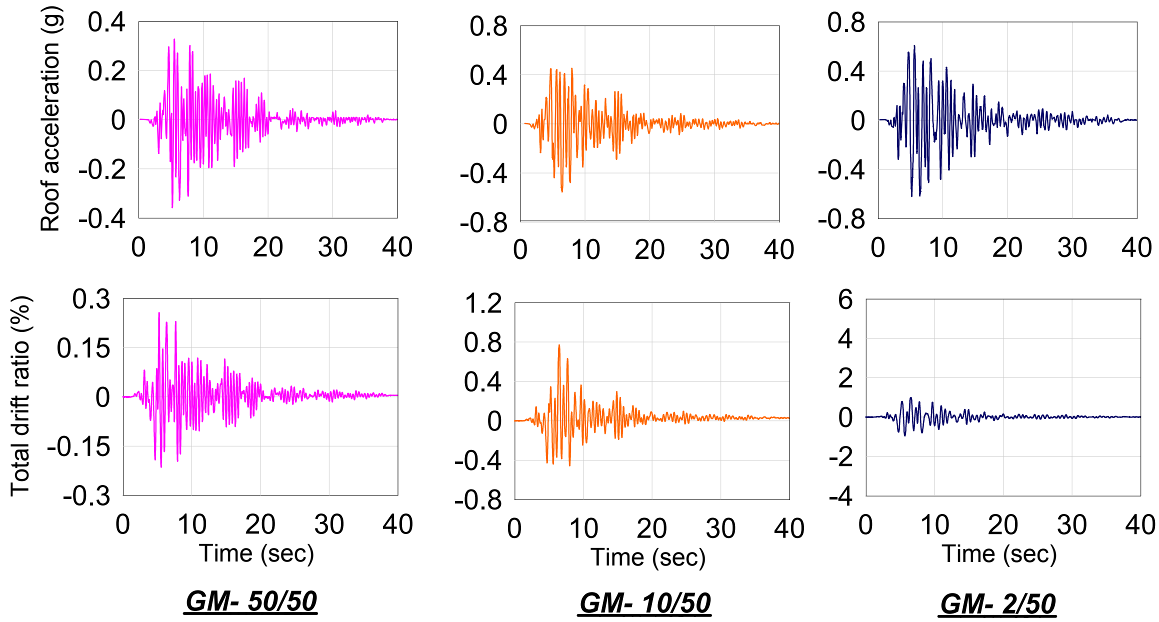

(a) BNWF model

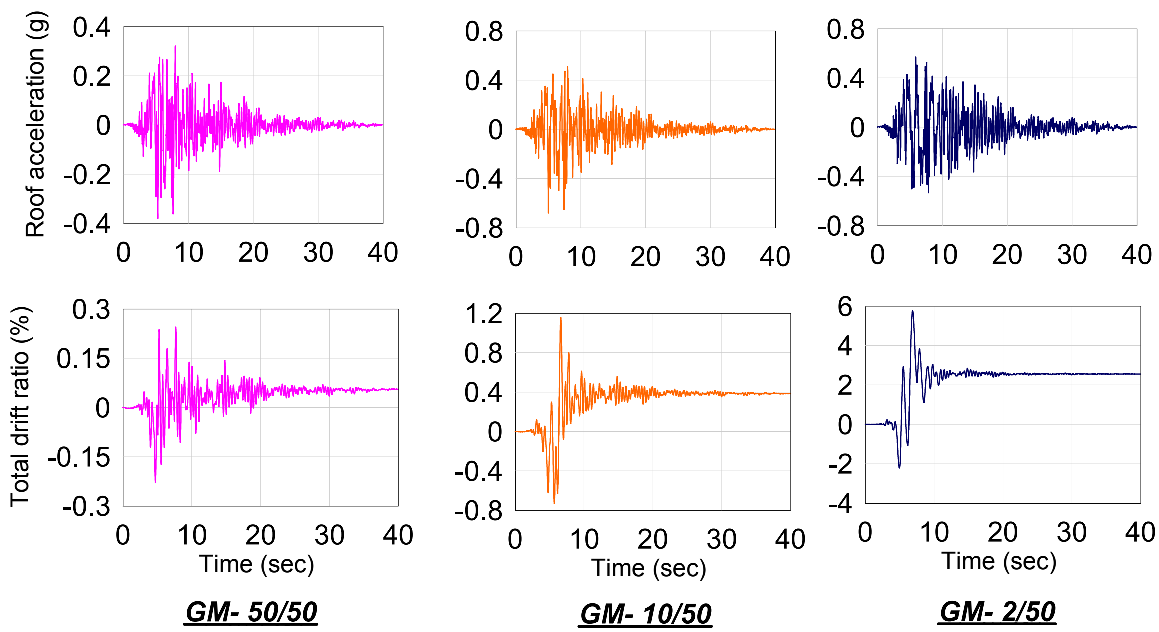

(b) CIM model

Fig 4.16 Structural response for 1-story building: (a) BNWF model (b) CIM model.

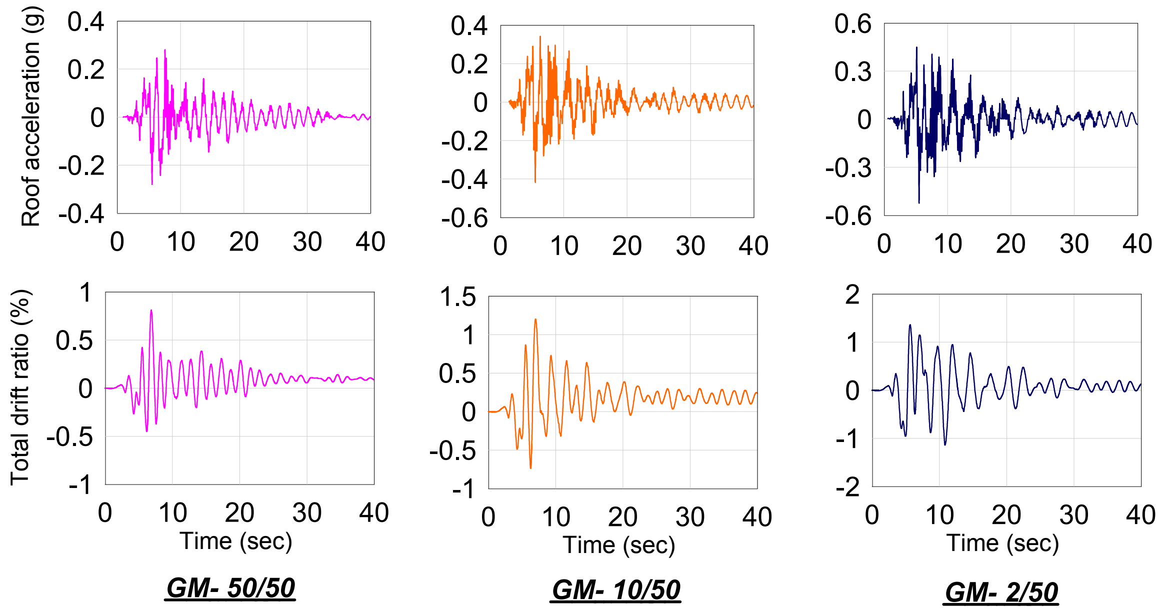

(a) BNWF model

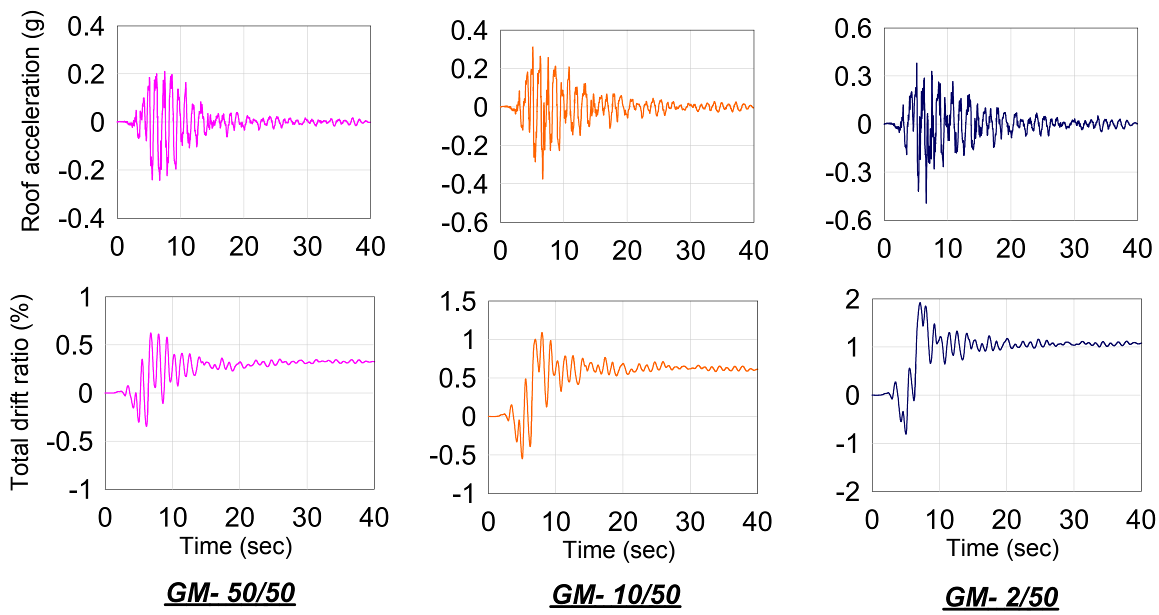

(b) CIM model

Fig 4.17 Structural response for 5-story building: (a) BNWF model (b) CIM model.

4.3.5 Ground Motion Analysis for Models with Coupled Footings

The analysis is extended for a case where the foundation of the building has a large shear capacity and stiffness, approximately restraining the building against sliding. This might be expected when individual spread footings for wall and columns are interconnected by grade beams possibly combined with slab-on-grade foundations. This is a common foundation configuration in California practice, which tends to produce large horizontal stiffness and capacity. Permanent horizontal displacements of foundations during earthquakes are very rare, and the few reported cases involve soil softening from liquefaction (e.g., Bray and Stewart 2000). Therefore, we increase the shear capacity and horizontal stiffness to account for this effect and the simulations are repeated. The shear capacity has been increased from 3.32 MN to 26 MN and the horizontal capacity from 750 MN/m to 1800 MN/m. These values are obtained from the shear capacity and stiffness associated with the full foundation dimensions of the building.

The analysis results considering these modifications for the four-story building are shown in Figure 4.18 for the mid-range ground motion (10%-in 50-years hazard level). For comparison, the modeling results for the uncoupled foundation are overlain in the same format in Figure 4.19. It is apparent that although there are still differences in terms of the responses of the footings, and particularly the maximum settlements predicted by the two models (the BNWF model calculates typically about half of the settlements from CIM), the BNWF and CIM predictions are much closer for the coupled foundation case. This occurs because the increased shear capacity is not exceeded by either model for the coupled foundations.

Figure 4.20 shows the results for all three models (four-, one-, and five-story) for the mid-range ground motion. Again, the BNWF and CIM results are relatively similar.

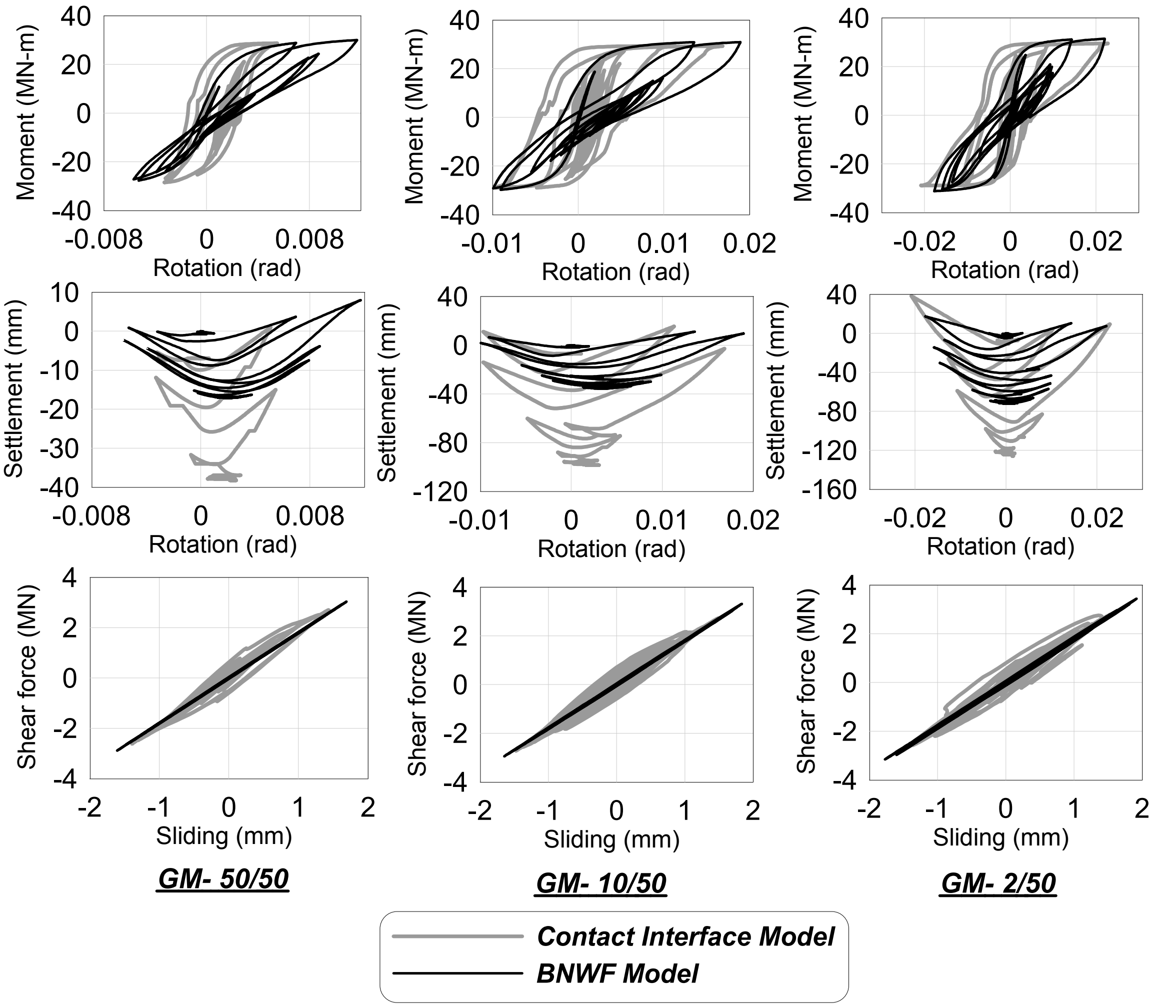

Fig 4.18 Comparison of model results for 4-story building (increased V_x and K_x).

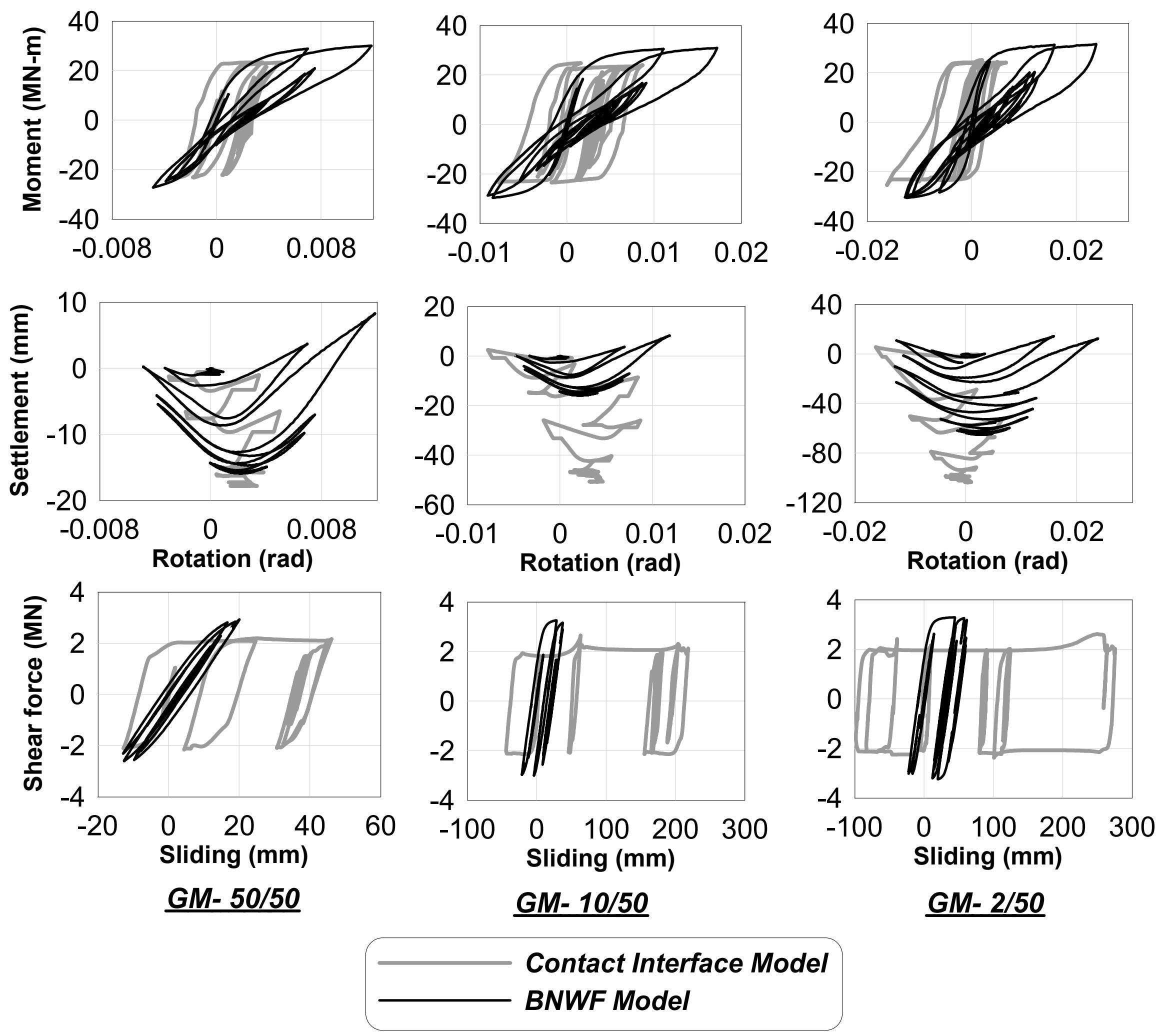

Fig 4.19 Comparison of model results for 4-story building (original K_x and V_x).

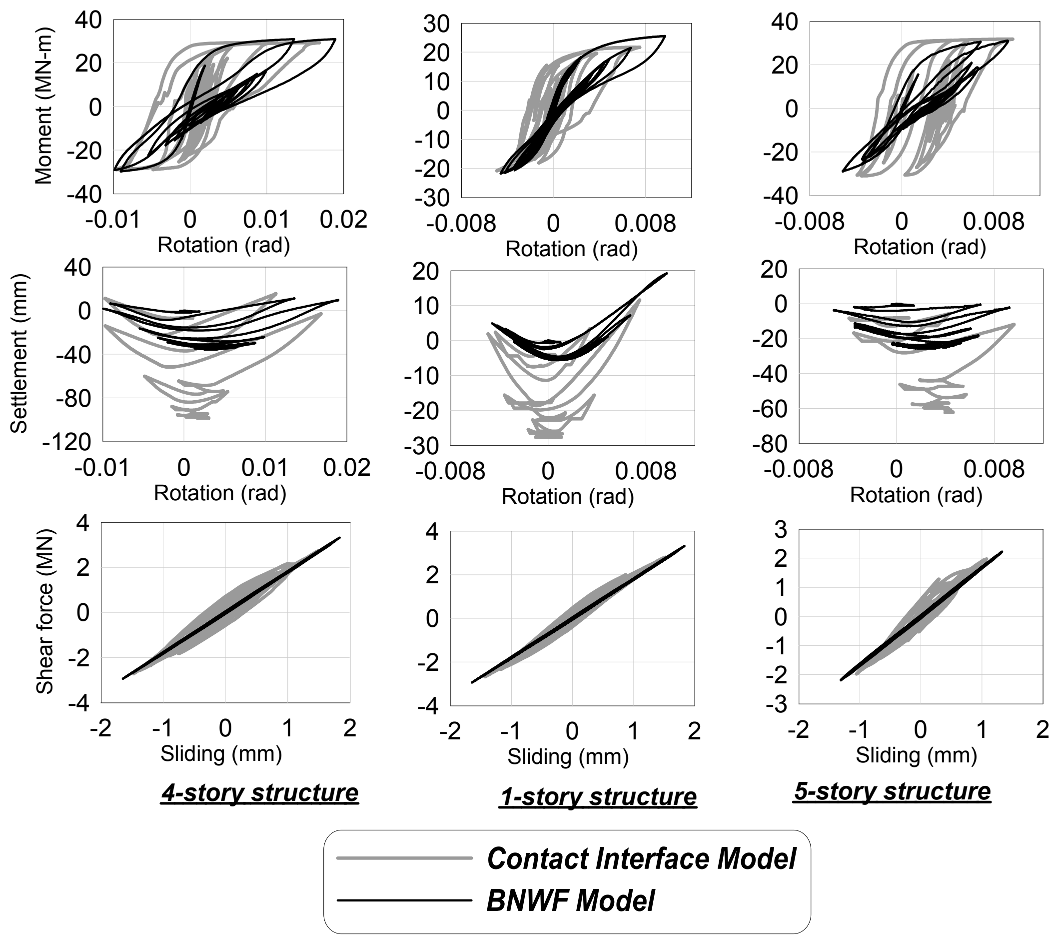

Fig 4.20 Comparison of results for GM-10/50 ground motion (increased V_x and K_x).

4.4 SUMMARY

In this chapter, the OpenSees simulations for typical shear wall structures supported by shallow foundations resting on clayey soil are presented. The simulations are carried out using both the beam on nonlinear Winkler foundation (BNWF) model and the contact interface model (CIM). The properties of the structure (height and weight) and the loading conditions (pushover, slow cyclic, and dynamic) were varied to consider the effects of moment/shear ratio, and inertial effects. The goals of this exercise are to gain insight into the significance of some of the different modeling assumptions contained in the BNWF and CIM models on the computed responses. Both models are capable of predicting the nonlinear responses of moment-rotation, settlement-rotation, and shear-sliding. The following are the similarities and differences observed during these comparisons:

- Small-displacement rotational and shear stiffness are comparable for both models. While initial shear stiffness is a direct input parameter for both models, the initial rotational stiffnesses vary as described in Section 4.3.1. Nonetheless, the flexible-base first mode periods estimated by the two models are generally within 10% of each other. The flexible-base periods estimated by both models agree reasonably well with the theoretical values obtained from expressions provided by Veletsos and Meek (1974).
- Both numerical models indicate that energy is dissipated at the footing-soil interface for the input motions and case study models considered. Both the BNWF and CIM model predictions indicate more energy dissipation through the rocking mode than through the sliding mode for the four and five story buildings. Energy dissipation through the sliding mode becomes more significant for the shorter building (one story).
- The moment and shear capacities predicted by both the BNWF and CIM model agree reasonably well in general, except for the shorter structure. The CIM prediction of the maximum moment of the 1 story structure is about 20% smaller than that of BNWF, due to the lack of coupling between the moment and the shear behavior of the BNWF model.
- The computed footing rotations during dynamic shaking are similar for the BNWF and CIM models. Settlement estimates are generally larger for the CIM model (up to a factor of 2), as compared with the BNWF model.
- Sliding displacement predictions by the CIM model are generally larger than those of the BNWF model, particularly for the shorter structure. This may be attributed to the lack of moment-shear coupling in the BNWF model, which results in a higher shear capacity.
- When the models are restrained against sliding, the general shape and amplitude of the moment-rotation and shear-sliding responses of the models are much more comparable. However, permanent settlements of the CIM model were still observed to be up to twice that of the BNWF model.

5 Validation against Centrifuge Test Data

5.1 VALIDATION AGAINST TESTS ON SHEAR WALL FOOTINGS

5.1.1 Centrifuge Tests on Shear Walls

A series of centrifuge experiments on shear wall structures with shallow footings were conducted at the UC Davis NEES facility. Figure 5.1 shows the experiment configuration inside the model container with structural setups for different types of loading conditions and instrumentation.

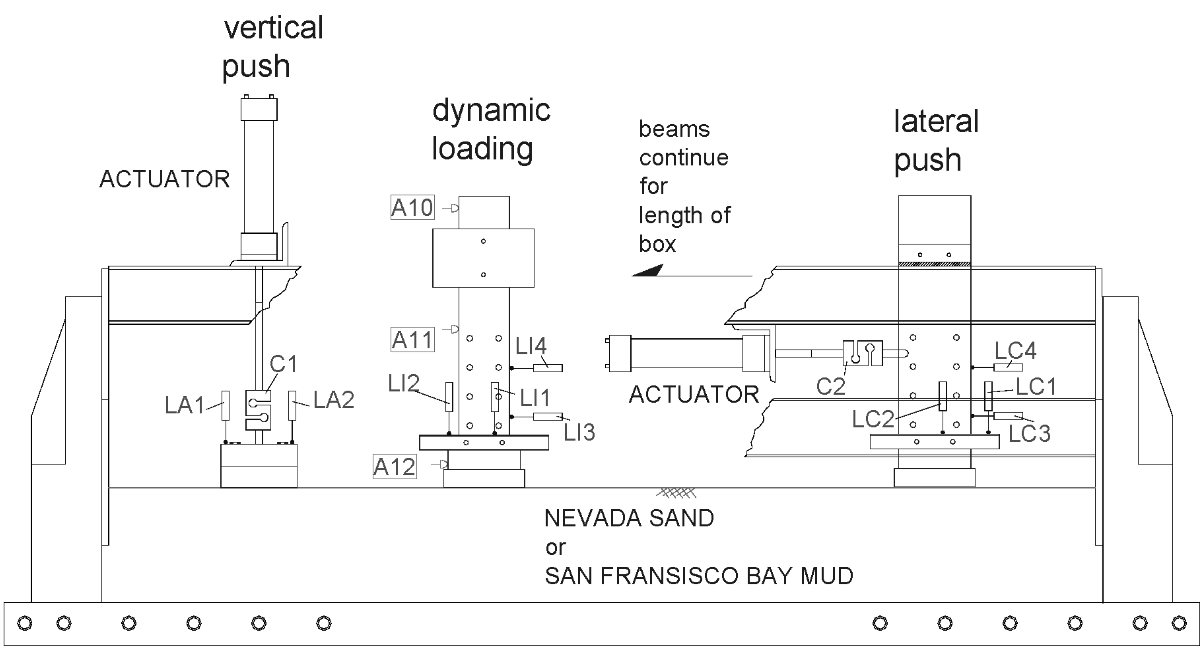

Fig. 5.1 Model container and experimental setup with instrumentation for vertical loading, slow lateral cyclic loading, and dynamic base shaking loading.

Each experiment included several shear wall–footing models tested under varying loading conditions. A variety of tests (slow lateral cyclic loading and dynamic base shaking loading) from these experiments covering a range of important parameters were chosen for validation of the OpenSees simulation tools. The structures at a specific station were tested during a given spin; the centrifuge was spun until the centrifugal acceleration normal to the sand surface was 20 g and the loading events were applied Experimental results are available for all the tested models in data reports (e.g., Gajan et al., 2003). Unless otherwise indicated, the model configurations and all the experimental results are presented using prototype-scale units in this document.

Figure 5.2 shows the geometry of the selected shear wall–footing structures, the instrumentation installed on the models, and the loading methods used in the experiments. The model structures consisted of an essentially rigid steel or aluminum shear wall with a rigid footing. The footing dimensions were length L = 2.8 m, width B = 0.65 m, and depth of embedment D = 0 or B. Both dry sand and overconsolidated clay foundation soils were used. The sand material used is Nevada Sand, which is uniform and fine-grained with a mean grain size of D_{50} = 0.17 mm. The sand was air pluviated to prepare the sand beds with relative density Dr=80%. The peak friction angle corresponding to Dr = 80% Nevada Sand is 42^o. The clay used in the experiments is San Francisco Bay Mud (PL = 35 ~ 40 and LL 88 ~ 93). The San Francisco Bay Mud was mixed with water and saturated to a water content of about 150%. Then the remolded clay was overconsolidated in a large press prior to centrifuge testing so that the strength variation with depth would be nominal. Assuming a uniform clay strength with depth, the undrained shear strength is back-calculated from static vertical bearing capacity to be c_u = 100 ± 10 kPa. This value is also consistent with Torvane shear tests and unconfined compression tests conducted on samples of the clay.

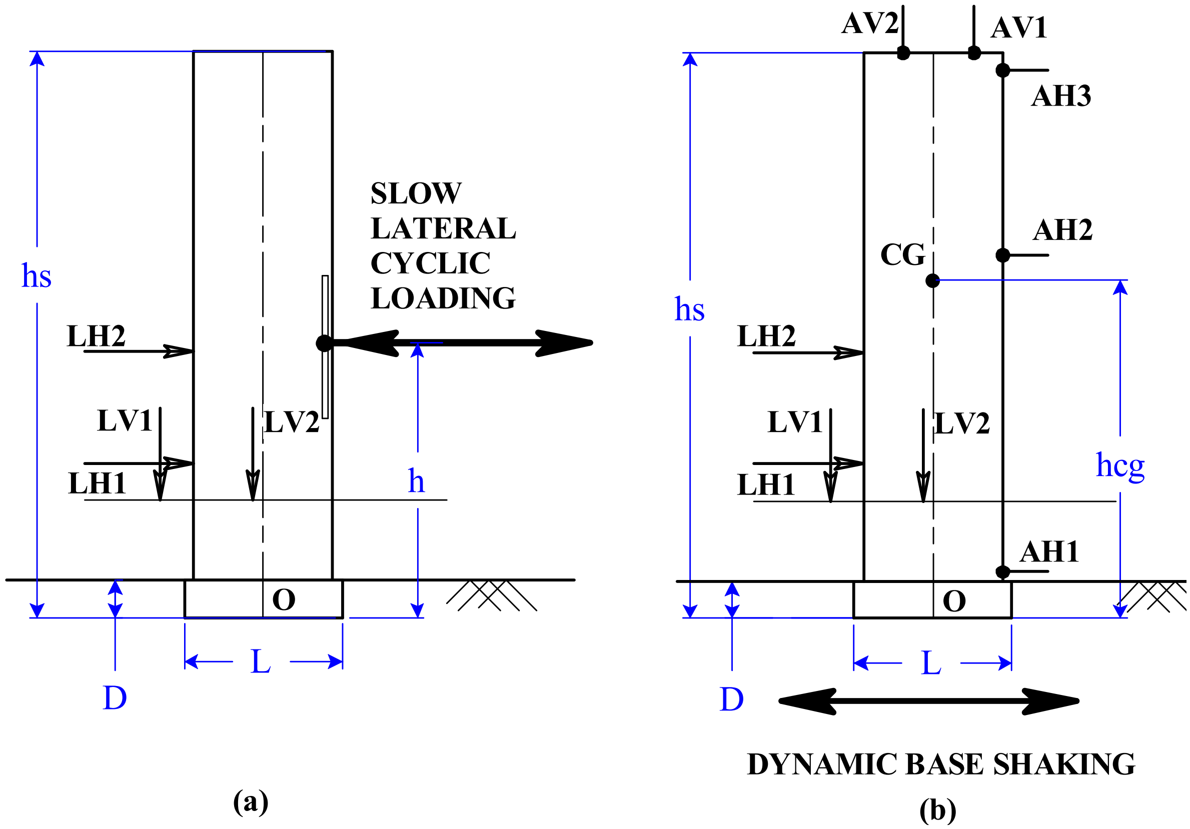

Fig. 5.2 Geometry, instrumentation, and loading methods for shear wall–footing structures tested in centrifuge experiments: (a) slow lateral cyclic tests and (b) dynamic base shaking tests.

The shear wall–footing structures were subjected to three types of loading: slow vertical loading to measure bearing capacity (not discussed further here), slow lateral cyclic loading by an actuator, and dynamic base shaking. The period of slow lateral cyclic loading was about 20 minutes and the clay strength is assumed to be governed by the undrained shear strength. The actuator and base shaking were both aligned in the direction of the long footing dimension, L. As shown in Figure 5.1, the actuator was fixed in the model container at the desired height. A pin and clevis attachment through a slot in the wall allowed the building to settle, slide, and rotate as the horizontal load was applied in slow lateral cyclic loading. The out of plane movement of the structure was limited by sliding Teflon bearing supports near the top of the shear wall. The supports were carefully placed to preclude binding. Theoretically, the lateral force on the Teflon is zero if the walls are perfectly aligned with the direction of loading. The supports were only required for stability. Due to known imperfections in the alignment, the lateral normal loads are estimated to be less than 1% of the vertical load, and the coefficient of friction is approximately 0.1, hence the moment error due to the Teflon friction is less than about 0.8% for the range of vertical loads used in the experiments.

The slow lateral cyclic tests were performed under displacement control. Hence, the displacement histories were applied as sinusoidal cycles and the forces required to produce those displacements were measured by a load cell attached to the actuator. The amplitude, the frequency, and the number of cycles varied slightly from test to test. Four linear potentiometers (LV1, LV2, LH1, and LH2), fixed at known locations (two in the vertical direction and two in the horizontal), were used to measure the displacements of the footing. The contact points of the linear potentiometers were allowed to slide along the structure during rigid body translation. Those data were used to calculate the settlement, sliding, and rotation at the base center point of the footing (indicated as "O" in Fig 5.2).

The instrumentation for dynamic base shaking tests included two vertical and two horizontal linear potentiometers (LV1, LV2, LH1, and LH2) to measure displacements and three horizontal and two vertical accelerometers (AH1, AH2, AH3, AV1, and AV2) to measure accelerations. Accelerometers were also placed at the base of the container, inside the soil and near the ground surface in the free-field. Note that the accelerometer contact points were fixed on the structure, whereas linear potentiometers were allowed to slide. The applied shaking histories consisted of tapered sinusoidal displacements, which were designed to produce different peak base accelerations (0.2 g, 0.5 g, and 0.8 g). The procedures used to calculate forces, moments, and dynamic and permanent translations and rotations of the structures using these sensors are described in Gajan et al. (2003) and Gajan (2006).

Tables 5.1 and 5.2 present the details of the centrifuge experiments used for verification of numerical analyses in this document. The factor of safety for static vertical loading (FS_V) was calculated based on the weight of the structure, and bearing capacity. Normalized moment to shear ratio [$M/(H \cdot L)$] is the normalized height of lateral loading (h/L) in slow lateral cyclic tests. The normalized heights of center of gravity (h_{cg}/L) are given in Table 5.2 for structures subjected to dynamic base shaking tests.

Table 5.1 Details of shear wall–footing structures used in slow lateral cyclic tests.

Test number	Mass (Mg)	Soil type	L (m)	B (m)	D/B	FS_V	$M/(H \cdot L)$
SSG04_06	68	Sand, Dr = 80%	2.8	0.65	0	2.3	1.20
SSG03_02	58	Sand, Dr = 80%	2.8	0.65	0	2.6	0.45
SSG02_05	58	Sand, Dr = 80%	2.8	0.65	0	2.6	1.72
SSG02_03	28	Sand, Dr = 80%	2.8	0.65	0	5.2	1.75
SSG03_03	28	Sand, Dr = 80%	2.8	0.65	1	14.0	1.77
KRR03_02	36	Clay, Cu = 100 kPa	2.7	0.65	0	2.8	1.80

Table 5.2 Details of shear wall–footing structures used in dynamic base shaking tests.

Test number	Mass (Mg)	Soil Type	L (m)	B (m)	D/B	FS_V	hcg/L
SSG04_10	36	Sand, Dr = 80%	2.8	0.65	0	4.0	1.80
SSG03_07	58	Sand, Dr = 80%	2.8	0.65	1	7.2	1.80
KRR03_03	36	Clay, Cu = 100 kPa	2.7	0.65	0	2.8	1.70

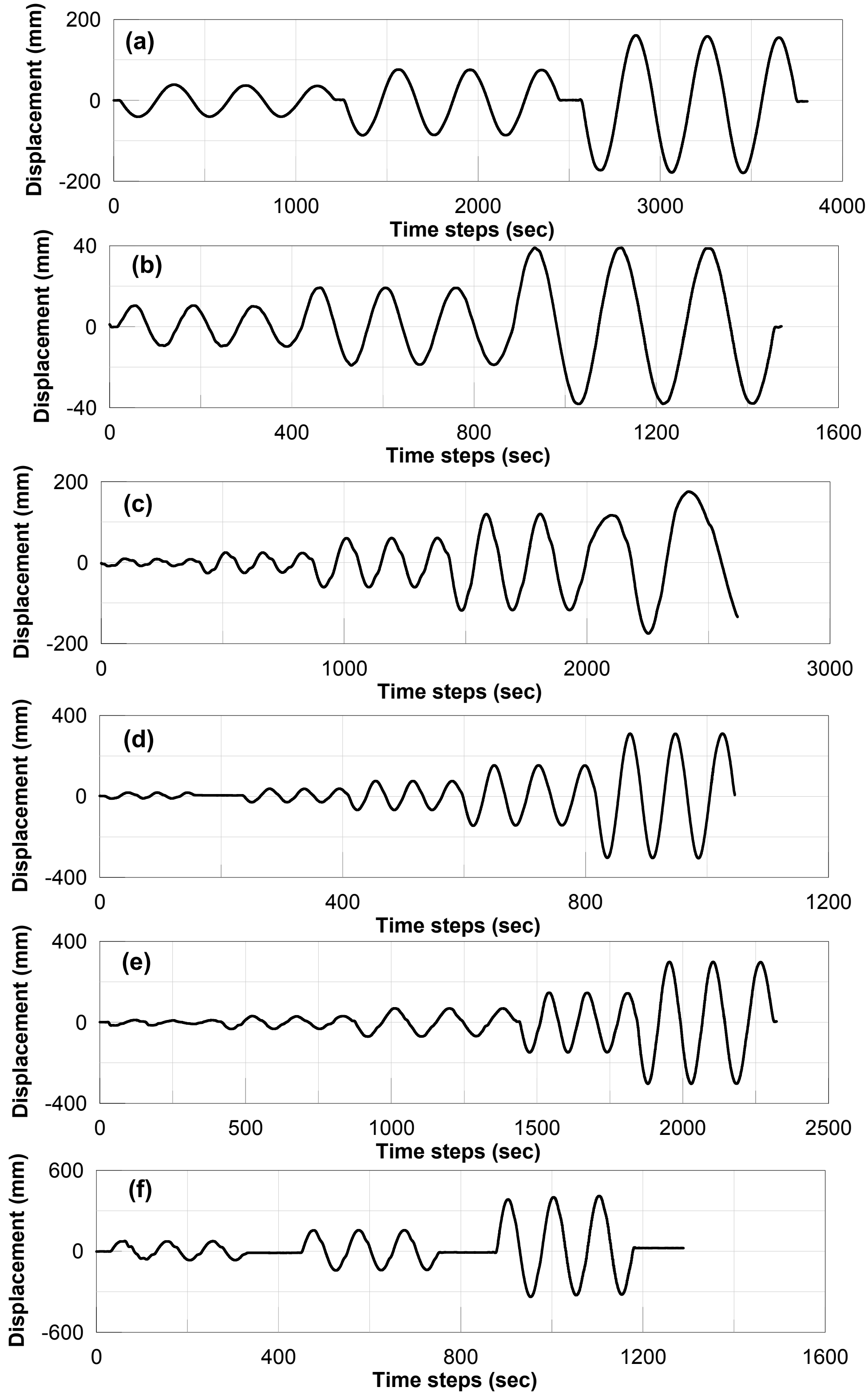

Fig. 5.3 (a) Horizontal input displacements for static lateral tests: (a) SSG04_06, (b) SSG03_02, (c) SSG02_05, (d) SSG02_03, (e) SSG03_03, (f) KRR03_02.

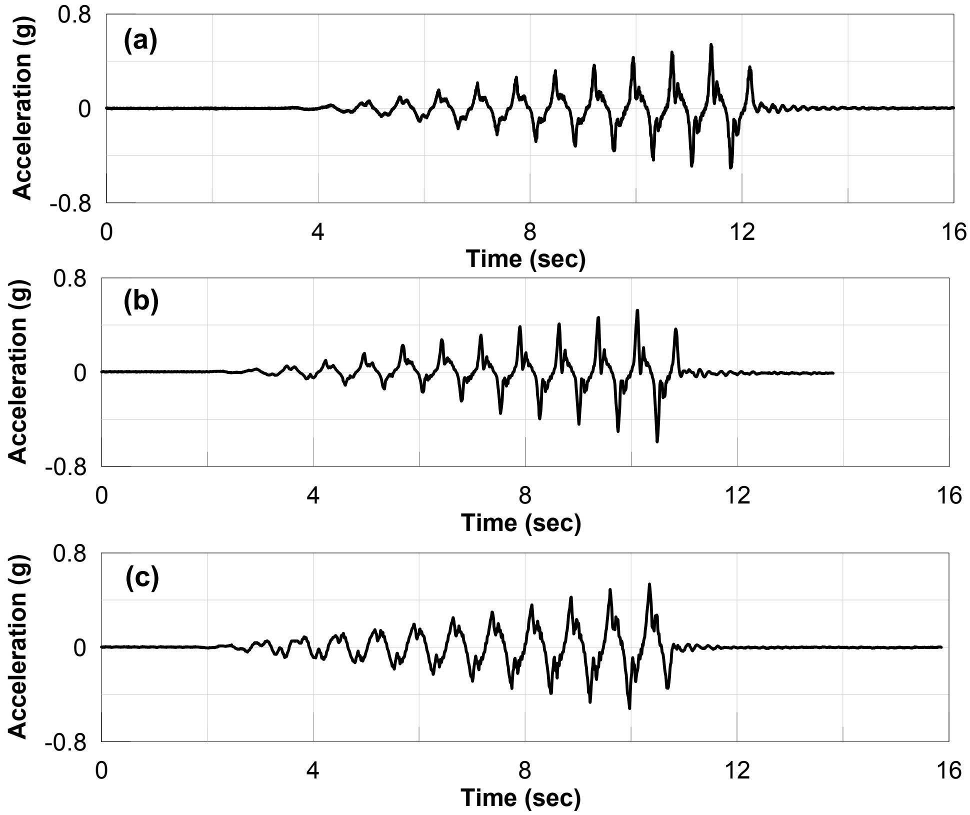

Fig. 5.3 (b) Input acceleration for dynamic tests: (a) SSG04_10, (b) SSG03_07, (c) KRR03_03.

Figure 5.3a presents the measured displacement histories from the slow lateral cyclic tests. Figure 5.3b shows the acceleration histories measured near the ground surface in the free-field. In the simulations that follow, the displacement histories in Fig 5.3a and the acceleration histories in Fig 5.3b represent the input demand.

5.1.2 Numerical Modeling of Experiments

(a) BNWFSimulation Results

BNWF models are constructed of each shear wall–footing specimen listed in Tables 5.1 and 5.2. The basic model geometry is shown in Figure 5.4. Namely, an elastic beam-column element is used to model the stiff shear wall having a defined Young's modulus, area, and moment of inertia. Note that there is only one superstructure node at the top of the model. The BNWF foundation mesh and associated input parameters are selected based on the protocols described in

Chapter 2. Specifically, qzMaterial, pyMaterial, and tzMaterial springs are specified as zero length elements (denoted "zeroLengthElement" in OpenSees) that are attached to footing nodes. One node of each zeroLengthElement is fixed in x, y, and θ degrees of freedom, while the other is connected to the beam-column elements used to represent the structural footing.

Table 5.3 summarizes the user input properties for developing the BNWF models for each experiment. Note that bearing capacity is calculated internally within the BNWF mesh code based on the weight and factor of safety given in Table 5.3. Vertical and horizontal stiffness is calculated using the equations of Gazetas (1991) in Table 2.1.

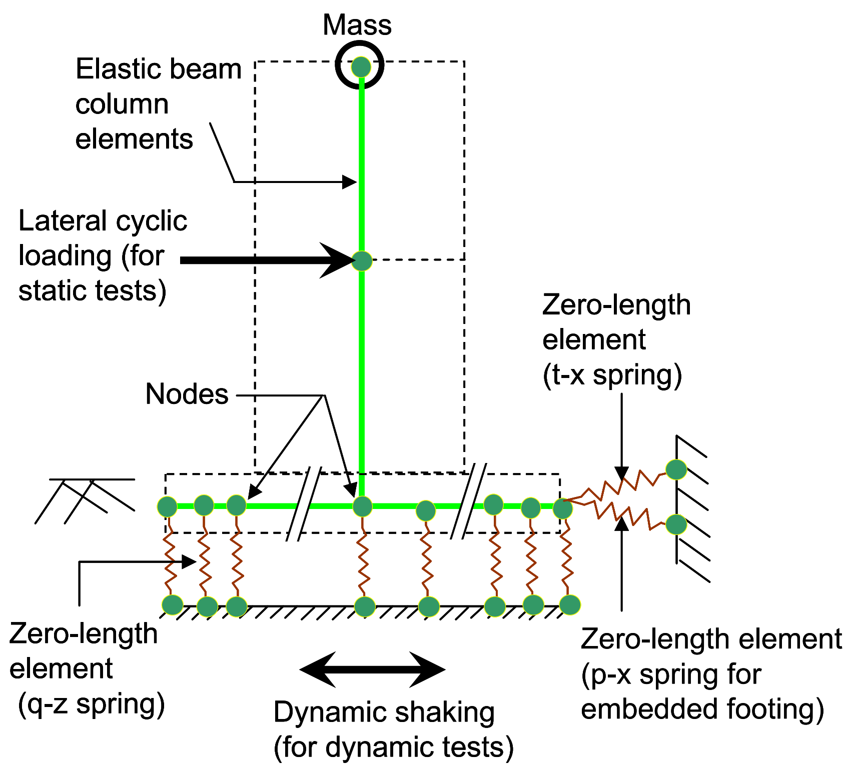

Fig. 5.4 OpenSees idealization of shear wall–footing system for BNWF modeling.

Loading begins with the application of model self-weight in the vertical direction at the superstructure node under load control. Slow lateral cyclic loading is applied as displacement histories at the superstructure node. Dynamic base shaking is applied as free-field accelerations input to the base of the wall-footing model (at the laterally fixed spring node). The superstructure node in this case is positioned at the superstructure center of mass. The Newmark integrator and

Newton algorithm are used to perform the dynamic nonlinear calculations, and recorders monitor the forces, the displacements, and the accelerations of the models.

Figures 5.5–5.13 compare the BNWF simulation results with the experimental data. Figures 5.5–5.10 pertain to the slow cyclic tests, whereas Figures 5.11–5.13 pertain to the dynamic base shaking tests. The relationships presented are moment-rotation, settlement-rotation, shear force-sliding, and settlement-sliding, with simulation results in black and experimental data in gray.

Table 5.3 User input parameters for BNWF models developed for each centrifuge experiment case summarized in Tables 5.1 and 5.2.

Parameters	SSG04_06	SSG03_02	SSG02_05	SSG02_03	SSG03_03	KRR03_02	SSG04_10	SSG03_07	KRR03_03
Input loading	Actuator disp	Actuator disp	Actuator disp	Actuator disp	Actuator disp	Actuator disp	Surface acc	Surface acc	Surface acc
L (m)	2.8	2.8	2.8	2.8	2.8	2.8	2.8	2.8	2.8
B (m)	0.65	0.65	0.65	0.65	0.65	0.65	0.65	0.65	0.65
Df (m)	0	0	0	0	0.65	0	0	0.65	0
FSv	2.3	2.5	2.6	5.2	14	2.8	4	7.2	2.8
E (MPa)	45	45	45	45	45	40	45	45	40
ν	0.4	0.4	0.4	0.4	0.4	0.5	0.4	0.4	0.5
c_{rad} (%)	5	5	5	5	5	5	5	5	5
TP (%)	10	10	10	10	10	10	10	10	10
L_{end}/L (%)	10	10	10	10	10	10	10	10	10
Rk	2.5	2.5	2.5	2.5	2.5	2.5	2.5	2.5	2.5
le/L (%)	2	2	2	2	2	2	2	2	2

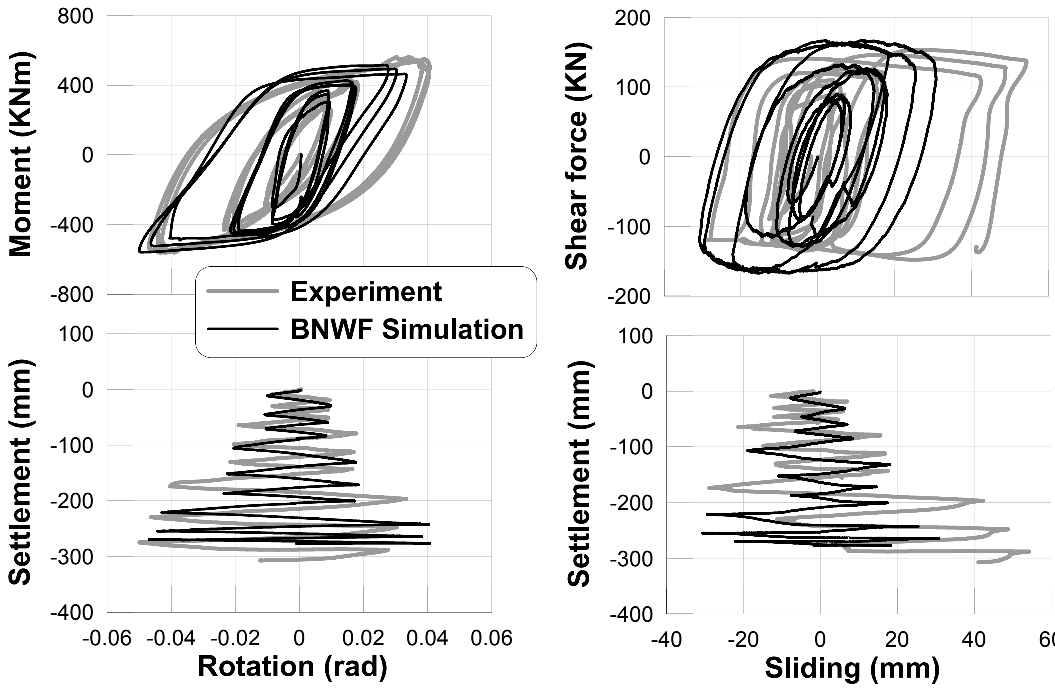

Fig. 5.5 Comparison of footing response for BNWF simulation and SSG04_06 centrifuge test.

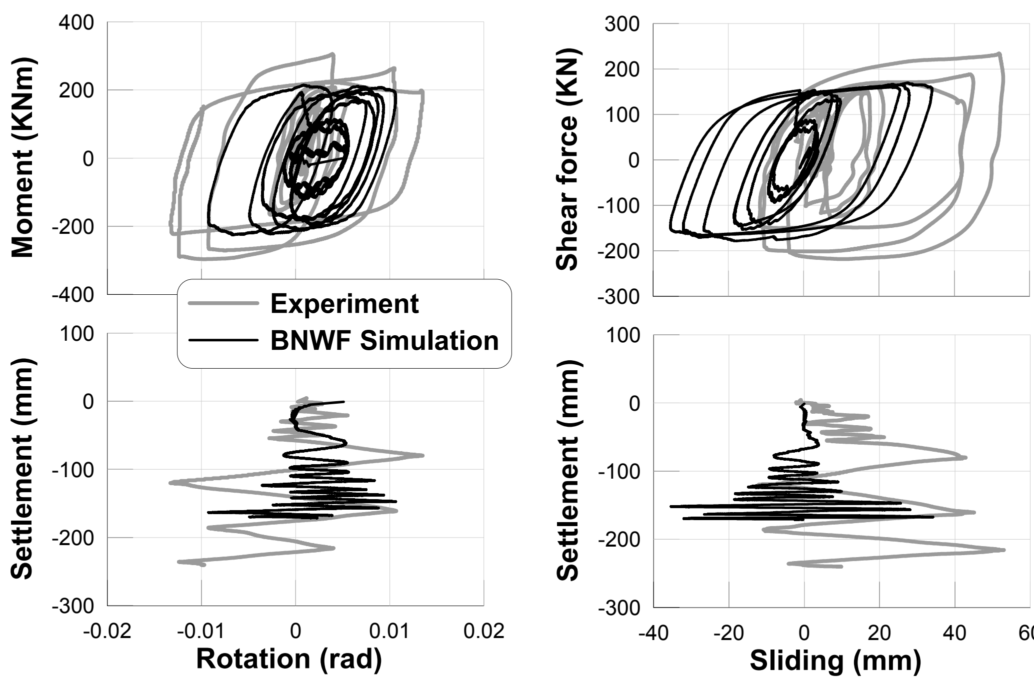

Fig. 5.6 Comparison of load-deformation behavior of footing for BNWF simulation and SSG03_02 centrifuge test (Dr = 80%, FS_v = 2.5, M/(H×L) = 0.45).

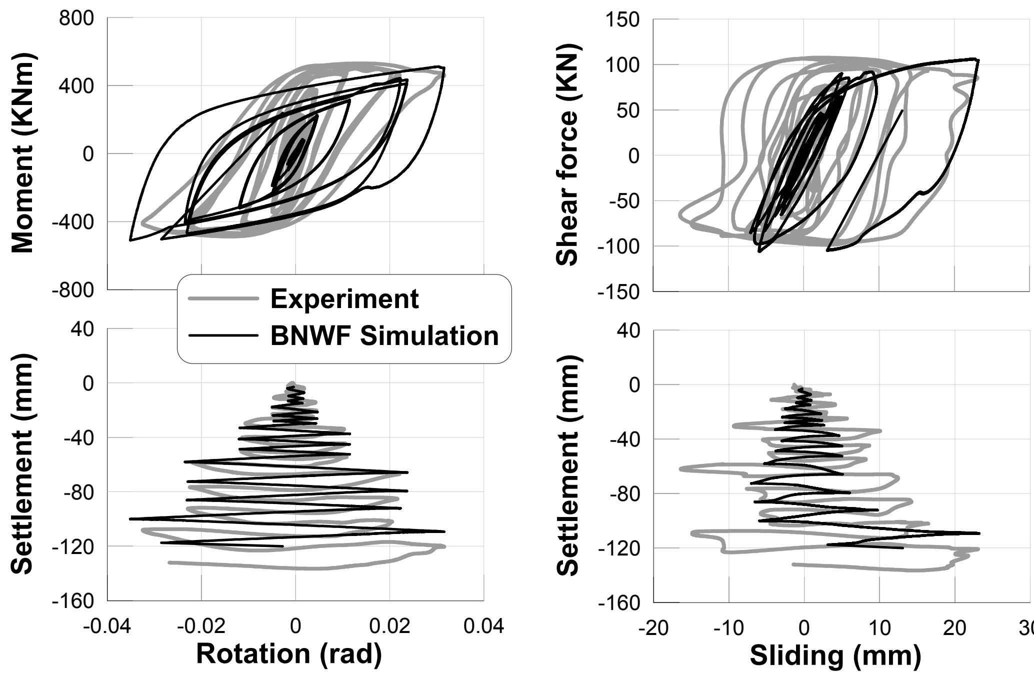

Fig. 5.7 Comparison of load-deformation behavior of footing for BNWF simulation and SSG02_05 centrifuge test (Dr = 80%, FS_v = 2.6, M/(H×L) = 1.72).

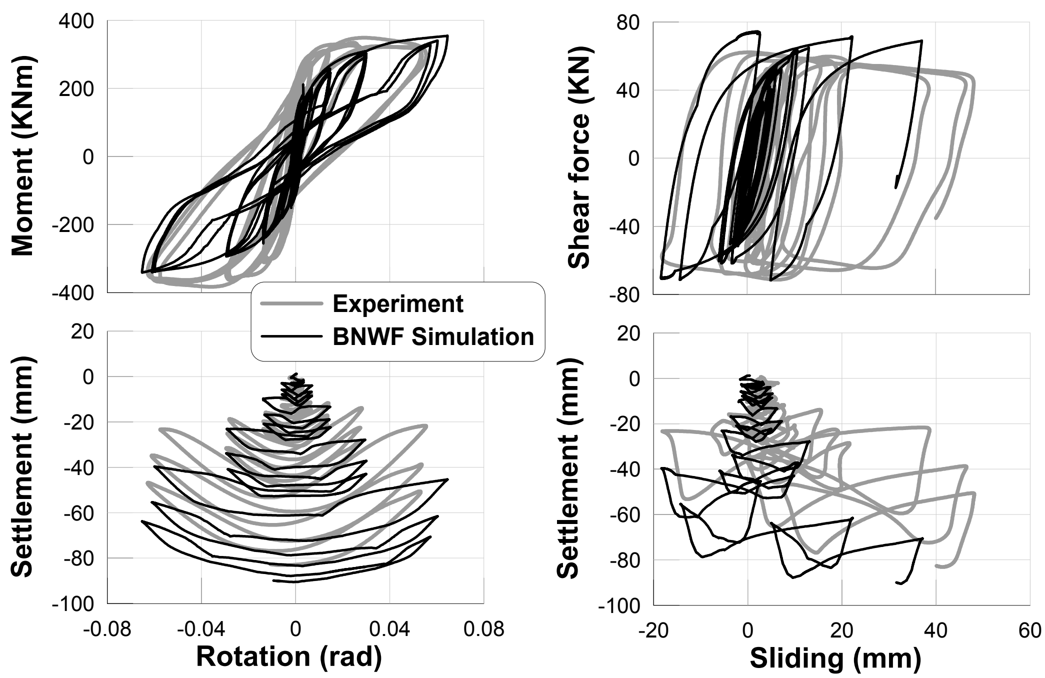

Fig. 5.8 Comparison of load-deformation behavior of footing for BNWF simulation and SSG02_03 centrifuge test (Dr = 80%, FS_v = 5.2, M/(H×L) = 1.75).

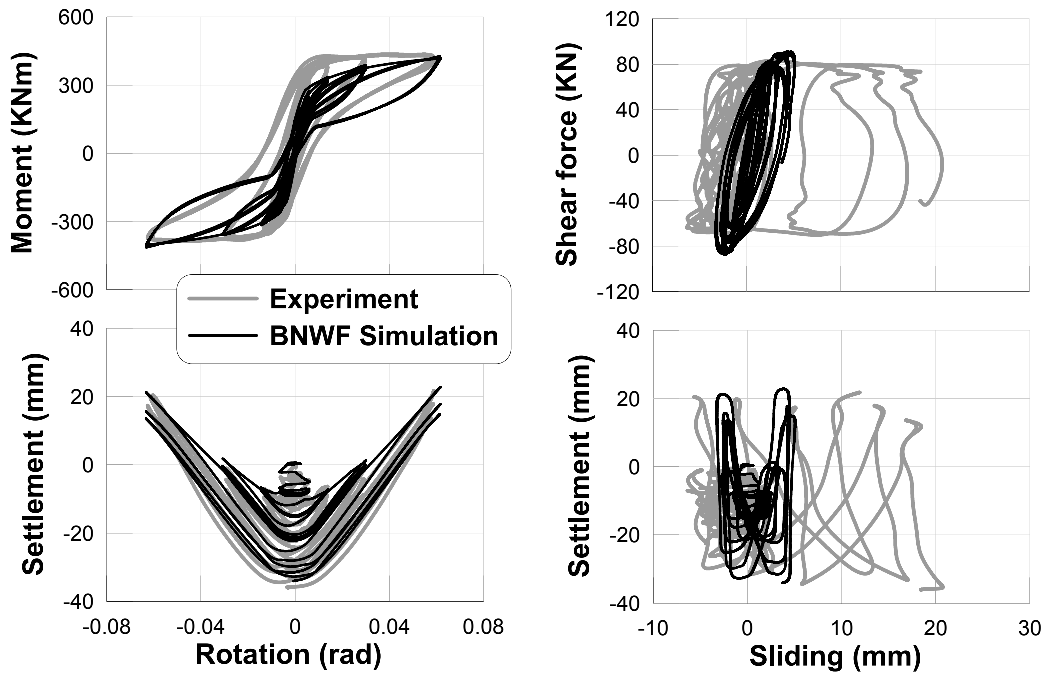

Fig. 5.9 Comparison of load-deformation behavior of footing for BNWF simulation and SSG03_03 centrifuge test (Dr = 80%, FS_v = 14.0, M/(H×L) = 1.77).

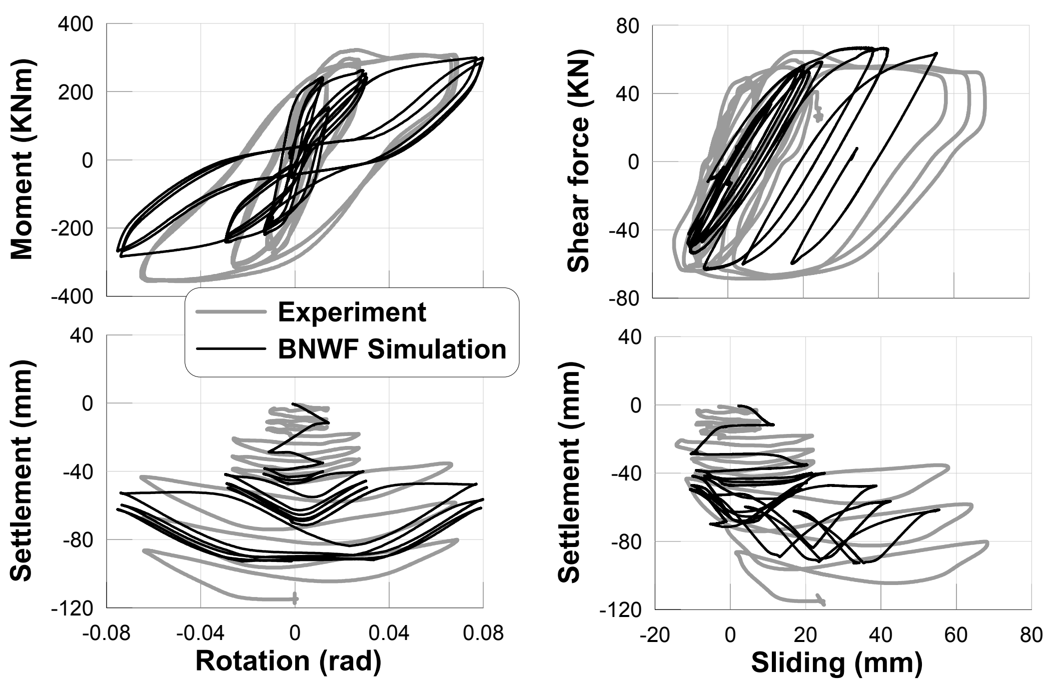

Fig. 5.10 Comparison of load-deformation behavior of footing for BNWF simulation and KRR03_02 centrifuge test (Cu=100 KPa, FS_v = 2.8, M/(H×L) = 1.80).

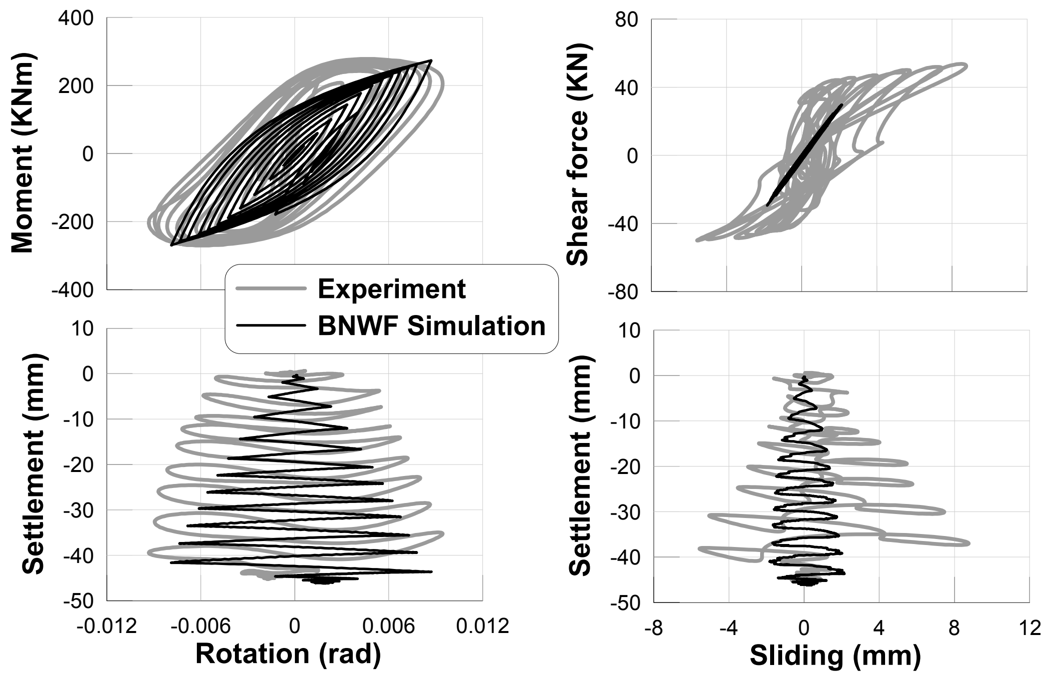

Fig. 5.11 Comparison of load-deformation behavior of footing for BNWF simulation and SSG04_10 centrifuge test (Dr = 80%, FS_v = 4.0, M/(H×L) = 1.80).

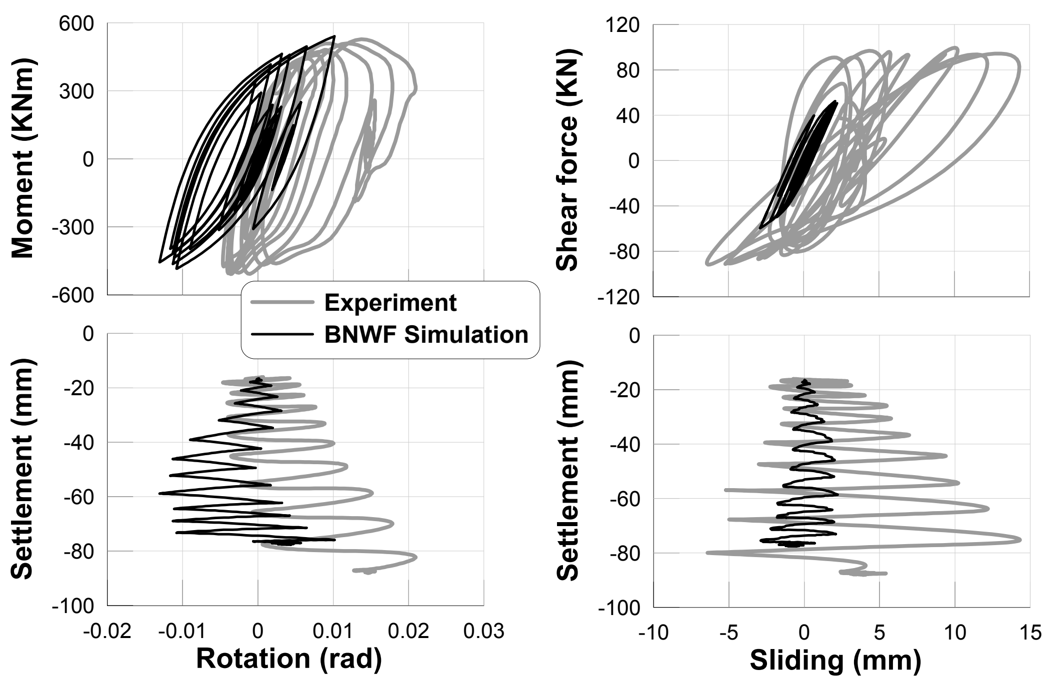

Fig. 5.12 Comparison of load-deformation behavior of footing for BNWF simulation and SSG03_07 centrifuge test (Dr = 80%, FS_v = 7.2, M/(H×L) = 1.80).

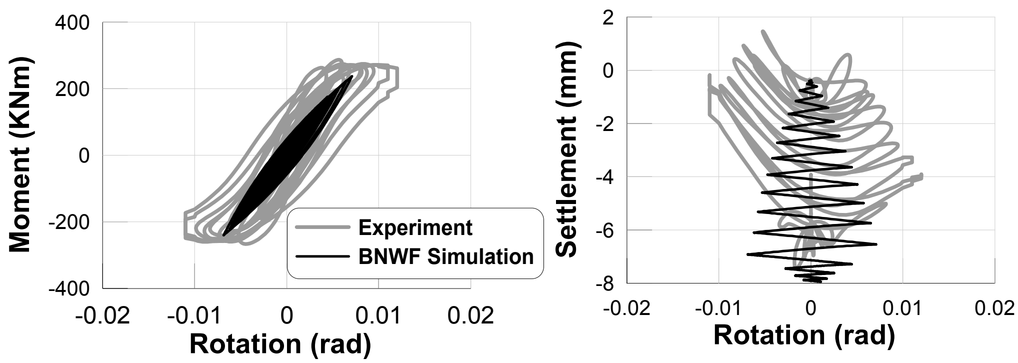

Fig. 5.13 Comparison of load-deformation behavior of footing for BNWF simulation and SSG04_10 centrifuge test (Cu = 100 KPa, FS_v = 2.8, M/(H×L) = 1.70).

(b) Interpretation of BNWF Simulation Results

Effect of M/(HL) Ratio: The geometry of the test specimens SSG04_06, SSG03_02, and SSG02_05 are similar with the exception of the M/(H×L) ratio, which ranges from low (0.45) to high (1.72). The design vertical factors of safety are nearly three (FSv~3.0), which is reasonable for realistic structures. Comparing the results in Figures 5.5–5.7, we observe that the model consistently captures the maximum measured moment and shear, with the exception of the lowest M/(H×L) model (Fig. 5.6, M/(H×L) = 0.45). In that case the experimental moment and shear demands are approximately 30% higher than the simulation results. The general shapes of the predicted hysteresis loops (unloading and reloading stiffness and fullness of the loops) are reasonably predicted, as are the settlement-rotation and settlement-sliding relationships. However, again the lowest M/(H×L) model has misfit.

As shown in Fig 5.6, for the low M/(H×L) model BNWF predicts large initial settlement with smaller settlements in subsequent cycles, whereas the data contain initially small cycles of settlement per rotation cycle. In addition, the maximum and the residual sliding are not fully captured for the low M/(H×L) model. The asymmetric shear-sliding response observed in the experiment may be due to slight asymmetry of the connection of the wall to the actuator.

Effect of FSv: The results in Figures 5.7–5.9 compare the results for models with varying vertical factors of safety (FSv = 2.6, 5.2, and 14, respectively). The vertical factor of safety is modified by either increasing the mass (Fig. 5.7) or embedding the footing (Fig. 5.8). These plots show that the shapes of the experimental moment-rotation histories become increasingly pinched as FSv increases, while the settlement-rotation histories become increasingly rounded. These attributes of the measured response are fairly well captured by the BNWF model. However, the model does not capture the asymmetric transient and permanent sliding response observed in the high FSv experiment (SSG03_03, Figure 5.9). Permanent settlement is calculated as approximately 5 mm for the experiment, where 18 mm was measured.

Effect of soil type: Tests SSG02_05 and KRR03_02 are similar except for the soil type, with the former resting on dense sand and the latter on clay. The results are shown in Figures 5.7 and 5.10, respectively. To maintain similar factors of safety, the mass of SSG02_05 is larger than that of KRR03_02. The clay model experiment shows an asymmetric moment demand (larger in the pull/negative direction), which is not captured by the model. This may be due to local modifications to the soil that could not be captured with a symmetric array of springs. Moreover, the model predicts a large initial settlement in the early cycles, whereas the experiment small settlements in the initial cycles. The peak permanent settlement is underestimated by approximately 18%, while the peak sliding is underestimated by approximately 21%. The model reasonably captures the rotational stiffness during the early cycles and the shear stiffness throughout the loading history.

Effects of loading rate: The effect of loading the models using dynamic base excitation versus slow cyclic loading can be evaluated by comparing SSG03_03 and SSG03_17 (Figs. 5.9 and 5.12, respectively) or KRR03_02 with KRR03_03 (Figs. 5.10 and 5.13, respectively). In each case, parameters other than the load rate are similar. Comparing the results for clay, much fatter hysteresis loops and larger settlement are observed the slow test (Fig. 5.10) than the fast test (Fig. 5.13). Comparing the results for sands, the slow test (Fig. 5.9) produces much more pinching in the moment-rotation response and greater shear sliding than in the fast test (Fig. 5.12). The shapes of the moment-rotation responses are completely different due to the lack of pinching in the dynamic tests. In both Figures 5.9 and 5.12, the BNWF model tends to underpredict the sliding response, and in each case the lack of shear capacity mobilization results in a nearly linear elastic shear-sliding response, therefore underpredicting the sliding displacements. A similar trend is observed in Figure 5.11, where the simulation maximum shear is approximately one half that of the experimentally determined shear capacity. The lack of shear capacity mobilization observed in the simulations presented in Figures 5.11 and 5.12 resulted in an 80 and 85% underprediction of the maximum sliding displacement.

The experimental results shown for the dynamic case in Figure 5.12 indicate that the model is ratcheting in the positive direction, whereas in the test the model moved in the negative direction. In comparing Figures 5.10 and 5.13, it should be noted that the peak rotation imposed on the model for the dynamic case is about one third of the rotation input for slow lateral cyclic loading (Fig. 5.13). Simulation results for the dynamic case SSG04_10 predict that the model does not mobilize moment capacity; therefore the moment-rotation histories are fairly thin in comparison with the data. Nonetheless, the maximum settlements and average settlement per cycle are similar.

(c) CIM Simulation Results

Figure 5.14 shows the CIM model for the shear wall–footing soil systems tested in the centrifuge. Since the shear wall is stiff compared to the soil, the shear wall is modeled using a single elastic beam-column element in OpenSees with a specified Young's modulus, cross-sectional area, and area moment of inertia (Gajan, 2006).

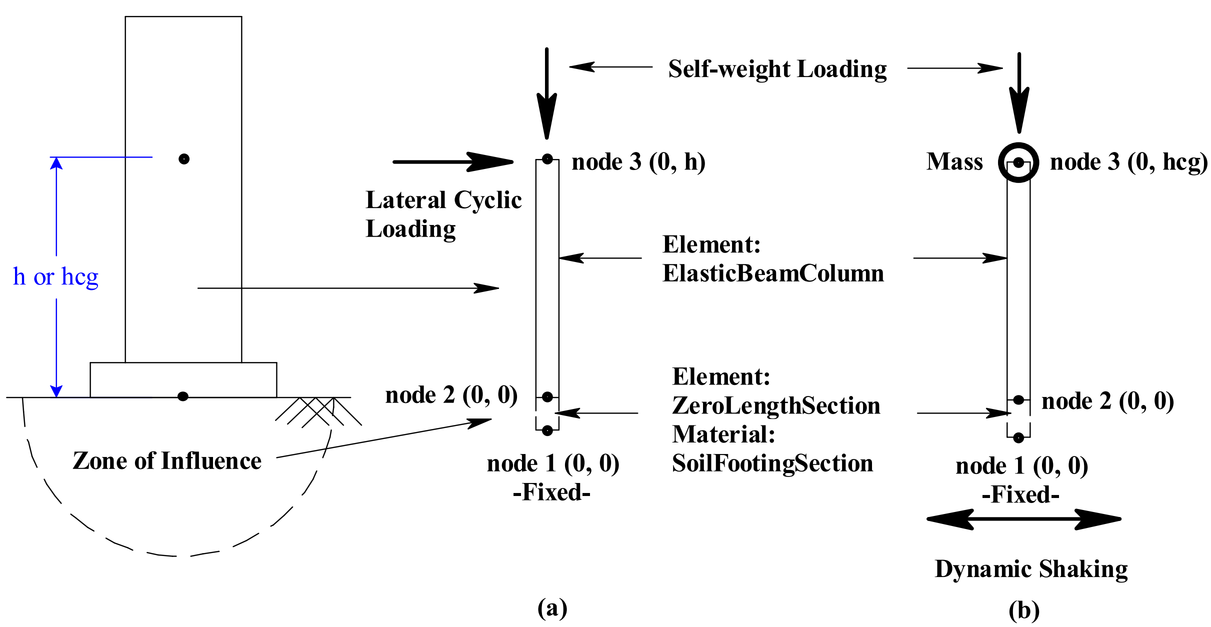

Fig. 5.14 OpenSees modeling of shear wall–footing soil system for (a) slow lateral cyclic tests and (b) dynamic base shaking tests.

The CIM model of the footing and the foundation soil is implemented as "SoilFootingSection2D" element in OpenSees. SoilFootingSection2D is used to relate stress resultants (forces and moments) to displacements. The SoilFootingSection2D material is used with a ZeroLengthSection element to represent the two-dimensional footing-soil interface that has three degrees of freedom (lateral displacement, vertical displacement, and rotation). The ZeroLengthSection element connects two nodes at the same location (nodes 1 and 2 in Fig. 5.14) with node 1 being fixed in all three degrees of freedom, while node 2 is allowed to settle, slide, and rotate. The bottom end of the elastic beam-column element is connected to the SoilFootingSection2D at node 2. The CIM input parameters are listed in Table 5.4. The definitions and descriptions of all the input parameters were presented in Chapter 3.

Table 5.4 Input parameters used for contact interface model analysis in OpenSees.

Parameter	SSG04_06	SSG03_02	SSG02_05	SSG02_03	SSG03_03	KRR03_02	SSG04_10	SSG03_07	KRR03_03
Input loading	Actuator disp.	Actuator disp.	Actuator disp.	Actuator disp.	Actuator disp.	Actuator disp.	Surface acc.	Surface acc.	Surface acc.
V_{ULT} (kN)	1500	1500	1500	1500	3850	985	1500	3850	985
L (m)	2.8	2.8	2.8	2.8	2.8	2.7	2.8	2.8	2.7
Kv (kN/m)	560	560	560	560	620	305	560	620	305
Kh (kN/m)	180	180	180	180	200	100	180	200	100
$\theta_{Elastic}$ (Rad.)	0.001	0.001	0.001	0.001	0.001	0.001	0.001	0.001	0.001
Rv (Ratio)	0.1	0.1	0.1	0.1	0.1	0.1	0.1	0.1	0.1
ΔL (m)	0.01	0.01	0.01	0.01	0.01	0.01	0.01	0.01	0.01

Initially the self-weight of the structure is applied at node 3 (Fig. 5.14) and the SoilFootingSection2D element is initialized based on this load and the foundation capacity. For simulations of slow lateral cyclic tests, input consists of the actuator displacement history applied at node 3. For simulations of dynamic base shaking, the total mass of the superstructure is attached at node 3 (which is positioned at the center of the mass of the shear wall–footing structure) and the measured free-field acceleration history is applied at the fully fixed node 1. The Newmark integrator and Newton algorithm in OpenSees are used for dynamic calculations. OpenSees recorders are used to record the acceleration of the structure, and the stress resultants and displacements at the base center point of the footing.

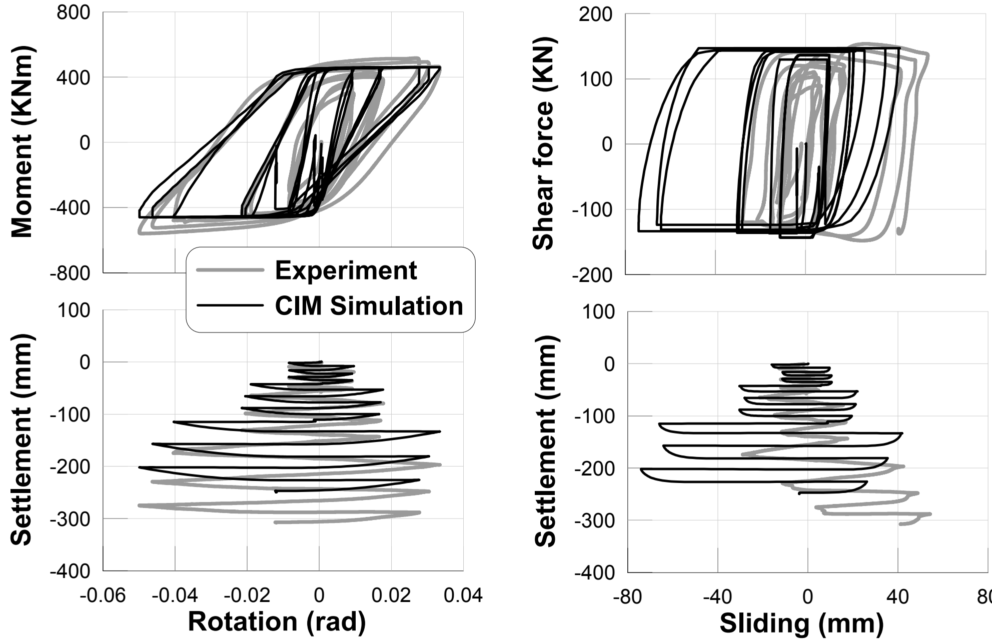

Fig. 5.15 Comparison of footing response for CIM simulation and SSG04_06 centrifuge test.

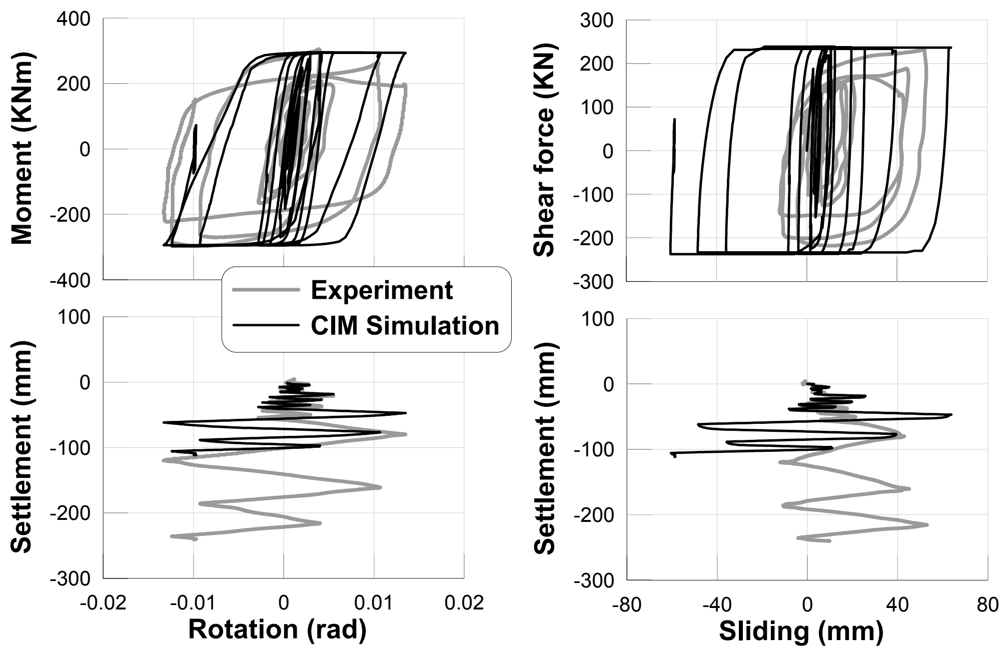

Fig. 5.16 Comparison of load-deformation behavior of footing for CIM simulation and SSG03_02 centrifuge test (Dr = 80%, FS_v = 2.5, M/(H×L) = 0.45).

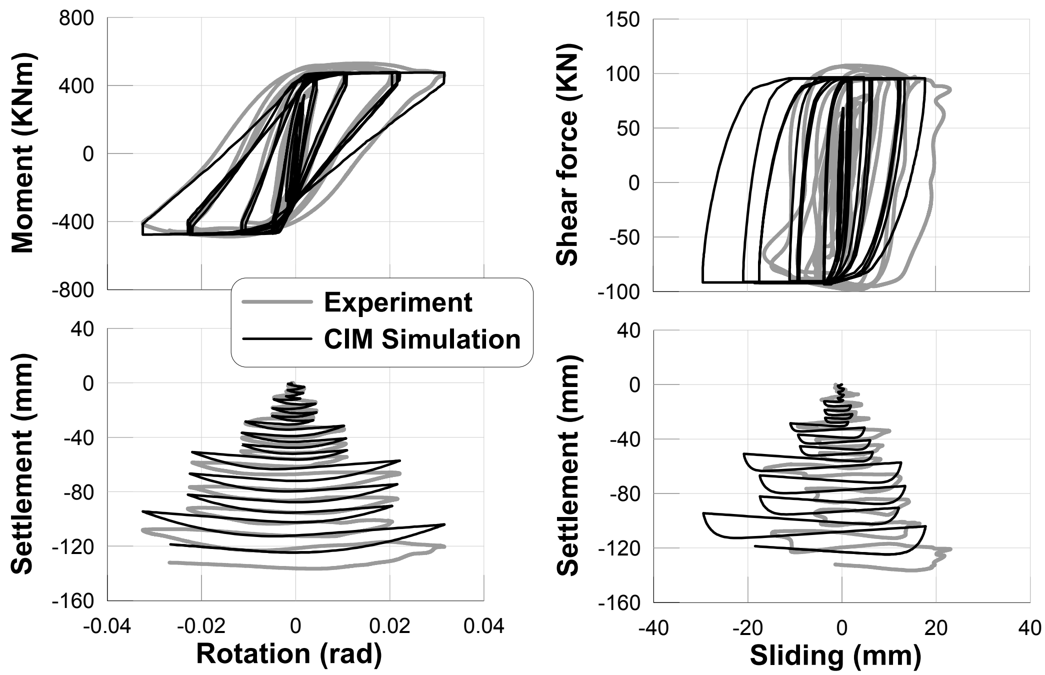

Fig. 5.17 Comparison of load-deformation behavior of footing for CIM simulation and SSG02_05 centrifuge test (Dr = 80%, FS_v = 2.6, M/(H×L) = 1.72).

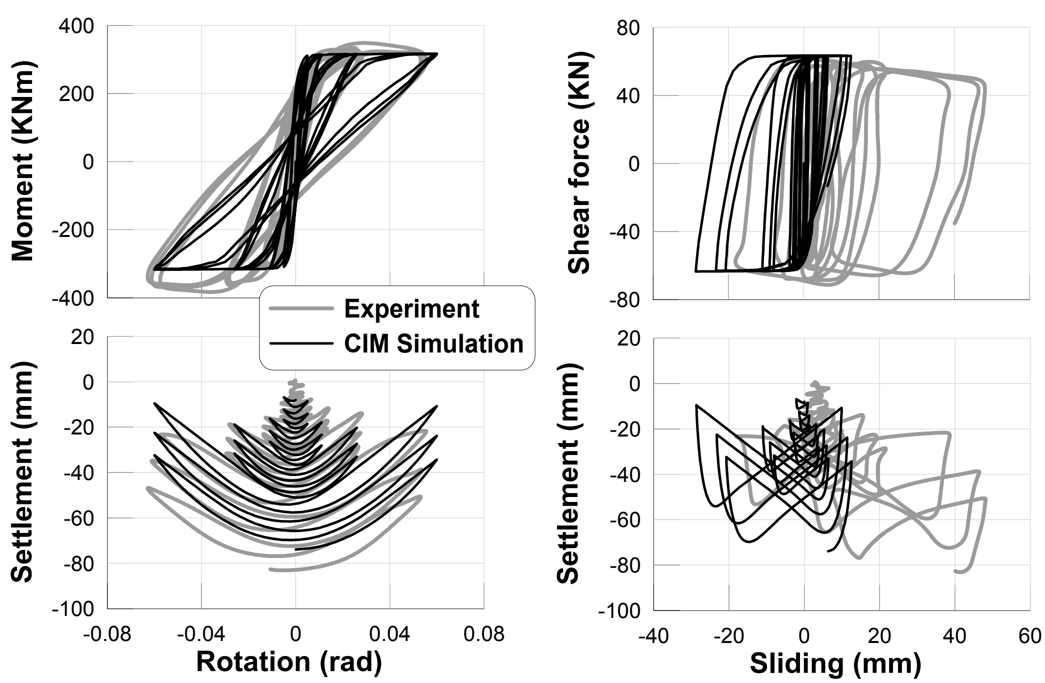

Fig. 5.18 Comparison of load-deformation behavior of footing for CIM simulation and SSG02_03 centrifuge test (Dr = 80%, FS_v = 5.2, M/(H×L) = 1.75).

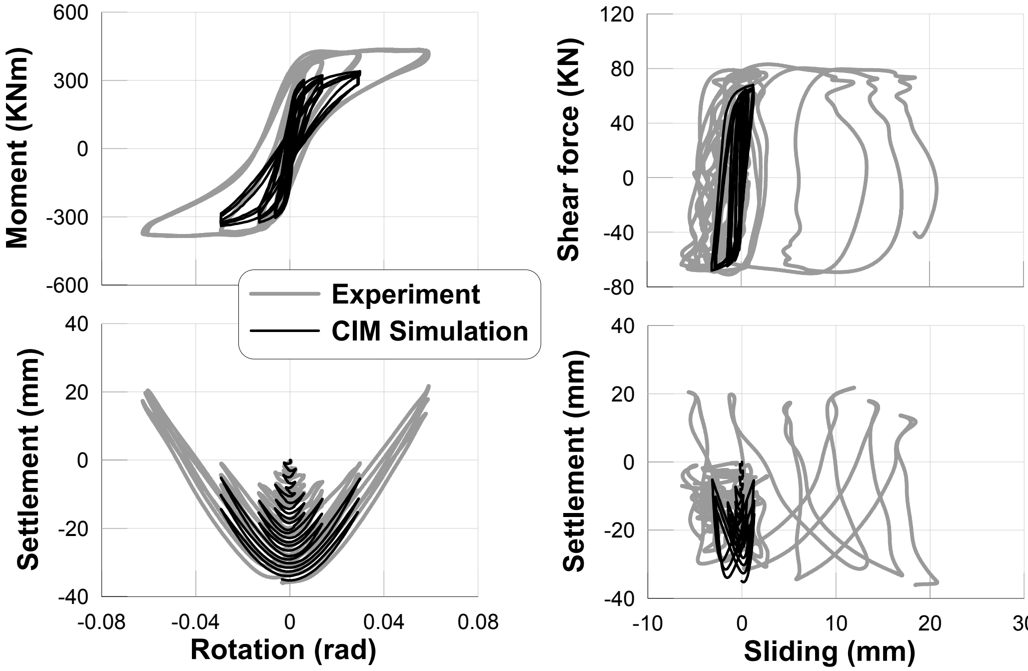

Fig. 5.19 Comparison of load-deformation behavior of footing for CIM simulation and SSG03_03 centrifuge test (Dr = 80%, FS_v = 14.0, M/(H×L) = 1.77).

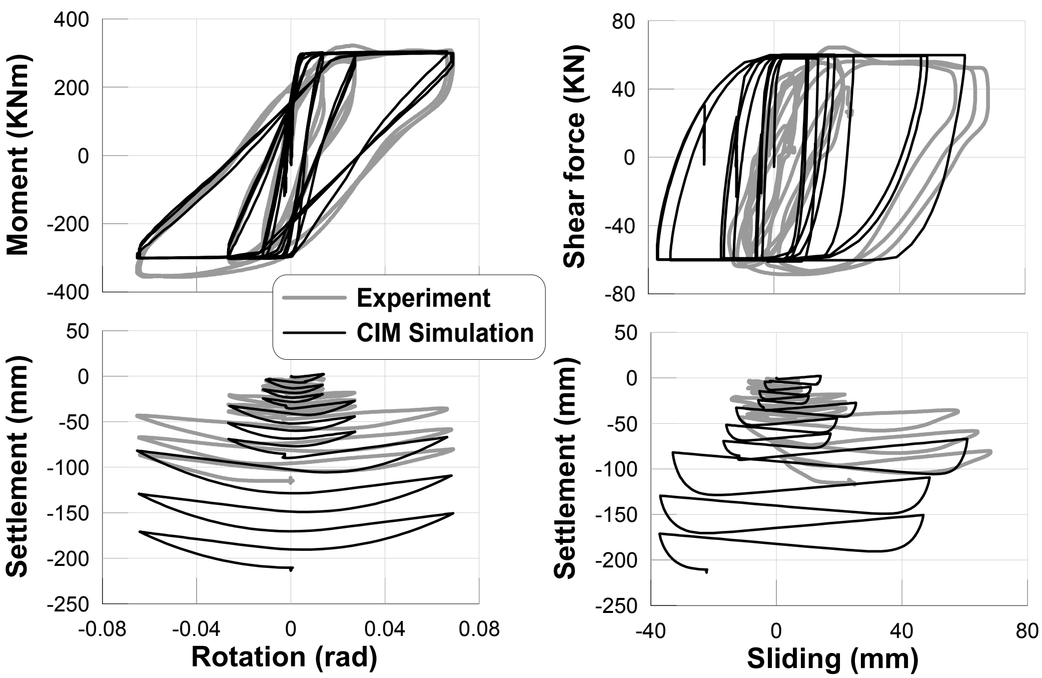

Fig. 5.20 Comparison of load-deformation behavior of footing for CIM simulation and KRR03_02 centrifuge test (Cu=100 KPa, FS_v = 2.8, M/(H×L) = 1.80).

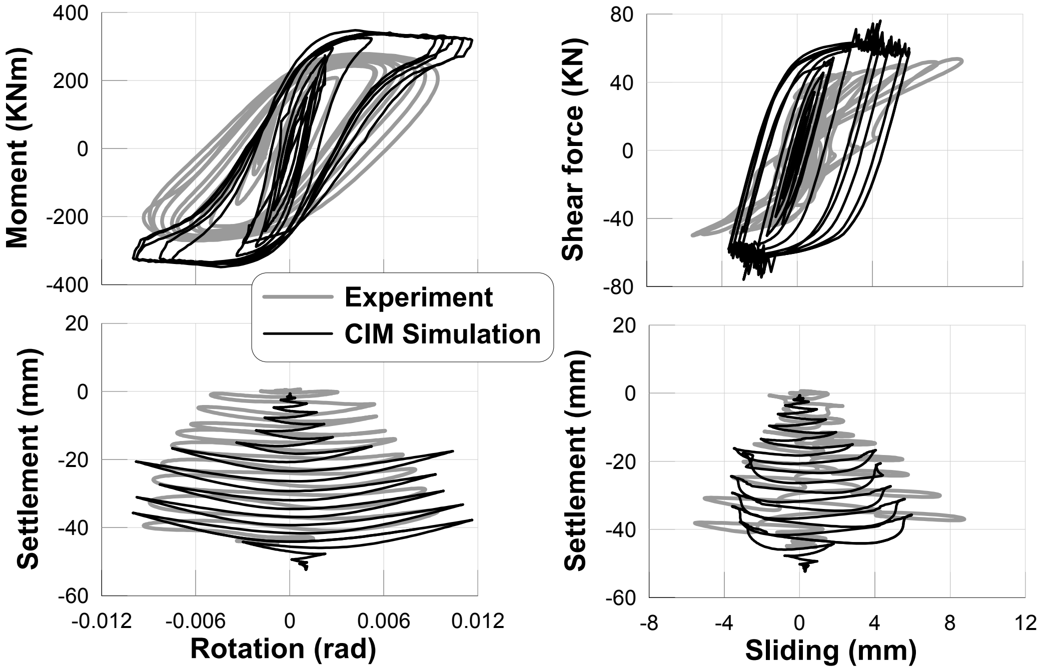

Fig. 5.21 Footing comparison of load-deformation behavior of footing for CIM simulation and SSG04_10 centrifuge test (Dr = 80%, FS_v = 4.0, M/(H×L) = 1.80).

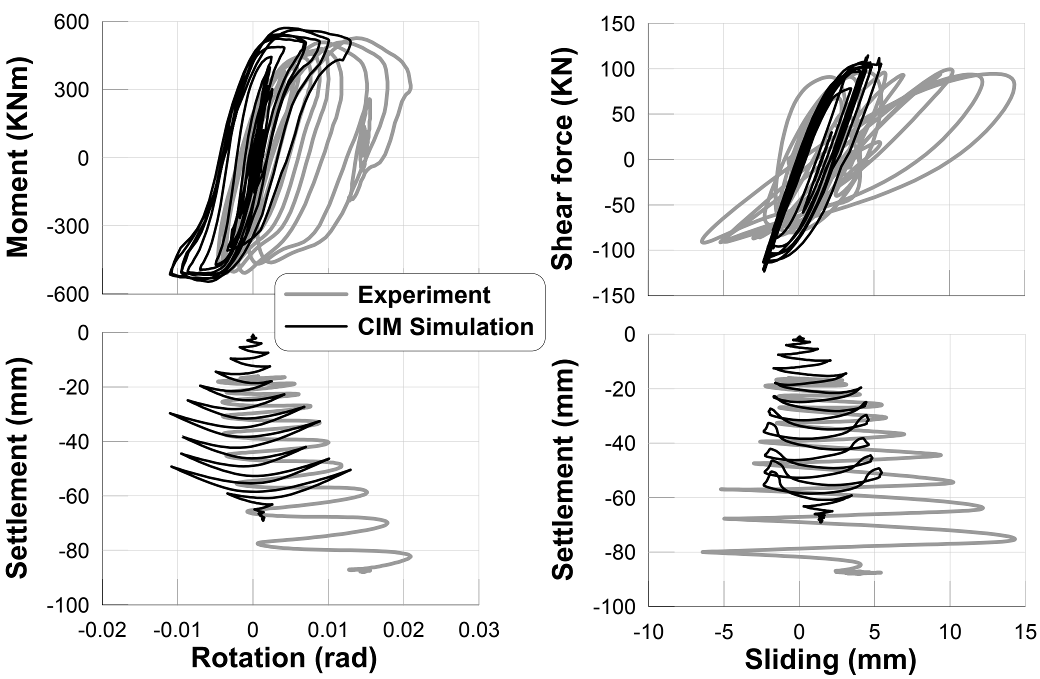

Fig. 5.22 Comparison of load-deformation behavior of footing for CIM simulation and SSG03_07 centrifuge test (Dr = 80%, FS_v = 7.2, M/(H×L) = 1.80).

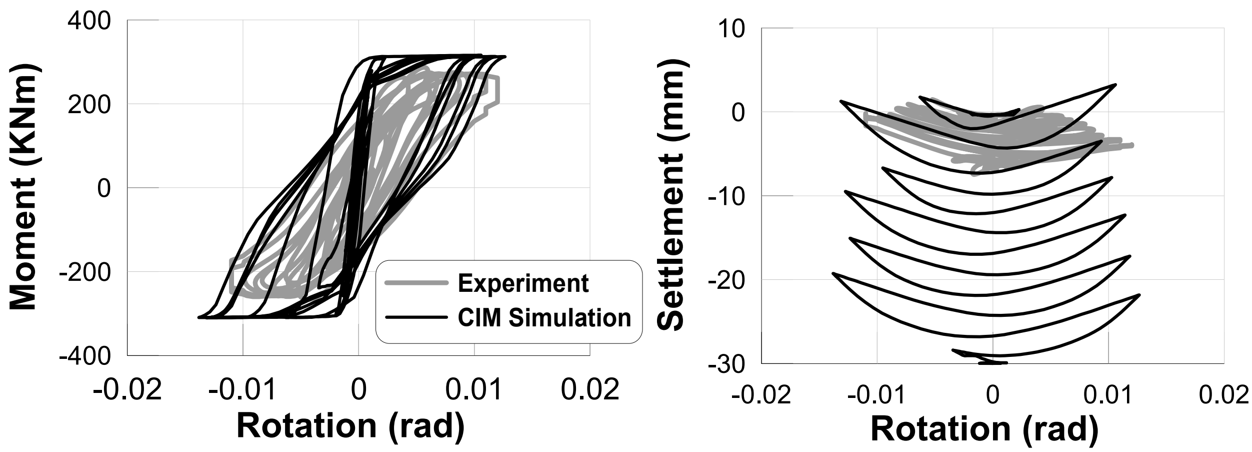

Fig. 5.23 Comparison of load-deformation behavior of footing for CIM simulation and SSG04_10 centrifuge test (Cu = 100 KPa, FS_v = 2.8, M/(H×L) = 1.70).

Figures 5.15–5.17 compare the simulation results to the data for footings with similar FS_V (2.3, 2.6, and 2.6) but different normalized moment-to-shear ratios (M/(H×L) = 1.2, 0.45, and 1.75). These are slow lateral cyclic tests with sand foundation soils. The results are presented in terms of moment, rotation, shear force, sliding, and settlement at the base center point of the footing. As can be seen from Figure 5.17, simulations for high M/(H×L)=1.75 compare well to data in all aspects. Figure 5.15 shows intermediate M/(H×L)=1.2 results for which maximum moment and shear and rotational stiffness degradation compare well to data. Cyclic sliding is overpredicted and the permanent settlement is underpredicted by about 20%. Figure 5.16 shows low M/(H×L)=0.45 results for which the model predicts reduced peak moment and increased peak shear (compare Figs. 5.17 and 5.16) as observed in the experiment. However, permanent settlement is underpredicted and cyclic sliding is overpredicted.

Figures 5.18 and 5.19 compare simulation results to data for two FS_V levels (5.2 and 14.0) and similar M/(H×L)=1.75 for models on sand. The larger FS_V level is created by embedding the footing. Figure 5.18 shows simulation results that compare well with data for FS_V = 5.2 except that the experiment shows unsymmetrical behavior in sliding. The results for FS_V = 14 in Figure 5.19 indicate underprediction of the maximum moment and shear, which could be due to the passive resistance of the soil against the embedded footing in the experiments. This passive reaction is not included in the CIM. Figure 5.20 presents the results for clay foundation soils (FS_V = 2.8 and M/(H×L) = 1.8). As with the sand results, the simulations for clay foundation soils compare well with data in terms of maximum moment and shear, energy dissipation, and rotational stiffness degradation. However, the model overestimates the measured settlement.

Figures 5.21 and 5.22 compare simulations to data for dynamic base shaking tests conducted with sand foundation soils and FS_V = 4.0 and 7.2, respectively. Figure 5.21 shows that the observed maximum moment is about 25% smaller than predicted for the FS_V = 4.0 case. For the embedded footing (FSV = 7.2), Figure 5.22 shows simulation results that compare reasonably well with data except for unsymmetrical behavior causing the accumulation of permanent rotation and sliding in the positive direction. Figure 5.23 shows that simulations for footings on clay overestimate the measured permanent settlement, as was found in the slow cyclic case.

5.2 VALIDATION AGAINST TESTS OF BRIDGE COLUMNS SUPPORTED ON SQUARE FOOTINGS

5.2.1 Centrifuge Tests on Bridge Columns

A centrifuge test series was performed at the UC Davis NEES facility by Ugalde et al. (2008) to investigate the rocking behavior of bridges on shallow foundations. The scope and test procedures of the centrifuge tests are described in this section. Additional details on the test setup, testing procedures, and data processing procedures can be found in the centrifuge data report for the JAU01 Test Series (Ugalde et al. 2008).

As shown in Figure 5.24, many model structures were tested in a given soil container. Each structure location was given a station name: A–G. Slow cyclic testing occurred at stations A and B with a hydraulic actuator, whereas specimens at stations C–G were excited by ground motions applied to the base of the soil container.

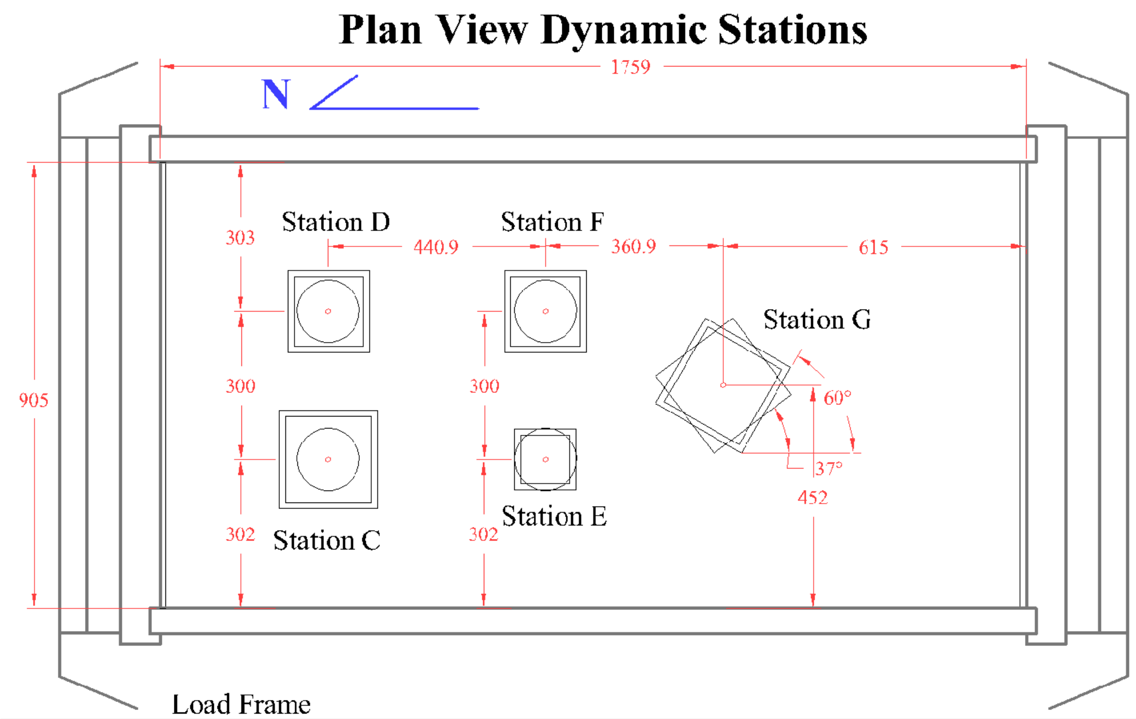

Fig. 5.24 Plan view of dynamic shaking stations where double line borders indicate footings and single lines indicate deck masses.

The model tests were scaled from typical bridge configurations used by Caltrans. The prototype footings were square with widths of three, four, or five times the diameter of the column (Dc =1.8 m). The prototype structure was a typical reinforced concrete single-column bridge bent connected to a shallow spread footing. The column resembles a "lollipop" structure with the deck mass lumped at the top. Figure 5.25 depicts the system modeled in the centrifuge tests. The deck mass was represented by a steel block. The reinforced concrete column was represented by an aluminum tube with bending stiffness (EI) scaled to match the cracked EI of the prototype concrete column. The footings were constructed of aluminum plate with sand glued to the base to provide a rough concrete-like interface with the soil.

At the time that the sand was placed, all seven model foundations were embedded to a depth of 40 mm (1.7 m prototype) at seven stations (A–G). Structures at one or two stations were tested during a given spin; the structures were bolted to their embedded foundation, then the centrifuge was spun until the centrifugal acceleration normal to the sand surface was 42.9 g's and the loading events were applied. After stopping the centrifuge, the model structures were removed and new structure(s) were placed at other station(s) for testing in the next spin.

For stations C–G, six accelerometers were placed on the foundation and six on the deck in order to resolve all six rotational and translational degrees of freedom for these relatively rigid bodies. Six displacement transducers were also placed against the footings to measure their six displacement degrees of freedom. A plastic frame, shown in Figure 5.25 was attached to the embedded footings to provide accurate surfaces on which to mount the displacement transducer probes.

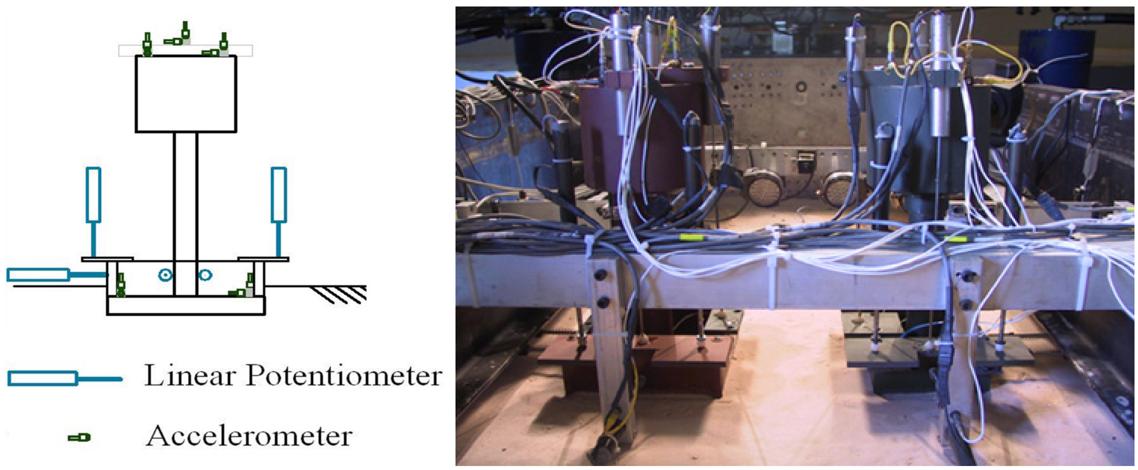

Fig. 5.25 Side view of typical structure setup and instrumentation.

The two structures considered here for verification analyses are at stations E and F. These two structures were shaken side by side and are identical except for the different footing sizes. The properties are shown in Table 5.5. The masses and moments of inertia specified for the footing and bridge deck come from summing the mass of everything above the midpoint of the column as the deck mass and everything below the midpoint of the column as the footing mass.

Table 5.5 Structural properties used to calculate experimental load-deformation behavior.

Station	FSv	Deck Mass (Mg)	Footing Mass (Mg)	Footing Width (Square) (m)	Icg Deck (kg*m^2)	Icg Foot (kg*m^2)	Embed-ment (m)	Hcg deck (m)	Hcg foot (m)	Icolumn (m^4)	Ecolumn (Pa)	hcg / L
E	17	926	173	5.4	3.34E+06	8.67E+05	1.7	13.47	1.215	1.07E-01	6.90E+10	2.14
F	31	926	246	7.1	3.34E+06	1.93E+06	1.7	13.47	1.238	1.07E-01	6.90E+10	1.54

Structures at stations E and F were subjected to dynamic loading using the shaking table mounted on the centrifuge to shake the entire model container. The ground motions imposed on the model container were scaled and filtered motions from recordings in the Tabas 1978 earthquake and a Los Gatos recording of the 1989 Loma Prieta earthquake. These motions come from the near-field records posted at the SAC Steel Project (2006) website. Twelve scaled motions were applied to each structure. The testing sequence for dynamic stations started with low-amplitude step waves, followed by scaled-down earthquake ground motions, then large-amplitude earthquake ground motions, and finally step waves similar to those applied before strong shaking. The peak ground accelerations ranged between 0.1 g and 0.8 g.

The motions considered for the verification studies were the fifth, sixth, and eighth events of the fifth spin of the JAU01 test series. Shaking events five, six, and eight were chosen because the relatively low-amplitude Events 1, 2, 3, 4, and 7 caused little settlement or nonlinear load-deformation behavior of the footing. The motion recorded at the footing level in the free field during the experiment was used as input at the base of the CIM and BNWF models. Figure 5.26 shows the acceleration times histories measured in the free field during the experiments. The response spectra are plotted in Figure 5.27.

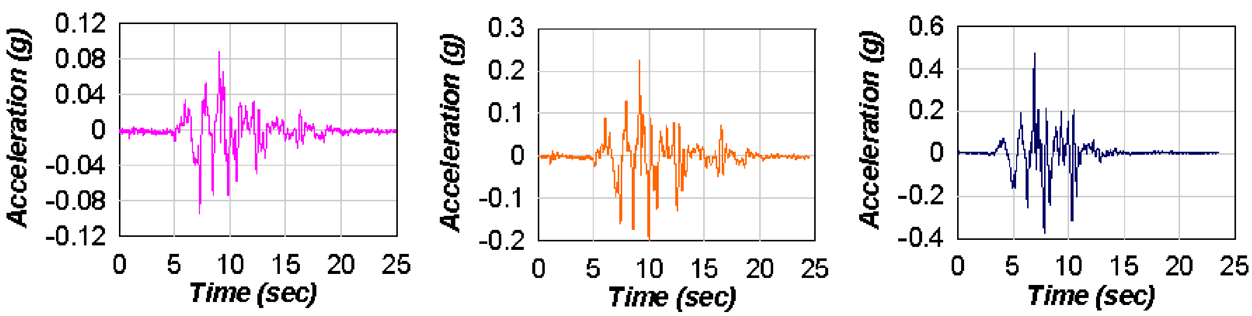

Fig. 5.26 Acceleration time history of free-field soil at footing level for motions during event (a)JAU01_05_05, (b) JAU01_05_06, and (c) JAU01_05_08.

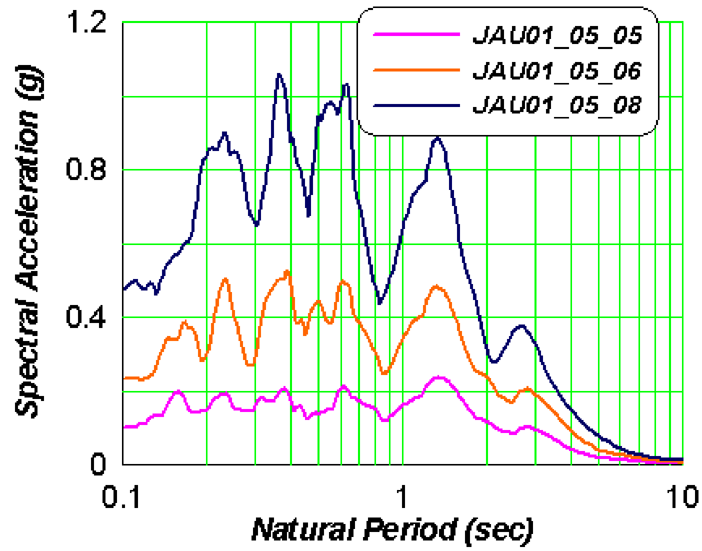

Fig. 5.27 Acceleration response spectra (for 5% damping ratio).

5.2.2 Experimental and Numerical Modeling and Results

Figure 5.28 shows a schematic depiction of the structural model. Five structural nodes are used in the model, which are located at the base of the footing, the center of gravity of the footing mass, the height of the fixity point at the base of the column, the height of the fixity point at the top of the column, and the center of gravity of the deck mass. All structural elements are elastic beam-columns. The element representing the structural column was given the properties of the aluminum tube used in the centrifuge test. The elements representing the deck mass, footing mass, and column fixity points are all approximately rigid by using elastic beam columns with 20 times the area moment of inertia, I, of the column.

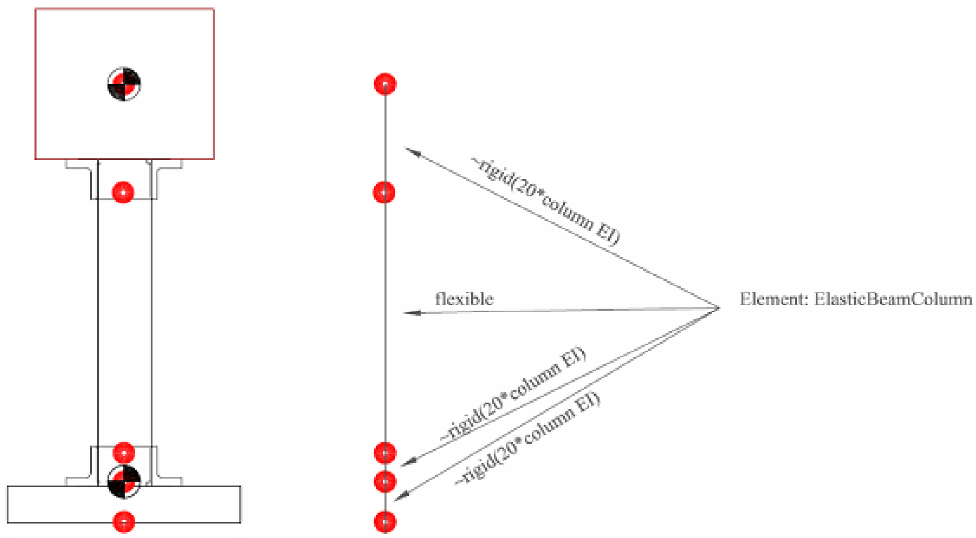

Fig 5.28 Simplified structural numerical model of experiment used for both simulations (note: foundation elements not shown).

(a) BNWF Results

A BNWF model was created of the system shown in Figure 5.28 using a bed of nonlinear Winkler springs as well as p-x and t-x springs attached to the base node. Model parameters selected according to the protocols given in Chapter 2 are summarized in Table 5.6.

Table 5.6 Parameters for BNWF model used in verification study of bridge columns.

Parameters	JAU01_05_05 (station-E)	JAU01_05_05 (station-F)	JAU01_05_06 (station-E)	JAU01_05_06 (station-F)	JAU01_05_08 (station-E)	JAU01_05_08 (station-F)
Input loading	Surface acc	Surface acc	Surface acc	Surface acc	Surface acc	Surface acc
L = B (m)	5.4	7.1	5.4	7.1	5.4	7.1
Df (m)	1.73	1.73	1.73	1.73	1.73	1.73
FSv	17	31	17	31	17	31
E (MPa)	45	45	45	45	45	45
ν	0.4	0.4	0.4	0.4	0.4	0.4
c_{rad} (%)	5	5	5	5	5	5
TP (%)	10	10	10	10	10	10
L_{end}/L (%)	16	16	16	16	16	16
Rk	5	5	5	5	5	5
le/L (%)	2	2	2	2	2	2

Recall that unlike the shear wall tests discussed in Section 5.1, the bridge-column tests all involve dynamic shaking. Figures 5.29–5.34 compare model predictions to data for the three applied motions and two footings. The BNWF model results for moment, rotation, and settlement are quite reasonable for all three motions and both of the footings. The shapes of the moment-rotation and settlement-rotation curves are also captured well. Further discussion of the results is provided in Section 5.2.3.

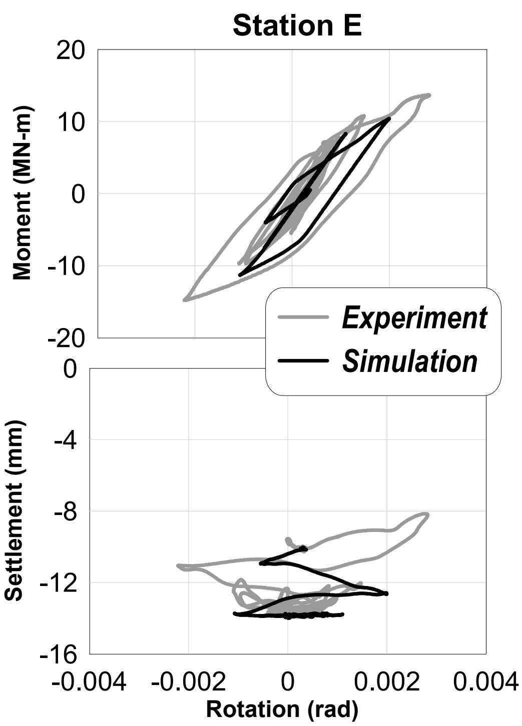

Fig. 5.29 Load-deformation behavior of footing for (a) station E and (b) station F during JAU01_05_05 (BNWF results).

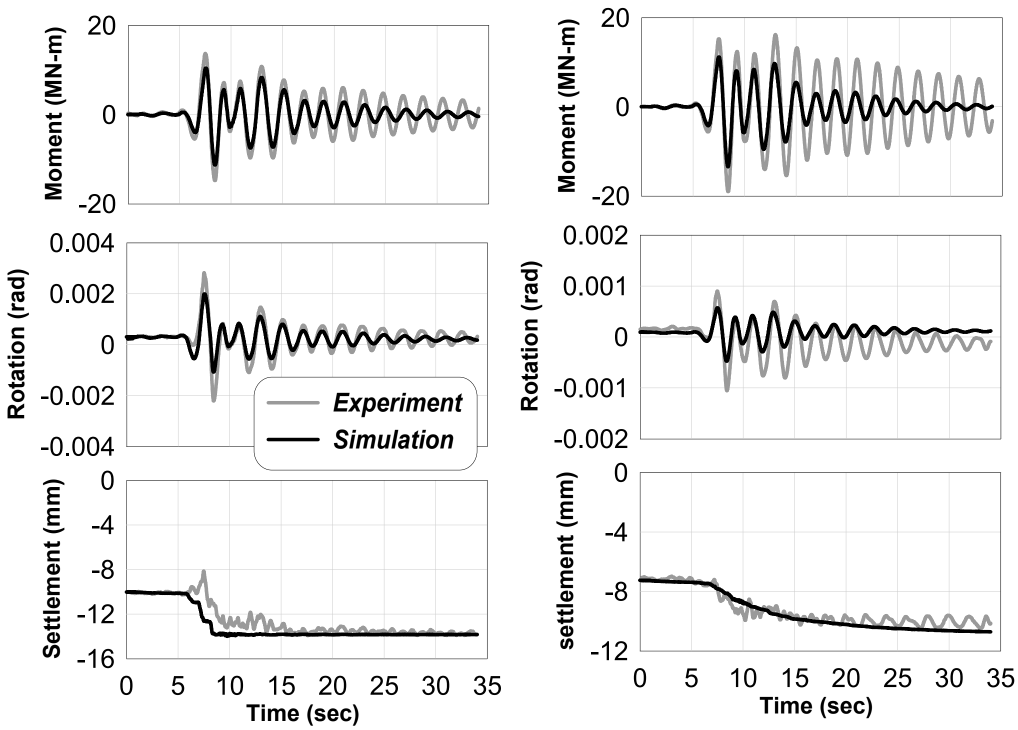

Fig. 5.30 Footing moment, rotation, and settlement time histories for (a) station E and (b) station F during JAU01_05_05 (BNWF results).

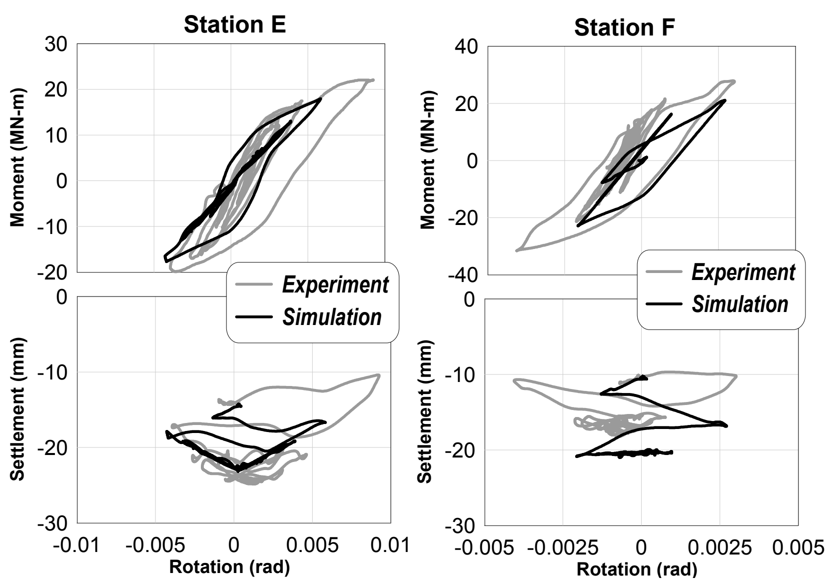

Fig. 5.31 Load-deformation behavior of footing for (a) station E and (b) station F during JAU01_05_06 (BNWF results).

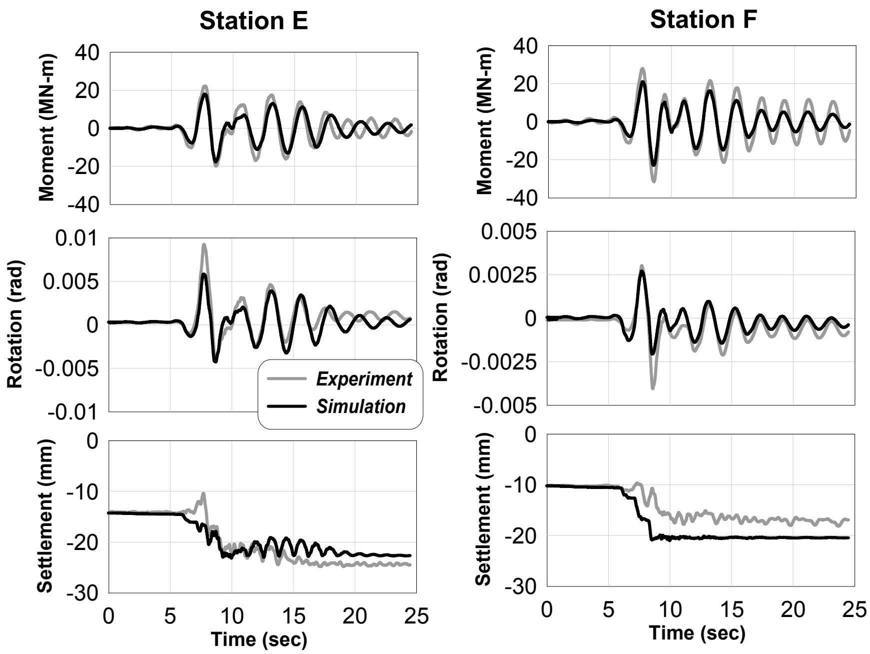

Fig. 5.32 Footing moment, rotation, and settlement time histories for (a) station E and (b) station F during JAU01_05_06 (BNWF results).

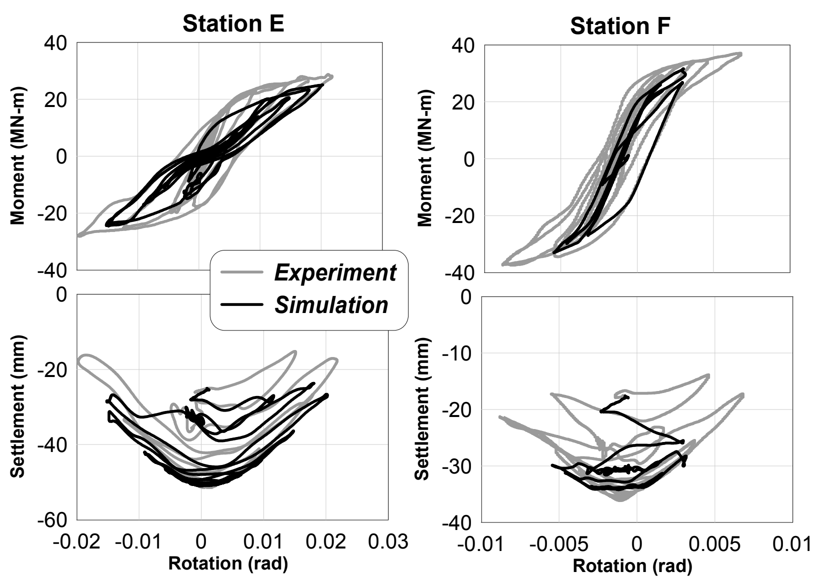

Fig. 5.33 Load-deformation behavior of footing for (a) station E and (b) station F during JAU01_05_08 (BNWF results).

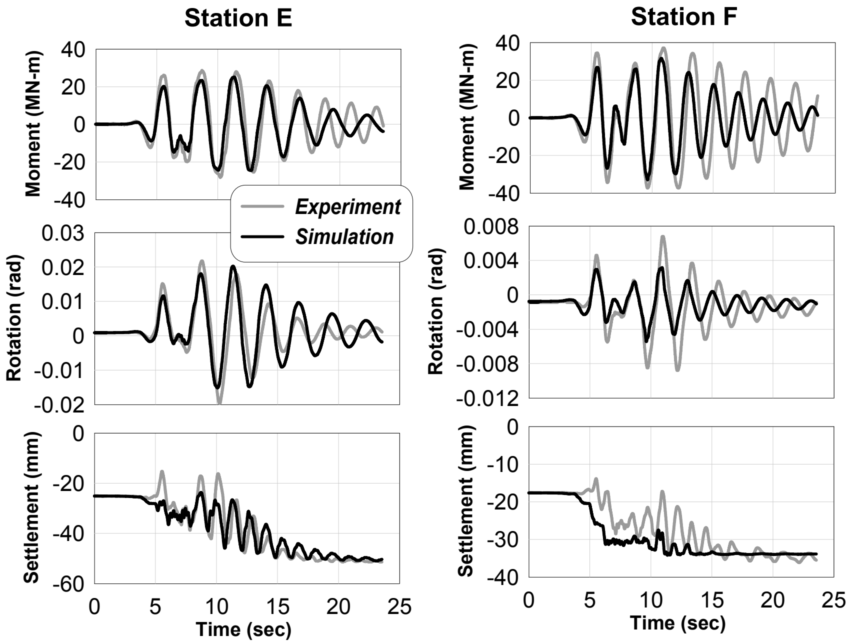

Fig. 5.34 Footing moment, rotation, and settlement time histories for (a) station E and (b) station F during JAU01_05_08 (BNWF results).

(b) CIM Results

The OpenSees model is generated using CIM element implemented in OpenSees as soilfootingsection2D. The following figures show the load-deformation responses of the two footings to three consecutive earthquake motions. The experimental results are compared to simulation results as before. The CIM input parameters listed in Table 5.7 were selected according to the protocols given in Chapter 3.

Table 5.7 Parameters for contact interface model used in verification study of bridge columns.

Parameter	JAU01_05_05 (station-E)	JAU01_05_05 (station-F)	JAU01_05_06 (station-E)	JAU01_05_06 (station-F)	JAU01_05_08 (station-E)	JAU01_05_08 (station-F)
Input	Surface acc	Surface acc	Surface acc	Surface acc	Surface acc	Surface acc
Vult (kN)	1.83E+05	3.58E+05	1.83E+05	3.58E+05	1.83E+05	3.58E+05
L = B (m)	5.4	7.1	5.4	7.1	5.4	7.1
Kv (kN/m)	1.18E+07	1.20E+07	1.18E+07	1.20E+07	1.18E+07	1.20E+07
Kh (kN/m)	6.90E+06	6.50E+06	6.90E+06	6.50E+06	6.90E+06	6.50E+06
$\theta_{Elastic}$ (Rad.)	0.001	0.001	0.001	0.001	0.001	0.001
Rv (Ratio)	0.15	0.1	0.15	0.1	0.15	0.1
ΔL (m)	0.002	0.005	0.002	0.005	0.002	0.005

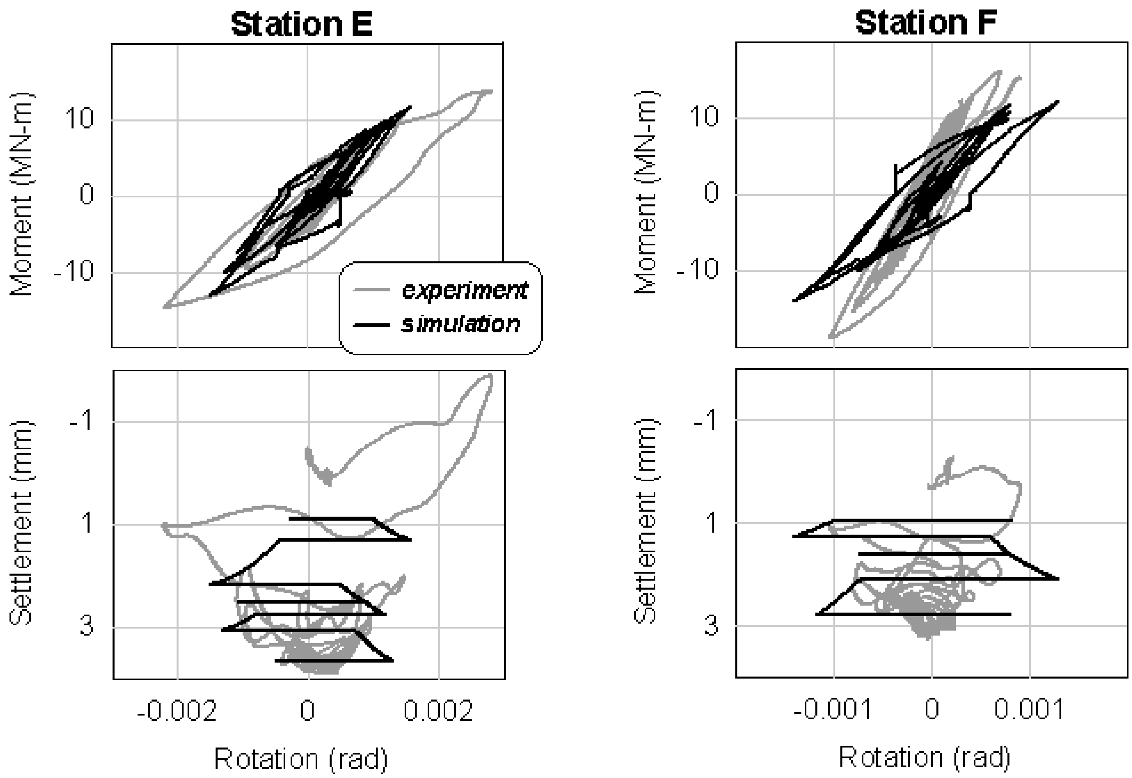

Fig. 5.35 Comparison of load-deformation behavior of footing for contact interface model simulation and JAU01_05_05 centrifuge test (a) station E and (b) station F.

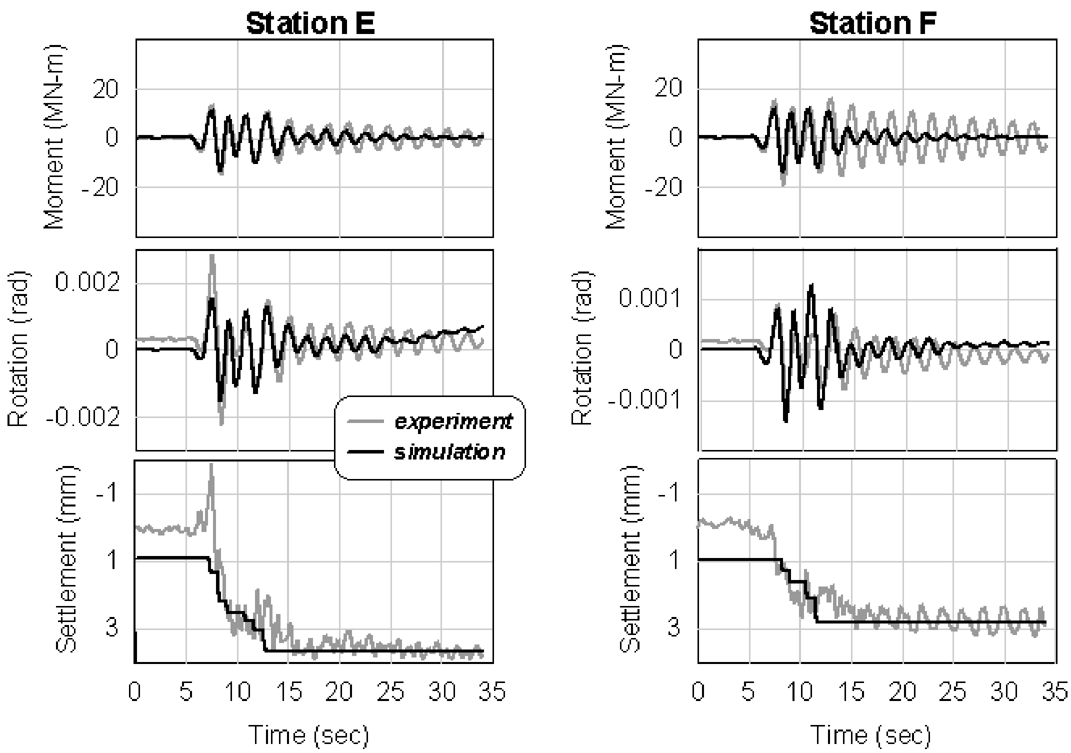

Fig. 5.36 Footing moment, rotation, and settlement time histories for (a) station E and (b) station F during JAU01_05_05.

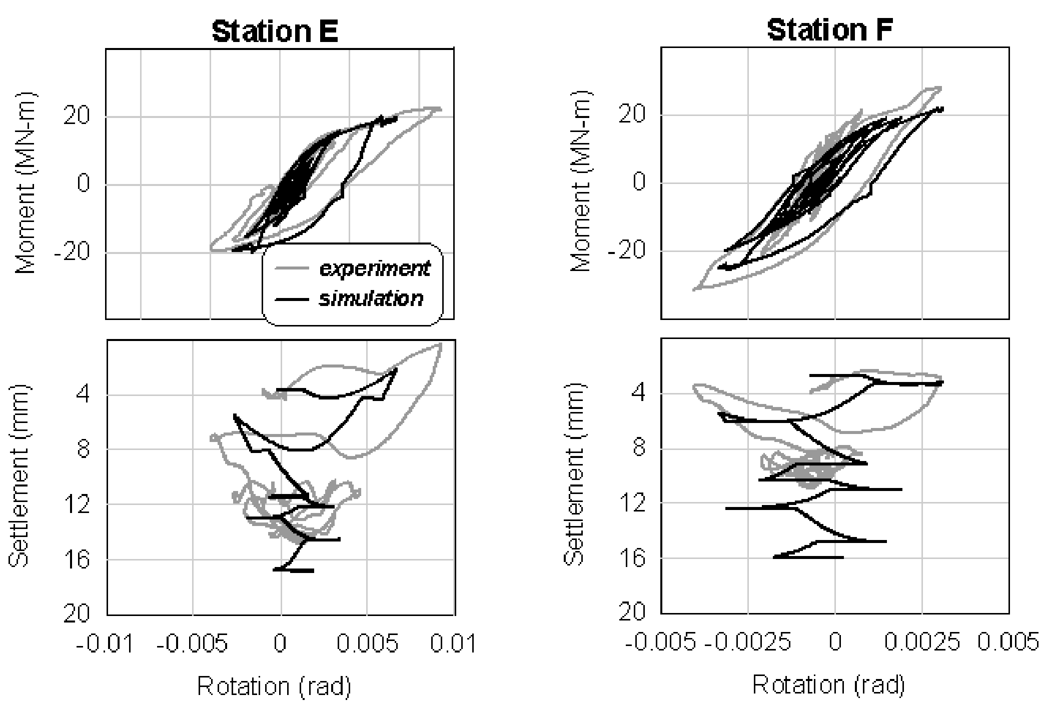

Fig. 5.37 Load-deformation behavior of footing for (a) station E and (b) station F during JAU01_05_06.

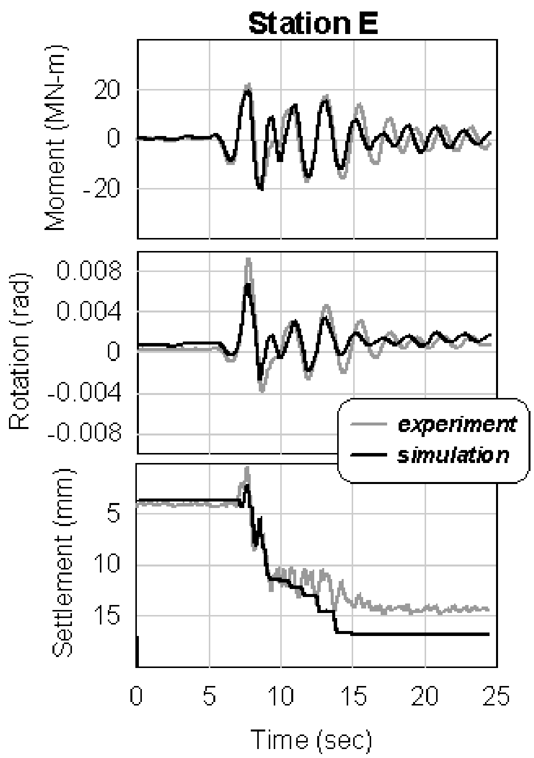

Fig. 5.38 Footing moment, rotation, and settlement time histories for (a) station E and (b) station F during JAU01_05_06.

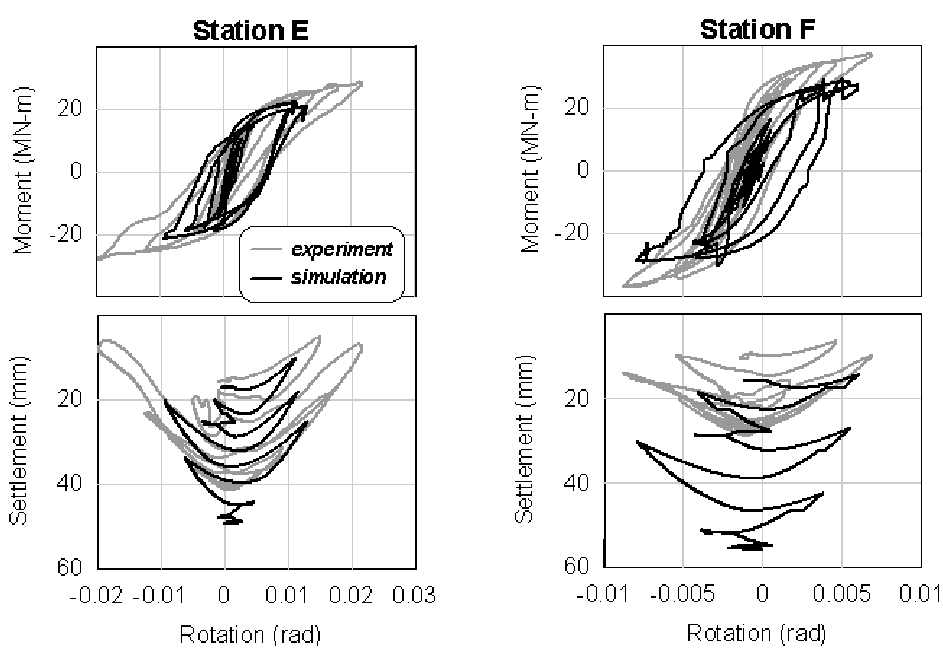

Fig. 5.39 Load-deformation behavior of footing for (a) station E and (b) station F during JAU01_05_08.

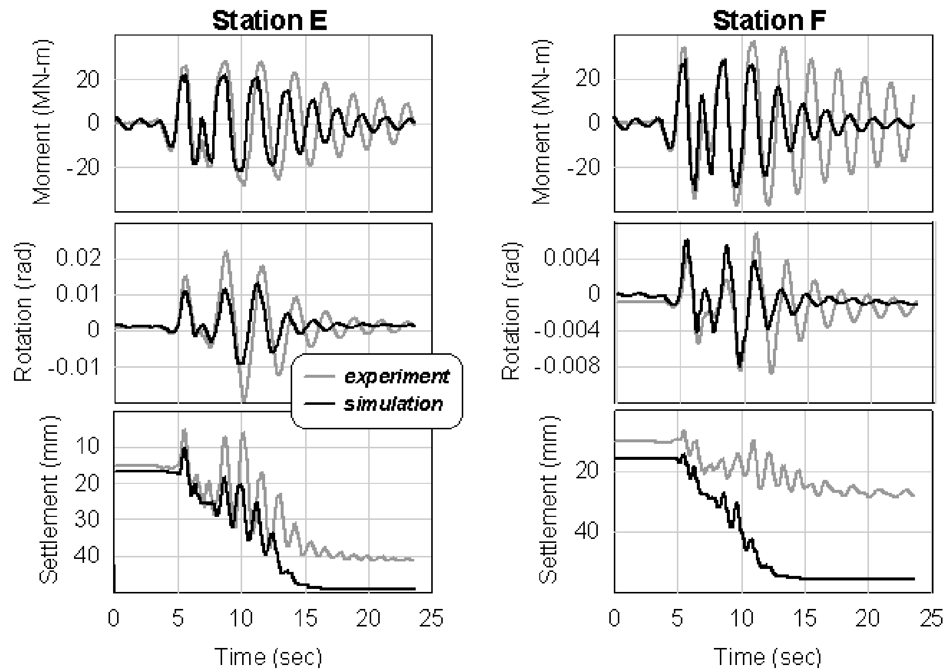

Fig. 5.40 Footing moment, rotation, and settlement time histories for (a) station E and (b) station F during JAU01_05_08.

5.2.3 Discussion of Bridge Results

In this section we discuss the comparisons of simulation results to data for bridge-column footing tests. The discussion is organized according to the response quantities of moment capacity, settlement, rotation, and energy dissipation.

(a) Maximum Moment

Both the CIM and BNWF models underpredict the maximum moment developed during the tests. The level of underprediction varies from 10 to 20% for CIM and 13% to 26% for BNWF. Potential causes include the use of 6% Rayleigh damping to achieve numerical convergence and possible underestimation of the vertical bearing capacity of the footings.

(b) Footing Displacements

For low-amplitude shaking events the level of permanent settlement is reasonably well predicted. However, the simulated response of the larger footing (station F) to the more intense earthquakes

(JAU01_05_06 and JAU01_05_08) overpredicts permanent settlements (both models). The CIM more accurately predicts the permanent settlement of the smaller footing (station E) although cyclic uplift is underpredicted. The BNWF model underestimates rotations by about 20–50%.

(c) Energy Dissipation

Both models reasonably capture the shape of the moment-rotation hysteresis loops and the area enclosed by them. The Rayleigh damping used in the simulations appears to overdamp the footing response after strong shaking is finished.

5.3 INTERPRETATION AND DISCUSSION

In this chapter, we verify predictions of the BNWF and CIM models against data from centrifuge experiments conducted on model shear walls supported by wall footings and bridge columns supported by square footings. The shear wall and bridge-column test specimens are different from each other in the following respects:

- The shear wall models consist of a stiff structural wall with uniformly distributed mass over its height and uniform cross-sectional properties. The bridge columns have a "lollipop" structure with deck mass concentrated at the top of the column.
- The shear wall has a strip footing, with a width to length (B/L) ratio of ~0.3, whereas the bridge model footings are square with prototype widths of 5.4 m 7.1 m. Vertical factors of safety for the shear wall footings range from FS_V=2–14, whereas the column footings range from FS_v=17–31. The bearing capacities and FS_V values are based on a state of shear failure in the foundation soils. The design of large footings on granular soils are often settlement-controlled, resulting in large FS_v.
- The shear wall specimens were tested under slow lateral cyclic loading applied by a horizontal actuator and dynamic shaking. The bridge-column specimens were only subjected to dynamic shaking.
- Input acceleration histories for the dynamic shaking were tapered sine waves for the shear wall specimens and recorded ground motions for the bridge columns.

A comparison of numerical-experimental results for the above cases demonstrates that in general both the CIM and BNWF models reasonably predict the footing response observed during the experiments, including the moment-rotation, settlement-rotation, and shear-sliding behavior. In addition, the initial unloading and reloading rotational and shear stiffness of the footings are generally captured by both models. An aggregate summary of key response quantities is presented in Figures 5.41–5.42. In these figures, simulated response quantities on the y-axis are compared to data on the x-axis. The observations are summarized below:

- The maximum moment developed at the footing (M_{max}) is generally well predicted by the CIM and BNWF models for the bridge columns but slightly underpredicted for the shear wall specimens. This may be partially due to the increased soil bearing capacity from previous loading cycles and the contributions of passive pressure and side friction on moment capacity, which are neglected by the CIM and BNWF models. The magnitude of underprediction is smaller for the strip footing cases (shear wall footings) because most of the footings were surface-resting and therefore initially have no side friction contribution to capacity.
- Simulated values of the maximum shear force developed at the footings (H_{ult}) are fairly well predicted by both models in all cases. Calculated values are within 30% of experimental estimates; however, 60% of the cases are within 10% of the experimental observations.
- Maximum footing rotations (θ_{max}) are generally predicted within error margins of approximately 10%. These response comparisons have meaning principally for the dynamic shaking experiments because rotation is effectively the input to the model for the slow cyclic tests.
- Maximum sliding displacements of the footings (U_{max}) are consistently underpredicted by the BNWF model. The CIM model overpredicts sliding for tall buildings (high M/(H×L) cases) and underpredicts sliding for low aspect ratio buildings. The BNWF underprediction of sliding displacement may be partly explained by the lack of coupling between lateral and vertical springs; i.e., the reduction of shear capacity when gapping occurs below the footing. In some cases, large sliding displacements in the experiments are asymmetric, which is attributed to slight asymmetry of the connection of the structural element (wall) to the actuator. The simulations did not include this condition and tended to respond almost symmetrically.

- Total footing settlements (S_{total}) were generally underpredicted by the BNWF model. The results for the CIM model were mixed. For sand foundation materials, CIM settlements were too low for the shear wall specimens and too high for the bridge-column specimens. For clay foundation materials, CIM settlements were too high.
- The total energy dissipation ED_{total}, which is calculated as the sum of the shear-sliding and moment-rotation energies (areas enclosed by moment-rotation and shear-sliding loops) is generally reasonably captured by both models. However, there are two outliers for each model involving overprediction of ED_{total} by the CIM model and underprediction by the BNWF model.

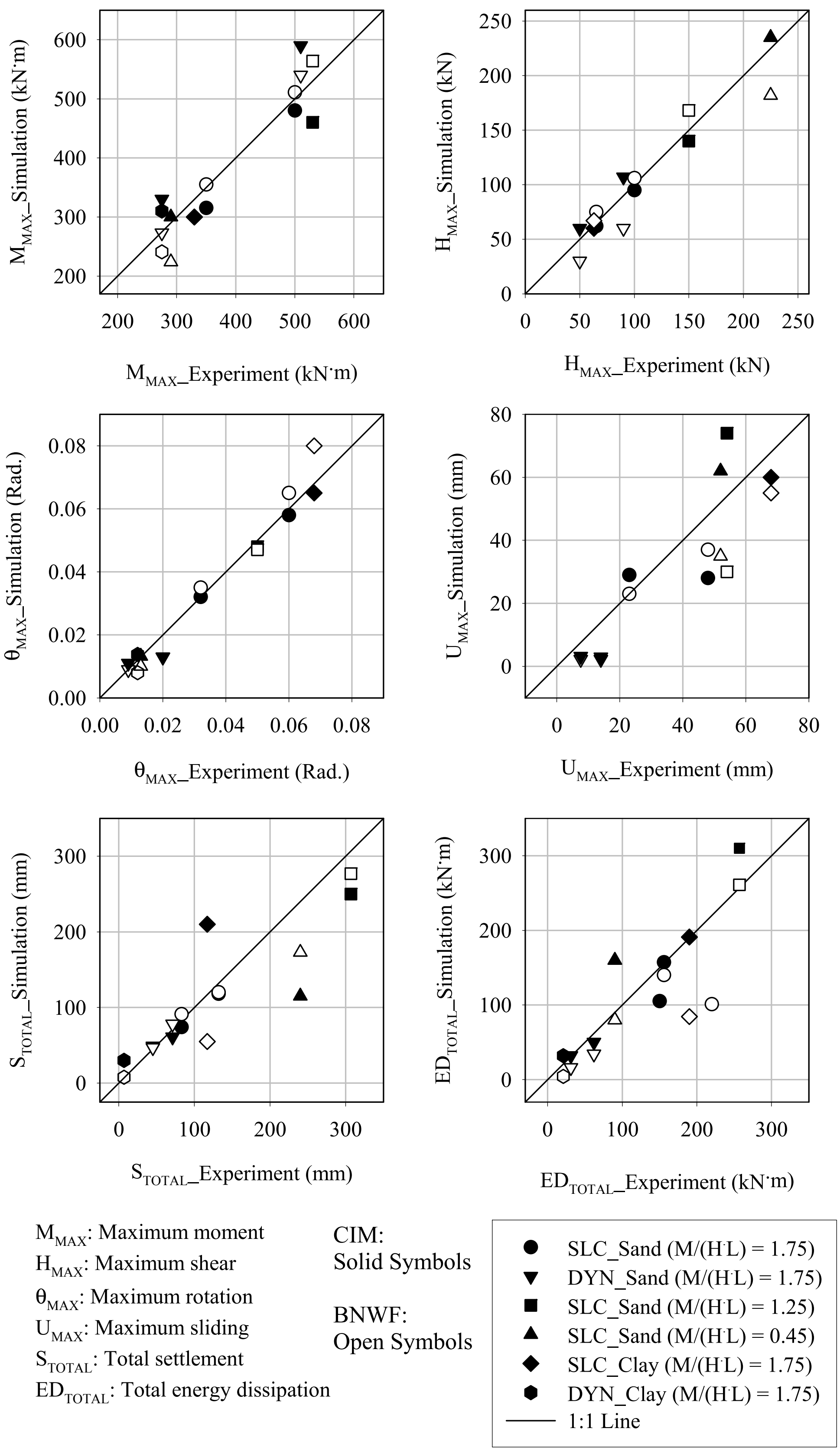

Fig. 5.41 Footing demand summary (shear wall modeling results).

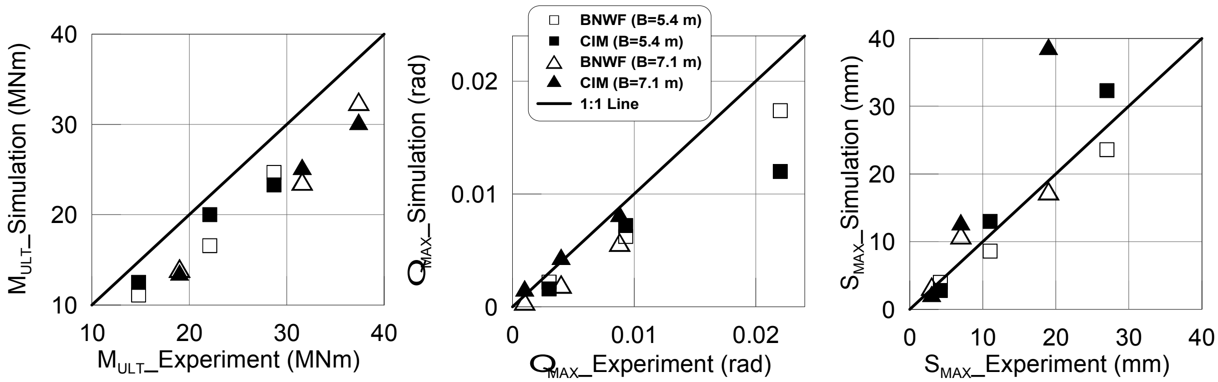

Fig. 5.42 Footing demand summary (bridge modeling results).

Finally, to put these findings in perspective, it must be recognized that the model predictions presented in this chapter follow the parameter selection protocols described in Chapters 2 and 3. This raises two points. First, those parameter selection protocols are based in part on empirical calibrations against these same experiments (e.g., of the Rv parameter in the CIM and the Cr parameter in the BNWF), especially for the shear wall tests. Hence, good fits are to be expected. Second, users should recognize the intimate link between model performance and parameter selection protocols. Different protocols would produce different results with different relative trends between models and across tests. Hence, all of the findings presented here are conditional not only on the model formulation but to equal degree on the parameter selection protocols.

6 Conclusions

6.1 SCOPE OF WORK AND FINDINGS

The potential benefits and consequences of nonlinear foundation-soil interaction for shallow foundations are well documented in the literature (e.g., Housner 1965; Priestley et al. 1978). However, modeling procedures that account for this nonlinear behavior are needed for use in practice. This report describes two numerical models for simulating soil-foundation interaction, documents the input parameters and parameter selection protocols for these models, and compares the results of model predictions for a fictional building structure on clay foundation soils and for a series of centrifuge model tests involving sand foundation soils. The two models considered are referred to respectively as a beam-on-nonlinear-Winkler-foundation (BNWF) model and a contact interface model (CIM).

The beam-on-nonlinear-Winkler-foundation (BNWF) model is a system of closely spaced independent nonlinear inelastic springs, capable of capturing gapping and radiation damping. Vertical springs distributed along the base of the footing are used to capture the rocking, uplift and settlement, while horizontal springs attached to the sides of the footing capture the resistance to sliding. The mechanistic springs are modifications of an earlier implementation by Boulanger (2000), which were developed for laterally loaded piles. The BNWF model can be implemented with a variable stiffness distribution over the length of the foundation to account for relatively large reaction stresses that tend to develop at the edges of stiff footings. A prescribed ground motion is applied at one end of the zero length BNWF springs while the other end is attached to elastic beam elements that represent the structural footing system.

The contact interface model (CIM) provides nonlinear constitutive relations between cyclic loads and displacements at the footing-soil interface of a shallow foundation that is subjected to combined moment, shear, and axial loading. The nonlinear interaction between the structural footing, which is assumed to be rigid, and the soil beneath the footing in the zone of influence are modeled as a single macro-element. The CIM tracks the geometry of the contact between the soil and the base of the footing along with the kinematics of the footing-soil system to predict the rocking and settlement. The CIM allows coupling between foundation displacements and shear, moment, and vertical capacities. The coupling between shear and moment and associated deformations are accounted for using a yield surface (interaction diagram) and an associative flow rule, similar to previously published macro element models. Coupling between the vertical and moment loads and associated deformations are not based on yield surfaces and flow rules; rather, they are natural outcomes of tracking the geometry of the contact and gapping between a rigid footing and the underlying foundation soil.

Chapters 2 and 3 describe the general attributes of the BNWF and CIM models, respectively, along with their respective capabilities, input parameter selection protocols, and inherent limitations. Chapter 4 presents a comparison between BNWF and CIM model predictions using the parameter selection protocols for three hypothetical shear wall buildings of different height. From these analyses, it is observed that (1) maximum moment, maximum shear, rotational stiffness, and shear stiffness are comparable for both models; (2) both models show significant energy dissipation at the base of the footing; (3) sliding displacement predictions by the CIM model were generally larger than those of the BNWF model, particularly for shorter structures; and (4) upon increasing the sliding resistance of the model shear wall–footing system (to account for the fact that the mat foundation is likely to constrain sliding displacements), the model-to-model shear-sliding response comparisons become more similar.

Chapter 5 presents the results of a verification exercise in which the BNWF and CIM models are used to simulate the results of centrifuge experiments for shear wall–footing systems and bridge column–footing systems. Again, the parameter selection protocols from Chapters 2 and 3 are used and attributes of the models' performance are identified. For the modeling conducted herein: it was found that (1) the salient hysteretic features (shapes, peaks, unloading and reloading of the footing response curves) as observed in the experiments were reasonably captured by both models, (2) the maximum moment tended to be underpredicted slightly for both models, which may be due to ignoring the increased soil capacity from previous loading cycles and the friction and passive pressure on the front and sides of the footings, (3) the maximum absolute sliding displacement was always underpredicted by the BNWF model, while the CIM model slightly overpredicted sliding for tall buildings (high M/(HL) cases) and underpredicted the sliding for low aspect ratio cases, and (4) the total energy dissipation observed in the experiments was reasonably captured by both models. In reference to the third finding above, the underprediction of sliding observed for the BNWF model may be due to overestimation of the sliding capacity due to neglecting the coupling between lateral and vertical springs, i.e., the reduction of shear capacity that occurs when the contact area reduces due rocking and the remaining elements in contact are subject to large bearing pressures

6.2 HIGH-LEVEL ACCOMPLISHMENTS OF THIS WORK

Over the course of the last several years, several series of centrifuge model tests have been performed with support from PEER. These tests along with others in the literature have provided a much clearer understanding of the mechanisms of behavior of rocking shallow foundations and further highlighted the potential benefits of allowing and properly simulating foundation movement during seismic loading. A key accomplishment of this work is the availability of an experimental database of footing test results for use in numerical model validation (Rosebrook and Kutter 2001a–c; Gajan et al. 2003a,b).

The work presented in this report capitalizes on these data by evaluating two numerical modeling approaches for capturing shallow footing response under cyclic loading. An additional high-level accomplishment of this work is the availability of these validated and cross-compared models to the community. The models are both implemented in OpenSees, and therefore are available to any OpenSees user.

6.3 PRACTICAL IMPLICATIONS

It is well documented that structural performance can be significantly affected by the nonlinear behavior of shallow foundations (e.g., Comartin et al. 2000). As compared to the yielding of the structural elements, the yielding behavior at the foundation-soil interface dissipates energy with a self-centering mechanism that can help reduce residual drift. Energy dissipation in the foundation may also reduce ductility demands in the structure. However, hysteretic energy dissipation comes at the expense of permanent settlements and rotations. We postulate that shallow foundations can be designed with a well-defined moment capacity and to exhibit ductile nonlinear behavior when that capacity is exceeded. While rocking foundations will tend to experience permanent settlements, the level of settlement can be characterized and incorporated into the design. Thus, we argue that the profession should move toward appropriate engineering characterization of nonlinear foundation performance for use in structural response simulations, as has been done for other components of structural systems. To accomplish this, the rocking footings would need to be considered as an integral component of the system design.

A key step towards realizing this objective is the availability of practical engineering tools for simulating foundation behavior in seismic design. This work has advanced the BNWF model and CIM from research tools used principally by the Ph.D. students that wrote the codes to working OpenSees models with well-defined (and at least partially validated) parameter selection protocols. We recognize that further validation against full-scale field performance data would be useful to gain additional insights and confidence in the models. However, in the meantime, we encourage the application of these models, in parallel with more conventional impedance function models, with the recognition that the simulation results from both established and new procedures should be interpreted with appropriate engineering judgment as part of the design process. It is hoped that the experimental and simulation results presented herein will help engineers understand the mechanisms and consequences of nonlinear response of shallow foundations, and hence will increase the knowledge upon which their engineering judgment is based.

6.4 ADVICE FOR POTENTIAL USERS

6.4.1 Creating a Model

Use of the models described in this report can be undertaken by following the parameter selection protocols described in Chapters 2 and 3. Example TCL scripts, used to drive the OpenSees analyses for the BNWF and CIM models, are provided in the Appendix to facilitate use by others.

6.4.2 Input Ground Motions

It is recommended that the input for both models should be the free-field ground motion at a depth of approximately half the footing width below the base of the footing. For large footings or footings below a basement, kinematic interaction effects may be accounted for by using a foundation input motion instead of a free-field motion. Procedures for the evaluation of foundation input motions are given in FEMA-440 (2005) and Stewart et al. (2004).

6.4.3 Post Processing

Example scripts are provided in the Appendix to help users perform the required post-processing. When compared to the CIM model, the BNWF model allows the user to more directly determine the internal moments and shears in the structural footing elements, as this model uses conventional beam elements to represent the structural footing. This would be useful for designing the structural footing section and reinforcement. In order to estimate the shear force and the bending moment distributions from the CIM model, the magnitude and the resultant force on the base of the footing may be directly determined from the output of the analysis, and then by assuming a suitable distribution of the resultant reaction stresses, the shear forces could be determined, albeit less directly than for the BNWF model.

6.4.4 Selecting Model: Relative Strengths and Limitations of BNWF and CIM Models

Many readers of this report will have a basic question — which model (BNWF or CIM) is better suited to a specific application? Some high-level attributes of the models may help guide this decision:

- If the simulations are to be used for structural design of footing elements, or the footing flexibility is anticipated to contribute to the foundation response, the BNWF model should be chosen. This model can be used to more directly evaluate internal moments and shears used for section design as described above.
- If the normalized moment to shear ratio $M/(H \cdot L)$ = (Moment)/((Horizontal shear force)*(Length of footing)) is less than approximately 1.5, and sliding is not restrained by slabs and grade beams, then the moment capacity of the footing will be sensitive to shear load and vice versa. In this case, the CIM model is preferred because of its ability to account for the coupling between the moment, shear, and axial responses. For cases with $M/(H \cdot L) > 1.5$ rocking will tend to dominate and both models should produce similar

results if the parameter selection protocols presented here are followed. Coupling may also be neglected for very small M/(H·L) ratios where sliding is known to dominate.

- If users would like to use another platform besides OpenSees, then implementation of the BNWF model will be more easily accomplished if bilinear spring, gap, and damping elements are available in the alternative platform. Implementation of the CIM in another platform would require implementation of a new element and hence access to the source code for the host platform.

6.5 RECOMMENDATIONS FOR FUTURE WORK

Additional work is needed to provide further insight into nonlinear foundation-soil interaction and the benefits of performing the type of simulations enabled by the BNWF and CIM models. Future research should include:

- Utilization of the models in structural simulations similar to those of Goulet et al. (2007), in which the full PEER framework for performance-based earthquake engineering was exercised, to evaluate the effect of SSI on loss estimation and life-cycle costs for a building system.
- Extension of the modeling exercise to consider multiply-connected footings and/or footings of various types (e.g., frame-wall–footing systems).
- Verification of model performance against full-scale field performance data derived from experiments or strong motion data in strongly shaken buildings.
- Currently, the models are implemented to evaluate two-dimensional response. Extension to three dimensions would be valuable for practical conditions.
- For the BNWF model, coupling of vertical and horizontal springs would help improve the performance of the model when analyzing intermediate aspect ratio, highly coupled moment-shear cases.
- Further efforts to improve the numerical robustness of the models, especially the CIM model would be valuable.
- Currently, both models are validated for footings on competent soil. The models should be exercised and extended as needed to predict footing behavior for liquefiable, unstable or reduced-strength supporting soils.

References

API. 1987. *American Petroleum Institute, Recommended Practice for Planning, Designing and Constructing Fixed Offshore Platforms API Recommended Practice Seventeenth Edition,* April 1.

Applied Technology Council (ATC). 1978. *Tentative Provisions for the Development of Seismic Regulations for Buildings*, ATC 3-06, Redwood City, CA.

Applied Technology Council (ATC). 1996. *Seismic evaluation and retrofit of concrete buildings*, Report No. 96-01, Seismic Safety Commission, State of California, November.

Boulanger, R. W., Curras, C. J., Kutter, B. L., Wilson, D. W., and Abghari, A. 1999. "Seismic soil-pile-structure interaction experiments and analyses." *ASCE, Journal of Geotechnical and Geoenvironmental Engineering*, 125(9), 750–759.

Boulanger, R. W. 2000. "The pysimple1, qzsimple1 and tzsimple1 material documentation." *Documentation for the OpenSees platform available at:* http://opensees.berkeley.edu/.

Briaud, J. L. and Gibbens, R. M. 1994. "Predicted and measured behavior of five spread footings on sand." *Geotechnical Special Publication*, 41.

Building Seismic Safety Council (BSSC), 2004. *NEHRP Recommended Provisions for Seismic Regulations for New Buildings and Other Structures*, Federal Emergency Management Agency, Washington D.C.

Comartin, C.D., Niewiarowski, R.W., Freeman, S.A., and Turner, F.M. 2000. Seismic retrofit and evaluation of concrete buildings: a practical overview of the ATC 40 document, *Earthquake Spectra*, 16, 241–262.

Coulomb, C. A. 1776. "Essai sur une application des règles des maximis et minimis à quelques problèmes de statique relatifs à l'architecture," *Mèm. acad. roy. près. Divers savants*, Vol. 7, Paris.

Cremer, C., Pecker, A. and Davenne, L. 2001. "Cyclic macro-element of soil structure interaction: Material and geometrical nonlinearities." *Int. Journal of Num. Anal. Meth. Geomech.*, Vol. 25, 1257-1284

Das, B. M., 2006. *Principles of Foundation Engineering*. Brooks/Cole Publishing Company, California.

Duncan, J. and Mokwa, R. L. 2001. "Passive earth pressures: Theories and tests." *ASCE Journal of Geotechnical and Geoenvironmental Engineering*, 127(3), 248-257.

EPRI. 1990. *Manual on Estimating Soil Properties for Foundation Design*. Electric Power Research Institute, Palo Alto, California.

Federal Emergency Management Agency (FEMA). 2000. *Prestandard and Commentary for the Seismic Rehabilitation of Buildings*, *FEMA (Series) 356*, Washington, D.C.

Federal Emergency Management Agency. 2004. *Improvement of inelastic seismic analysis procedures*, FEMA 440, Federal Emergency Management Agency, Washington, D.C.

Gadre, A. and Dobry, R. 1998. "Lateral Cyclic Loading Centrifuge Tests on Square Embedded Footing." *ASCE Journal of Geotechnical and Geoenvironmental Engineering* 124 (11). 1128-1138.

Gajan, S., Phalen, J. D. and Kutter, B. L. 2003. "Soil-foundation-structure interaction: Shallow foundations." *Centrifuge Data Report for test series SSG02*. Report No. UCD/CGMDR-03/01, Center for Geotechnical Modeling, University of California, Davis, California.

Gajan, S., Kutter, B. L. and Thomas, J. 2005. "Physical and Numerical Modeling of Cyclic Moment-Rotation Behavior of Shallow Foundations" *Proc. 16th Intl. Conf. Soil Mechanics and Geotechnical Engineering,* Sept., 2005, Osaka, Japan, Vol. 2, 795-798.

Gajan, S. 2006. "Physical and numerical modeling of nonlinear cyclic load-deformation behavior of shallow foundations supporting rocking shear walls". Ph.D. Dissertation, Department of Civil and Environmental Engineering, University of California, Davis, California.

Gajan. S. and Kutter, B. L. 2007. "A contact interface model for nonlinear cyclic moment-rotation behavior of shallow foundations" *Proc. 4th Intl. Conf. Earthquake Geotechnical Engineering.,* Paper No. 1458, Thessaloniki, Greece. June 25-28, 2007

Gajan, S. and Kutter, B. L. 2008. "Numerical simulations of rocking behavior of shallow footings and comparisons with experiments", *Proc. British Geotechnical Association (BGA) International Conference on Foundations*, Dundee, Scotland, June 24-27, 2008 (accepted for publication)

Gazetas, G., 1991. "Displacement and soil-structure interaction under dynamic and cyclic loading." *Proceedings of the 10th European Conference on Soil Mechanics and Foundation Engineering,* Florence.

Gazetas, G. 1991. "Foundations Vibrations." Foundation Engineering Handbook, Ch 15, Fang, H. Y. (ed.), Van Nostrand Reinhold, New York.

Goulet, C.A., Haselton, C.B., Mitrani-Reiser, J., Beck, J.L., Deierlein, G.G., Porter, K.A., and Stewart, J.P. 2007. "Evaluation of the seismic performance of a code-conforming reinforced-concrete frame building - from seismic hazard to collapse safety and economic losses," *Earthquake Engineering and Structural Dynamics*, 36 (13), 1973-1997.

Harden, C. W. 2003. "Numerical modeling of the non-linear cyclic response of shallow foundations." *M.S. Thesis, University of California, Irvine.*

Harden, C. W., Hutchinson, T., Martin, G. R., and Kutter, B. L. 2005. "Numerical Modeling of the Nonlinear Cyclic Response of Shallow Foundations", *Report for Pacific Earthquake Engineering Research Centre, PEER 2005/04*, August 2005.

Houlsby, G. T., Cassidy, M. J. 2002. "A plasticity model for the behavior of footings on sand under combined loading." *Geotechnique*, Vol. 52, No. 2, 117 – 129

Housner, G. 1963. "The Behavior of Inverted Pendulum Structures During Earthquakes," *Bulletin of the Seismological Society of America*, v. 53, 2, 403-417.

Matlock, H. 1970. "Correlations for design of laterally loaded piles in soft clay." *Proceedings, 2nd Annual O_shore Technological Conference*, Houston, Texas, 1(1204), 577–594.

Meyerhoff, G. G., 1963. "The ultimate bearing capacity of foundations." *Geotechnique*, 2, 301–332.

Mosher, R. 1984. "Load transfer criteria for numerical analysis of axially loaded piles in sand", *US Army Engineers Waterways Experiments Station, Vicksburg,* MS*,* Vol. 1.

Nova, R. and Montrasio, L. 1991. "Settlements of shallow foundations on sand." *Geotechnique*, Vol. 41, No. 2, 243 – 256

OpenSees 2008. "Open system for earthquake engineering simulation – development platform by peer." *http://opensees.berkeley.edu/.*

Priestley, M.J.N., Evison, R.J., and Carr, A.J. 1973. "Seismic response of structures free to rock on their foundations." *Bulletin of the New Zealand National Society for Earthquake Engineering*. 11(3): 141-150.

Rankine, W. J. M. 1857. “On the stability of loose earth”. *Philosophical Transactions of the Royal Society of London*, Vol. 147.

Raychowdhury, P. and Hutchinson, T. 2008. “Nonlinear material models for Winkler-based shallow foundation response evaluation.” *In the Proceedings of GeoCongress 2008*, New Orleans, Louisiana, March. (In Press).

Reese, L. C. and Neill, M. 1988. “Field load tests of drilled shafts.” *Deep Foundations on Board and Auger Piles*, Van IMpe Edited, Balkema, Rotterdam, 145–191.

Rollins, K. and Cole, R. 2006. “Cyclic lateral load behavior of a pile cap and backfill.” *ASCE Journal of Geotechnical and Geoenvironmental Engineering*, 132(9), 1143-1153.

Rosebrook, K. R. and Kutter, B. L. 2001. “Soil-foundation structure interaction: Shallow foundations.” *Centrifuge Data Report for the KRR01 Test Series: Center for Geotechnical Modeling Data Report UCD/CGMDR-01/01.*

Salgado, R. 2006.. *The Engineering of Foundations*. McGraw-Hill Science Engineering.

Stewart, J.P., Comartin, C.D., and Moehle, J.P. 2004. “Implementation of soil-structure interaction models in performance based design procedures,” *Proc. 13th World Conf. Earthquake Engrg*., Vancouver, B.C., Canada, Paper 1546.

Stewart, J.P., Kim, S., Bielak, J., Dobry, R., and Power, M. 2003. “Revisions to soil structure interaction procedures in NEHRP design provisions,” *Earthquake Spectra*, 19 (3), 677-696.

Stewart, J. P., Seed, R. B., and Fenves, G. L., 1999. Seismic soil-structure interaction in buildings. I: Analytical aspects, *J. Geotech. & Geoenv. Engrg.*, ASCE, 125, 26-37.

Terzaghi, K., 1943. *Theoretical Soil Mechanics*. John Wiley, New York.

Ugalde, J. A., Kutter, B. L., Jeremic, B., and Gajan, S. 2007. “Centrifuge modeling of rocking behavior of structures on shallow foundations” *Proc. 4th Intl. Conf. Earthquake Geotechnical Engineering.,* Paper No. 1484, Thessaloniki, Greece. June 25-28, 2007.

Veletsos, A. S., and Nair V. V., 1975. Seismic interaction of structures on hysteretic foundations, *J. Struct. Engrg*., ASCE, 101, 109-129.

Vijayvergiya, V. 1977. “Load-movement characteristics of piles.” Prceeding, *Ports 77 Conference, ASCE*, Long Beach, California, March.

Appendix

1. TCL Code for OpenSees Simulations of Benchmark Building Using CIM Model: 4-Story, Slow Lateral Cyclic Loading

```
# Tcl file for Benchmark building simulations
# written by: S. Gajan <s.gajan@ndsu.edu>
# units used: mass [Kg], length [m], time [s], and force [N]

# wipe out everything
wipe

# build a 2D model with 3 DOF
model BasicBuilder -ndm 2 -ndf 3

# height of each floor and foundation
set hFloor 3.355
set hFooting 1.82

# define nodes
node 1 0 0
node 2 0 0
node 3 0 $hFooting

for {set n 1} {$n <= 4} {incr n 1} {
	node [expr $n+3] 0 [expr $hFooting + $n*$hFloor]
}

# linear coordinate transformation
geomTransf Linear 1

# define CIM – implemented as soilFootingSection2d in OpenSees
# section SFS2d matID Vult L Kv Kh Theta_Elastic Rv deltaL
section soilFootingSection2d 1 1.81e+7 14.63 8.14e+8 7.5e+8 0.001 0.1 0.01

# SFS2d material must be used with a zeroLengthSection (ZLS) element
# element ZLS eleID iNode jNode matID <orientation vectors>
element zeroLengthSection 1 1 2 1 -orient 0 -1 0 1 0 0

# define elasticBeamColumn elements for structural footing and shear wall
# element elasticBeamColumn eleID iNode jNode A E I coord-trans
set E 2.0e+9
```

```
# footing element
element elasticBeamColumn 2 2 3 63.93 $E 1140.33 1

# shear wall elements
for {set n 1} {$n <= 4} {incr n 1} {
	element elasticBeamColumn [expr $n+2] [expr $n+2] [expr $n+3] 22.32 $E 99.69 1
}

# fix the base node in all three directions – the bottom end of CIM (SFS2d)
fix 1 1 1 1

# defining gravity loads – done in 10 increments
set wFooting -2.67e+5
set hFloor -7.8e+4

pattern Plain $n Linear {
	     load [expr $n+2] 0 $wFooting 0
	    load [expr $n+3] 0 $wFloor 0
	    load [expr $n+4] 0 $wFloor 0
	    load [expr $n+5] 0 $wFloor 0
	    load [expr $n+6] 0 $wFloor 0
	}


# define analysis objects for gravity loading
test NormDispIncr 1e-12 10 1
algorithm Newton
system SparseGeneral
constraints Plain
numberer Plain
analysis Static

# define recorders
set name "node"
for {set n 1} {$n <= 7} {incr n 1} {
	set fileName [join [list $name $n] {}]
	recorder Node -file $fileName -node $n -dof 1 2 3 disp
}

set name "element"
for {set n 1} {$n <= 6} {incr n 1} {
	set fileName [join [list $name $n] {}]
	recorder Element -file $fileName -time -ele $n force
}

# apply gravity loads first
analyze 10

# set time back to zero again – before shaking
loadConst -time 0.0

# slow lateral cyclic test analysis
# define a load pattern where the displacement is controlled
pattern Plain 2 {Sine 0 8000 1000 -shift 0 -factor 1} {load 7 1 0 0}

# read the input file and apply displacement
set f1 [open "input.txt"]
```

```
set itr 50
set lineNumber 0
set curr 0
set prev 0

while {[gets $f1 line] >= 0} {
	puts "[incr lineNumber]: $line"
	set curr $line
	set d [expr $curr-$prev]

	integrator DisplacementControl 7 1 $d

	test NormDispIncr 1e-12 $itr 0
	set ok [analyze 1]

	if {$ok != 0} {
		test NormDispIncr 1e-10 $itr 0
		set ok [analyze 1]
	}

	if {$ok != 0} {
		test NormDispIncr 1e-8 $itr 0
		set ok [analyze 1]
	}

	if {$ok != 0} {
		test NormDispIncr 1e-6 $itr 0
		set ok [analyze 1]
	}
	set prev $curr
}

close $f1

# print out final node and element outputs on screen

for {set n 1} {$n <= 7} {incr n 1} {
    print node $n
}
print ele

# done - wipe out everything again
wipe
```

2. TCL Code for OpenSees Simulations of Benchmark Building Using CIM

Model: 4-Story, Motion: b (GM 10/50)

```
# Tcl file for Benchmark building simulations
# written by: S. Gajan <s.gajan@ndsu.edu>
# units used: mass [Kg], length [m], time [s], and force [N]

# wipe out everything
wipe

# build a 2D model with 3 DOF
model BasicBuilder -ndm 2 -ndf 3

# height of each floor and foundation
set hFloor 3.355
set hFooting 1.82

# define nodes
node 1 0 0
node 2 0 0
node 3 0 $hFooting

for {set n 1} {$n <= 4} {incr n 1} {
	node [expr $n+3] 0 [expr $hFooting + $n*$hFloor]
}

# linear coordinate transformation
geomTransf Linear 1

# define CIM – implemented as soilFootingSection2d in OpenSees
# section SFS2d matID Vult L Kv Kh Theta_Elastic Rv deltaL
section soilFootingSection2d 1 1.81e+7 14.63 8.14e+8 7.5e+8 0.001 0.1 0.01

# SFS2d material must be used with a zeroLengthSection (ZLS) element
# element ZLS eleID iNode jNode matID <orientation vectors>
element zeroLengthSection 1 1 2 1 -orient 0 -1 0 1 0 0

# define elasticBeamColumn elements for structural footing and shear wall
# element elasticBeamColumn eleID iNode jNode A E I coord-trans
set E 2.0e+9

# footing element
element elasticBeamColumn 2 2 3 63.93 $E 1140.33 1

# shear wall elements
for {set n 1} {$n <= 4} {incr n 1} {
	element elasticBeamColumn [expr $n+2] [expr $n+2] [expr $n+3] 22.32 $E 99.69 1
}

# fix the base node in all three directions – the bottom end of CIM (SFS2d)
fix 1 1 1 1

# defining gravity loads – done in 10 increments
set wFooting -2.67e+5
set hFloor -7.8e+4
```

```
pattern Plain $n Linear {
        load [expr $n+2] 0 $wFooting 0
       load [expr $n+3] 0 $wFloor 0
       load [expr $n+4] 0 $wFloor 0
       load [expr $n+5] 0 $wFloor 0
       load [expr $n+6] 0 $wFloor 0
    }


# define analysis objects for gravity loading
test NormDispIncr 1e-12 10 1
algorithm Newton
system SparseGeneral
constraints Plain
numberer Plain
analysis Static

# define recorders
set name "node"
for {set n 1} {$n <= 7} {incr n 1} {
    set fileName [join [list $name $n] {}]
    recorder Node -file $fileName -node $n -dof 1 2 3 disp
}

set name "node_acc"
for {set n 1} {$n <= 7} {incr n 1} {
    set fileName [join [list $name $n] {}]
    recorder Node -file $fileName -time -node $n -dof 1 accel
}

set name "element"
for {set n 1} {$n <= 6} {incr n 1} {
    set fileName [join [list $name $n] {}]
    recorder Element -file $fileName -time -ele $n force
}

# apply gravity loads first
analyze 10

# set time back to zero again – before shaking
loadConst -time 0.0

# wipe gravity analysis objects
wipeAnalysis

# define mass at each floor (for seismic loading)
set mass_floor 3.75e+5

for {set n 1} {$n <= 4} {incr n 1} {
    mass [expr $n+3] $mass_floor 0 0
}

# define analysis objects for seismic loading
algorithm Newton
system UmfPack
constraints Plain
```

```
numberer RCM

# define Newmark integrator with VariableTransient analysis method
integrator Newmark 0.6 0.32
analysis VariableTransient

# define Rayleigh damping for energy dissipation – in structure
rayleigh 0.05 0 0.05 0

# define ground motion characteristics
set dT 0.005
set dTmin [expr $dT/10]
set dTmax $dT

# acceleration time history is read from an external file WVC270b.txt
set Series "Path -filePath WVC270b.txt -dt $dT -factor 9.81"

# acceleration is applied at the fixed base node in horizontal direction (1)
pattern UniformExcitation 2 1 -accel $Series

# apply shaking
set steps 8000
set itr 50


for {set i 1} {$i < $steps} {incr i 1} {
            test NormDispIncr 1e-12 $itr 0
            set ok [analyze 1 $dT $dTmin $dTmax $itr]

             if {$ok != 0} {
             test NormDispIncr 1e-10 $itr 0
             set ok [analyze 1 $dT $dTmin $dTmax $itr]
           }

           if {$ok != 0} {
           test NormDispIncr 1e-8 $itr 0
           set ok [analyze 1 $dT $dTmin $dTmax $itr]
           }

           if {$ok != 0} {
           test NormDispIncr 1e-6 $itr 0
           set ok [analyze 1 $dT $dTmin $dTmax $itr]
           }
}

# print out final node and element outputs on screen

for {set n 1} {$n <= 7} {incr n 1} {
      print node $n
}
print ele

# done - wipe out everything again
wipe
```

3. TCL Code for OpenSees Simulations of Shear Wall Structures Tested in Centrifuge Using CIM

SSG02_03: Slow Lateral Cyclic Loading

```
# Tcl file for shear wall structures tested in centrifuge (test code: ssg02_03)
# written by: S. Gajan <s.gajan@ndsu.edu>
# units used: mass [Kg], length [m], time [s], and force [N]

# wipe out everything
wipe

# build a 2D model with 3 DOF
model BasicBuilder -ndm 2 -ndf 3

# define nodes
node 1 0 0
node 2 0 0
node 3 0 5.0

# linear coordinate transformation
geomTransf Linear 1

# define CIM – implemented as soilFootingSection2d in OpenSees
# section SFS2d matID Vult L Kv Kh Theta_Elastic Rv deltaL
section soilFootingSection2d 1 1.5e+6 2.8 5.6e+5 1.8e+5 0.001 0.1 0.01

# SFS2d material must be used with a zeroLengthSection (ZLS) element
# element ZLS eleID iNode jNode matID <orientation vectors>
element zeroLengthSection 1 1 2 1 -orient 0 -1 0 1 0 0

# define elasticBeamColumn element shear wall
# element elasticBeamColumn eleID iNode jNode A E I coord-trans
set E 2.0e+10

# shear wall element
element elasticBeamColumn 2 2 3 1.3 $E 0.74 1

# fix the base node in all three directions – the bottom end of CIM (SFS2d)
fix 1 1 1 1

# defining gravity loads – done in 10 increments

pattern Plain $n Linear {
        load 3 0 -28500 0
    }


# define analysis objects for gravity loading
test NormDispIncr 1e-12 10 1
algorithm Newton
system SparseGeneral
constraints Plain
numberer Plain
analysis Static

# define recorders
```

```
set name "node"
for {set n 1} {$n <= 3} {incr n 1} {
	set fileName [join [list $name $n] {}]
	recorder Node -file $fileName -node $n -dof 1 2 3 disp
}

set name "element"
for {set n 1} {$n <= 2} {incr n 1} {
	set fileName [join [list $name $n] {}]
	recorder Element -file $fileName -time -ele $n force
}

# apply gravity loads first
analyze 10

# set time back to zero again – before shaking
loadConst -time 0.0

# slow lateral cyclic test analysis
# define a load pattern where the displacement is controlled
pattern Plain 2 {Sine 0 1500 100 -shift 0 -factor 1} {load 3 1 0 0}

# read the input file and apply displacement
set f1 [open "input.txt"]
set itr 50
set lineNumber 0
set curr 0
set prev 0


while {[gets $f1 line] >= 0} {
		puts "[incr lineNumber]: $line"
		set curr $line
		set d [expr $curr-$prev]

		integrator DisplacementControl 3 1 $d

		test NormDispIncr 1e-12 $itr 0
		set ok [analyze 1]

		if {$ok != 0} {
			test NormDispIncr 1e-10 $itr 0
			set ok [analyze 1]
		}

		if {$ok != 0} {
			test NormDispIncr 1e-8 $itr 0
			set ok [analyze 1]
		}

		if {$ok != 0} {
			test NormDispIncr 1e-6 $itr 0
			set ok [analyze 1]
		}
		set prev $curr
}
```

```
close $f1

# print out final node and element outputs on screen

for {set n 1} {$n <= 3} {incr n 1} {
	print node $n
}
print ele

# done - wipe out everything again
wipe
```

4. TCL Code for OpenSees Simulations of Shear Wall Structures Tested in Centrifuge Using CIM

SSG04_10: Dynamic Base Shaking

```
# Tcl file for shear wall structures tested in centrifuge (test code: ssg04_10)
# written by: S. Gajan <s.gajan@ndsu.edu>
# units used: mass [Kg], length [m], time [s], and force [N]

# wipe out everything
wipe

# build a 2D model with 3 DOF
model BasicBuilder -ndm 2 -ndf 3

# define nodes
node 1 0 0
node 2 0 0
node 3 0 5.0

# linear coordinate transformation
geomTransf Linear 1

# define CIM – implemented as soilFootingSection2d in OpenSees
# section SFS2d matID Vult L Kv Kh Theta_Elastic Rv deltaL
section soilFootingSection2d 1 1.5e+6 2.8 5.6e+5 1.8e+5 0.001 0.1 0.01

# SFS2d material must be used with a zeroLengthSection (ZLS) element
# element ZLS eleID iNode jNode matID <orientation vectors>
element zeroLengthSection 1 1 2 1 -orient 0 -1 0 1 0 0

# define elasticBeamColumn element shear wall
# element elasticBeamColumn eleID iNode jNode A E I coord-trans
set E 2.0e+10

# shear wall element
element elasticBeamColumn 2 2 3 1.3 $E 0.74 1

# fix the base node in all three directions – the bottom end of CIM (SFS2d)
fix 1 1 1 1

# defining gravity loads – done in 10 increments

pattern Plain $n Linear {
        load 3 0 -37000 0
    }


# define analysis objects for gravity loading
test NormDispIncr 1e-12 10 1
algorithm Newton
system SparseGeneral
constraints Plain
numberer Plain
analysis Static

# define recorders
```

```
set name "node"
for {set n 1} {$n <= 3} {incr n 1} {
	set fileName [join [list $name $n] {}]
	recorder Node -file $fileName -node $n -dof 1 2 3 disp
}

set name "element"
for {set n 1} {$n <= 2} {incr n 1} {
	set fileName [join [list $name $n] {}]
	recorder Element -file $fileName -time -ele $n force
}

# apply gravity loads first
analyze 10

# set time back to zero again – before shaking
loadConst -time 0.0

# wipe gravity analysis objects
wipeAnalysis

# define mass at node 3 in direction 1 (for seismic loading)
Mass 3 3.65e+4 0 0

# define analysis objects for seismic loading
algorithm Newton
system UmfPack
constraints Plain
numberer RCM

# define Newmark integrator with VariableTransient analysis method
integrator Newmark 0.6 0.32
analysis VariableTransient

# define Rayleigh damping for energy dissipation – in structure
rayleigh 0.05 0 0.05 0

# define ground motion characteristics
set dT 0.005
set dTmin [expr $dT/10]
set dTmax $dT

# acceleration time history is read from an external file input_motion.txt
set Series "Path -filePath input_motion.txt -dt $dT -factor 9.81"

# acceleration is applied at the fixed base node in horizontal direction (1)
pattern UniformExcitation 2 1 -accel $Series

# apply shaking
set steps 4000
set itr 50


for {set i 1} {$i < $steps} {incr i 1} {
		test NormDispIncr 1e-12 $itr 0
		set ok [analyze 1 $dT $dTmin $dTmax $itr]
```

```
            if {$ok != 0} {
            test NormDispIncr 1e-10 $itr 0
            set ok [analyze 1 $dT $dTmin $dTmax $itr]
          }

          if {$ok != 0} {
          test NormDispIncr 1e-8 $itr 0
          set ok [analyze 1 $dT $dTmin $dTmax $itr]
          }

          if {$ok != 0} {
          test NormDispIncr 1e-6 $itr 0
          set ok [analyze 1 $dT $dTmin $dTmax $itr]
          }
}

# print out final node and element outputs on screen

for {set n 1} {$n <= 3} {incr n 1} {
      print node $n
}
print ele

# done - wipe out everything again
wipe
```

5. TCL Code for OpenSees Simulations of Bridge Structures Tested in Centrifuge Using CIM

JAU_01_05: Dynamic Base Shaking

```
# Created by Jose Ugalde 2-07
# units used: Newton, meter, Kg and sec.

# wipe out everything
wipe

# name of this file
set filename dynamic6node_Eall.tcl

# build a 2D model with 3 DOF
model BasicBuilder -ndm 2 -ndf 3

set bla [clock seconds]
#set dataDir [clock format $bla -format "%a_%b_%d_%H-%M-%S_%Y"];
# name for data directory
set dataDir v1.13
set appendTag 6nodeEall_freeslidingsmalldL2_6percent_Rv0.15;
set dataDir [concat $appendTag$dataDir];
file mkdir $dataDir/;                          # create data directory
set GMdir [pwd]

# copy this file to folder with data saved
file copy -force $filename $dataDir/$filename

set pi [expr acos(-1)];

# Structure Properties
set E 6.9e10
set I 0.107
set A 0.348
set Hdeckcg 13.47
set Hfootcg 1.215;          # Structure E (3 Dc)
set Hfoot 1.63
set Hcol  9
set Mdeck 926e3
set Mfoot 173e3; # Structure E (3 Dc)
set Ideck 3.34e6
set Ifoot 8.67e5;   # Structure E (3 Dc)



#Define Paramters for macro element use
#---------------------------------------
# B, Df, gamma, phi, c, nu, and N160 not teeded if defining stiffnesses and FS manually

# Non-physical parameters
set Rv 0.15;                                   #Rebound ratio
set deltaL 0.002;                      #internal footing node spacing

# Physical parameters
set L 5.4;                                     #length of footing for Station E (B=3Dc)
set B $L;                                      #width of footing
set Vtot [expr ($Mdeck+$Mfoot)*9.81];          #Vertical load on bottom of footing
```

```
set Vfoot [expr $Mfoot*9.81];           #Weight of footing
set Vdeck [expr $Mdeck*9.81];           #Weight of deck
set Df    1.7;                          #Depth of embedment

# use FScalc script to calc FS
set gamma 16000;                        # Bouyant unit weight of soil (N/m^3)
set phi 40;                             # friction angle in degrees
set c 0;                                # "cohesion"
source FScalc.tcl;                # calc FS

set Vult [expr $Vtot*$FS]

# stiffness calculator input
set nu 0.3;                             # poison's ratio
set N160 30;                            # SPT blow count normalized for energy and overburden
source GazetasStiff_1.0.tcl;            # calculate Kv and Kh using FEMA356 formulas


# define nodes
node 1 0 0;                             #base node of macro element
node 2 0 0;                             #soil/footing interface
node 3 0 $Hfoot;                        #bottom of column
node 4 0 $Hfootcg;                      #Hcg of footing mass
node 5 0 [expr $Hfoot + $Hcol];   #top of column
node 6 0 $Hdeckcg;                      #Hcg of deck mass

# Create Elements

# Geometry of column elements
geomTransf Linear 1



# Foudations/ Soil element
# section SFS2d matID Vult L Kv Kh Theta_Elastic Rv deltaL
section soilFootingSection2d 1  $Vult  $L  $Kv  $Kh    0.001   $Rv     $deltaL

# element ZLS                   eleID    iNode    jNode    matID
element zeroLengthSection       1        1        2        1        -orient 0 -1 0 1 0 0

# Structure Elements
# element EBC              eleID iNode      jNode    area       E          I           crdTransTag
element elasticBeamColumn     2    2     3    [expr $A*4]    [expr $E*4]     [expr $I*5]     1 #to bot. of column almost
rigid (much stiffer than column)
element elasticBeamColumn     3    3     4     [expr $A*4]     [expr $E*4]     [expr $I*5]  1
element elasticBeamColumn     4    4     5     $A        $E        $I
element elasticBeamColumn     5    5     6     [expr $A*4]     [expr $E*4]            [expr $I*5]   1  #top of column to
center of deck mass almost rigid

# Boundary Conditions
fix 1 1 1 1;
fix 2 0 0 0;
fix 3 0 0 0;
fix 4 0 0 0;
fix 5 0 0 0;
fix 6 0 0 0;
```

```
# defining gravity loads
pattern Plain 1 Linear {load 4 0 -$Vfoot 0};
pattern Plain 2 Linear {load 6 0 -$Vdeck 0};

# define static analysis objects
test NormDispIncr 1e-10 800 1
algorithm Newton
system UmfPack
constraints Plain
numberer Plain
analysis Static

# define recorders
set dispSuffix disp.out;
set accelSuffix accel.out;

for {set n 1} {$n <= 6} {incr n 1} {
	recorder Node -file $dataDir/node$n$dispSuffix -time -node $n -dof 1 2 3 disp
	recorder Node -file $dataDir/node$n$accelSuffix -time -node $n -dof 1 2 3 accel
}


for {set n 1} {$n <= 5} {incr n 1} {
    recorder Element -file $dataDir/element$n.out -time -ele $n force
}

puts " ";
puts "---------  Static Analysis Started --------";
puts " ";

# apply gravity loads first
analyze 1
loadConst -time 0.0

# wipe static analysis
wipeAnalysis
puts "----------  Static Analysis Done  ----------";

# Dynamic Analysis

# nodal masses
mass 4 $Mfoot $Mfoot $Ifoot
mass 6 $Mdeck $Mdeck $Ideck


# define dynamic analysis objects
test NormDispIncr 1e-12 1 1
algorithm Newton
system UmfPack
constraints Plain
numberer RCM
integrator Newmark 0.5 0.25;
analysis VariableTransient;				# enable for substepping

# define DAMPING-----------------
# apply Rayleigh DAMPING from $xDamp
# D=$alphaM*M + $betaKcurr*Kcurrent + $betaKcomm*KlastCommit + #$beatKinit*$Kinitial
```

```
set xDamp 0.06;                                    # 5% damping ratio
set lambda [eigen 1];                         # eigenvalue mode 1
set omega [expr pow($lambda,0.5)];
set alphaM 0.;                                # M-prop. damping; D = alphaM*M
set betaKcurr 0.;                 # K-proportional damping;      + beatKcurr*KCurrent
set betaKcomm [expr 2.*$xDamp/($omega)];   # K-prop. damping parameter;   #+betaKcomm*KlastCommitt
set betaKinit 0.;                         # initial-stiffness proportional damping      #+beatKinit*Kini

rayleigh $alphaM $betaKcurr $betaKinit $betaKcomm;
#RAYLEIGH damping

# Dyanmic Loading

# time step
set dT 0.002618408

set dTmin [expr $dT/150];
set dTmax $dT;

# Motion file
set motionName benchmarkStringMotion1.txt
set scaleFactor 0.001
set Series "Path -filePath $GMdir/$motionName -dt $dT -factor $scaleFactor"

# copy motion file to folder with data saved
file copy -force $GMdir/$motionName $dataDir/$motionName

# Time analysis
set startT [clock seconds]

# Apply to base node
# pattern UE              tag       direction           time series type    $Motion
pattern UniformExcitation         3         1                   -accel                              $Series

set steps 31353; #for string of events 5,6,8
set itr 90
set disptag 0

#set TestType NormDispIncr;
set TestType EnergyIncr;

# Set 4 tolerances
set tol1 1e-17;
set tol2 5e-14;
set tol3 1e-12;
set tol4 1e-7;

puts " ";
puts "---------  Dynamic Analysis Started --------";
puts " ";



# do dynamic analysis
source analysisMultiTol_substep.tcl;                  # enable for substeping
puts " ";
```

```
puts "-------------------------------------------";
puts "----------  Dynamic Analysis Done ------";

# end timing
set endT [clock seconds]
set dt [expr $endT-$startT]
set timeMin [expr $dt/60]

# print to screen
puts "-------------------------";
puts "$dt seconds";
puts "$timeMin minutes";

# wipe out everything again
wipe
```

 # Name of this file: FScalc.tcl

```
set phi [expr $phi*$pi/180];
set Nq [expr pow(tan($phi/2+$pi/4),2)*exp($pi*tan($phi))];
set Nc [expr ($Nq-1)/tan($phi)];
set Ng [expr 2*($Nq+1)*tan($phi)];

set Fqs [expr 1 + ($B/$L)*tan($phi)];
set Fcs [expr 1 + ($B/$L)*($Nq/$Nc)];
set Fgs [expr 1 - 0.4*($B/$L)];

# Depth Factors (Hansen 1970) for Df<B
# need to edit or add conditional statement if Df>B

set Fcd [expr 1 + 0.4*($Df/$B)];
set Fqd [expr 1 + 2*tan($phi)*($Df/$B)*pow((1-sin($phi)),2)];
set Fgd 1;

set qu [expr $c*$Nc*$Fcs*$Fcd + $gamma*$Df*$Nq*$Fqs*$Fqd + 0.5*$gamma*$B*$Ng*$Fgs*$Fgd];
set q [expr $Vtot/($B*$L)];

set FS [expr $qu/$q];
```

 # Name of this file: GazetasStiff_1.0.tcl

```
# subroutine to calculate Gazetas Stiffnesses

# Calculate Shear Modulus under foundation (equn 4-5) in FEMA 356

# in Pa
set sv [expr $Vtot/($B*$L)]
# in psf
set sv [expr $sv/47.88]
set Go [expr 20000*pow($N160,0.33)*sqrt($sv)]
set G_overGo 1.0
set G [expr $Go*$G_overGo]
# in Pa
set G [expr $G*47.88]

# Calculate stiffnesses
# at surface
set Kxsurf [expr $G*$B/(2-$nu)*(3.4*pow(($L/$B),0.65)+1.2)]
set Kzsurf [expr $G*$B/(1-$nu)*(3.4*pow(($L/$B),0.65)+0.8)]

# embedment factors
# for JAU01 hieght of effective sidewall contact is same as depth of embedment
set d $Df

# therefore depth to centroid of effective sidewall contact is half Df
set h [expr $Df/2]

set BetaX [expr (1+0.21*sqrt($Df/$B))*(1+1.6*pow(($h*$d*($B+$L)/($B*$L*$L)),0.4))]
set BetaZ [expr (1+$Df/(21*$B)*(2+2.6*$B/$L))*(1+0.32*pow(($d*($B+$L)/($B*$L*$L)),(2/3)))]

# Embedded Stiffnesses

set Kh [expr $BetaX*$Kxsurf]
set Kv [expr $BetaZ*$Kzsurf]
```

 # Name of this file: analysisMultiTol_substep.tcl

```
# analysis using 4 tolerance levels

# set counters for how many steps per tolerance
set b1 0;
set b2 0;
set b3 0;
set b4 0;

for {set i 1} {$i < $steps} {incr i 1} {
puts $i;                                                #Display increment number
      test $TestType $tol1 $itr $disptag;          #Test convergence with tight tolerance
      set b1 [expr $b1 + 1];
      set ok [analyze 1 $dT $dTmin $dTmax $itr];          #Substep if doesnt converge

           if {$ok!=0} {                    ;
           test $TestType $tol2 $itr $disptag;
           set b2 [expr $b2 + 1];
           set ok [analyze 1 $dT $dTmin $dTmax $itr];
           }

           if {$ok!=0} {                    ;
           test $TestType $tol3 $itr $disptag;
           set b3 [expr $b3 + 1];
           set ok [analyze 1 $dT $dTmin $dTmax $itr];
           }

           if {$ok != 0} {
            error "no convergence"
      }
}

set Ntol1 [expr $b1-$b2];
set Ntol2 [expr $b2-$b3];
set Ntol3 [expr $b3-$b4];
set Ntol4 $b4;
set Total [expr $Ntol1+$Ntol2+$Ntol3+$Ntol4];

puts $Ntol1
puts $Ntol2
puts $Ntol3
puts $Ntol4
puts $Total
```

6. TCL Codes for OpenSees Simulations of Benchmark Building Using BNWF Model: 4-Story, Slow Lateral Cyclic Loading

```
#####################################################
# Tcl file for Benchmark building simulations
# Written by: P. Raychowdhury <pri@ucsd.edu>
# Units used: mass [Kg], length [m], time [s], and force [N]
# Name of file: "Main.tcl"; this is the main file; the other files mentioned in the code need to be sourced
#####################################################

wipe
wipeAnalysis

set PI 3.143
set g 9.81;	#--m/s^2
set inFile Cyclic_mm.dat; #--name of the input cyclic load input file
set path out/cyclic
#-------------------------------
# Assign Structural Dimensions
#-------------------------------
set Lwall 7.32;	#----length, width and height of shear wall in m
set Bwall 3.05
set Hwall 13.42
#-------------------------------
# Assign Mass and weight
#-------------------------------
set Mg [expr 3.75*pow(10,5)];	#---mass per floor (kg)
set Wg [expr 5.78*pow(10,6)];	#---total gravity load on footing
set massFooting  [expr 2.72*pow(10,5)]
#---------------------------------------------
# Assign Soil Properties and Footing Dimension
#---------------------------------------------
set soilType 1;	#---soiltype clay 1, sand 2
set cd 0.;	#---ratio of maximum drag to ultimate resistance
set phi 0.0001;	#---friction angle (in deg; cohesionless soil; but given a very small value to avoid solution failure)
set gamma 16200.; #---unit wt (N/m^3)
set beta 0.;		#---angle of load applied
set c [expr 52.0*pow(10,3)];	#---cohesion
set Gmax [expr 26.33*pow(10,6)];  #---provided by Christine
set neu 0.5;		#---Poisson's ratio
set crad 0.05;	#---radiation damping (default value=5%)
set damping 0.05;	#---rayleigh damping (default value=5%)
set tp 0.10;	#---uplift capacity (default value=10%)
set stripL 14.63;  #-length, width and height of the strip footing in m
set stripB 4.37
set stripH 1.82
set Df 0.0;	#---depth of embedment
#-------------------------------
# Assign FEM mesh properties
#-------------------------------
set ndive 20;		#----no of divisions at end region; should always be even
set ndivm $ndive;
set ratioe 20.;	#----End length ratio (Lend/L)
#-------------------------------
```

```
# Create ModelBuilder
#-------------------------------
model BasicBuilder -ndm 2 -ndf 3
geomTransf Linear 1
geomTransf Linear 2
#-------------------------------
# Calling Source Files
#-------------------------------
source Nodes.tcl
source Foundation.tcl
source Materials.tcl
source Elements.tcl
source Recorder.tcl
source eigen.tcl
source Analysis.tcl
#-------------------------------
# End of Main.tcl
#-------------------------------
```

```
##############################################
## File Name: Nodes.tcl
##############################################
set L $stripL
set Le [expr $ratioe*$L/100.];       #end length
set Lm [expr $L-2*$Le];              #mid length
set ratiom [expr ($Lm/$L)*100.];     #Mid length ratio
set le  [expr $Le/$ndive];        #---element length at end region
set lm  [expr $Lm/$ndivm];        #---element length at mid region
set nom [expr $ndivm-1];          #---no of nodes in mid region
set noe [expr $ndive+1];          #---no of nodes in each end region
set not [expr $nom+2*$noe];       #---total no of nodes in the footing
set elet [expr $not-1] ;       #---total no of elements in the footing

#nodes at the footing level starts from 1
#nodes at the spring level starts from 1001

for {set ix 1} {$ix<=$noe} {incr ix 1} {
##--left end portion
  node    $ix                        [expr $le*($ix-1)]      0.
  node    [expr 1000+$ix]   [expr $le*($ix-1)]      0.
  fix [expr 1000+$ix]          1  1  1
##--right end portion
node      [expr $ix+$noe+$nom]        [expr $L-$Le+$le*($ix-1)]     0.
node      [expr 1000+$ix+$noe+$nom]   [expr $L-$Le+$le*($ix-1)]     0.
fix [expr 1000+$ix+$noe+$nom]    1  1  1
 }
##--mid portion
for {set im 1} {$im<=$nom} {incr im 1} {
node      [expr $im+$noe]        [expr $Le+$lm*$im]     0.
node      [expr 1000+$im+$noe]      [expr $Le+$lm*$im]     0.
fix [expr 1000+$im+$noe]     1  1  1
 }
#------------------------------
# set the midnode and mid ele
#------------------------------
set midnode [expr ($not+1)/2]
set endnode [expr $not]
```

```
set midele1 [expr $midnode-1]
set midele2 [expr $midnode]
set endSpring [expr 1000+$endnode]

#nodes created for horizontal springs
#node IDtag  x      y
node 8001    0.     0.
node 8002    0.     0.

#fix  IDTag    x  y  rot
fix   8001              1  1  1
fix   8002              1  1  1

#---shear wall nodes-----
#node IDtag   x     y
node 8003     0.    [expr $Hwall*0.25+$stripH/2.]
node 8004     0.    [expr $Hwall*0.5+$stripH/2.]
node 8005     0.    [expr $Hwall*0.75+$stripH/2.]
node 8006     0.    [expr $Hwall*1.0+$stripH/2.]

##################################################
## End of Nodes.tcl
##################################################


##################################################
## File Name: Foundation.tcl
##################################################
##---bearing capacity of the foundation is calculated as Meyerhof, 1963
set PI 3.143
set radphi [expr $PI*$phi/180.]
set theta [expr $PI/4.+$radphi/2.]
set Nphi1 [expr pow(tan($theta),2)]
set Nq [expr $Nphi1*exp($PI*tan($radphi))]
#set Nc [expr ($Nq-1.0)/(tan($radphi))]
set Nc 5.14
set Ngamma [expr ($Nq-1.0)*tan(1.4*$radphi)]
puts "Nc = $Nc, Nq = $Nq, Ngamma = $Ngamma"
set B $stripB
set L $stripL
set H $stripH

##--ALL BEARING CAPACITY FACTORS ARE CALCULATED AFTER MEYERHOF, 1963
#---shape factors---
set Fcs [expr 1+ 0.2*($B/$L)*$Nphi1]
set Fqs [expr 1+ 0.1*($B/$L)*$Nphi1]
set Fgammas [expr $Fqs]
#puts "Fcs = $Fcs, Fqs = $Fqs, Fgammas = $Fgammas"

#---depth factors---
set Fcd [expr 1.+ 0.2*($Df/$B)*(pow($Nphi1,0.5))]
set Fqd [expr 1.+ 0.1*($Df/$B)*(pow($Nphi1,0.5))]
set Fgammad [expr $Fqd]
#puts "Fcd = $Fcd, Fqd = $Fqd, Fgammad = $Fgammad"

#---inclination factors---
set Fci [expr pow((1-$beta/90),2)];   #--beta in the angle of load application wrt vertical
```

```
set Fqi [expr $Fci]
set Fgammai [expr pow((1-$beta/$radphi),2)]
#puts "Fci = $Fci, Fqi = $Fqi, Fgammai = $Fgammai"

#---ultimate bearing capacity----
set q1 [expr $c*$Nc*$Fcs*$Fcd*$Fci]
set q2 [expr $gamma*$Df*$Nq*$Fqs*$Fqd*$Fqi]
set q3 [expr 0.5*$gamma*$B*$Ngamma*$Fgammas*$Fgammad*$Fgammai]
set qu [expr $q1+$q2+$q3]
set Qult [expr $qu*$L*$B];            #--ultimate load capacity
set FSv [expr $Qult/$Wg]
set qult [expr $Qult/$stripL]; #-bearing capacity per unit length (N/m)
set q1mid [expr $qult*$lm];    #---capacity of the each mid-spring
set q1end [expr $qult*$le*0.5];#---capacity of each extreme end spring
set q2end [expr $qult*$le];    #---capacity of other end region springs
##-------------------
## Sliding Capacity
##-------------------
set Qf [expr $stripB*$stripL*$c];  #--Frictional sliding capacity
#set Qf [expr 26.*pow(10,6)] ; #----provided by John Stewart on Jan-07
##----------------------------
## Stiffness Calculation
##----------------------------
#---soil stiffness is calculated as Gazetas, 1991
#set G [expr $E/(2.*(1+$neu))];
set G [expr $Gmax]; #given by Christina Goulet

#---for horizontal soil springs---
set kx [expr $G*$L/(2.-$neu)*(2.+2.5*((pow ($B, 0.85))/(pow ($L,0.85))))]
set kxf $kx

#---for vertical soil springs-----
set ratioK 3.0
set kmid [expr $kz/($Lm+2.*$Le*$ratioK)];            #mid region intensity
set kend [expr $kmid*$ratioK];                       #end region intensity
set kzm [expr $kmid*$lm]                          ;#stiffness of mid springs
set kze1 [expr $kend*$le*0.5]                     ;#stiffness of extreme end springs
set kze2 [expr $kend*$le]                         ;#stiffness of other end springs
puts "k1end=$kze1, k2end=$kze2, kmid=$kzm,"
###############################################
## End of Foundation.tcl
###############################################

###############################################
## File Name: Materials.tcl
###############################################
set Ist [expr $stripB*pow($stripL,3)/12]; #---I of total footing
set Ie [expr $Ist/$elet];       #---I for each footing element
set Ast [expr $stripB*$stripH];    #----area of whole footing
#set Ast [expr $Bxx*$Lxx]; #for increased K_x and Q_f case
set Ae [expr $Ast/$elet];
set Ae $Ast;                 #-----area of each element
set Awall [expr $Bwall*$Lwall]
set alpha 0.1
set Econc [expr $alpha*2.15*pow(10,10)];      #----[N/m^2];
set Iwall [expr $Bwall*pow($Lwall,3)/12.]
set EI [expr $Iwall*$Econc]
```

```
set EIfoot [expr $Ist*$Econc]

#uniaxialMaterial Elastic $matTag $E
uniaxialMaterial Elastic   1       $Econc

#---------------------------------------------------
# QzSimple1 MATERIAL, PySimple1 and TzSimple1 Material
#---------------------------------------------------
if {$soilType ==1} {
##Qz Properties
     set z1mid [expr 0.525*$q1mid/$kzm]
     set z1end [expr 0.525*$q1end/$kze1]
     set z2end [expr 0.525*$q2end/$kze2]
##Py Properties
#     set y50 [expr 8.0*$Pult/$kx]
##Tz Properties
     set zt50 [expr 0.708*$Qf/$kx]
 }
if {$soilType ==2} {
set z1mid [expr $q1mid*1.39/$kzm]
set z1end  [expr $q1end*1.39/$kze1]
set z2end  [expr $q2end*1.39/$kze2]

##Py Properties
#    set y50 [expr 0.542*$Pp/$kxp]
##Tz Properties
     set zt50 [expr 2.05*$Qf/$kxf]
 }
#puts "z501=$z1end, y50=$y50, zt50= $zt50"

##--material      QzSimple1   $matTag   $soilType     $qult     $z50     $TP    $crad
uniaxialMaterial  QzSimple1    3       $soilType     $q1mid    $z1mid    $tp    $crad
uniaxialMaterial  QzSimple1    4       $soilType     $q1end    $z1end    $tp    $crad
uniaxialMaterial  QzSimple1    5       $soilType     $q2end    $z2end    $tp    $crad
#
##--material      PySimple1   $matTag   $soilType     $pult     $y50   $Cd
##uniaxialMaterial  PySimple1    6      $soilType     $Pult     $y50   $cd
#
##--material      TzSimple1   $matTag   $soilType     $tult    $zt50     $Cd
uniaxialMaterial   TzSimple1    7       $soilType     $Qf      $zt50     $cd
###--material      Elastic   $matTag    $E
uniaxialMaterial  Elastic      8      $kxf
uniaxialMaterial  Elastic      9      $kzm
uniaxialMaterial  Elastic      10      $kze1
uniaxialMaterial   Elastic      11      $kze2
##################################################
## End of Materials.tcl
##################################################
##################################################
## File Name: Elements.tcl
##################################################
#---------------------------------
# mass assignment
#---------------------------------
for {set im 8003} {$im<=8006} {incr im 1} {
mass  $im   $Mg    0.01    0.01
 }
```

```
#mass  $midnode   $massFooting    0    0

#-------------------------------------
#Footing elements
#-------------------------------------
##--end portion
for {set iz 1} {$iz<=$ndive} {incr iz 1} {
 #element elasticBeamColumn    $eleTag    $iNode     $jNode    $A    $E   $I    $transfTag
 element elasticBeamColumn    $iz        $iz      [expr $iz+1]     $Ae      $Econc    [expr $Ie+$Ae*pow(($le*$iz-$le),2)]        1
 element elasticBeamColumn   [expr $iz+$noe+$nom] [expr $iz+$noe+$nom]  [expr $iz+$noe+$nom+1]  $Ae $Econc    [expr $Ie+$Ae*pow(($L-2*$Le+$Le*$iz),2)]   1
#element elasticBeamColumn    $iz $iz      [expr $iz+1]     $Ae     $Econc    [expr $Ie+$Ae]        1
#element elasticBeamColumn   [expr $iz+$noe+$nom] [expr $iz+$noe+$nom]  [expr $iz+$noe+$nom+1]  $Ae $Econc    [expr $Ie+$Ae]        1
}
##--mid portion
for {set im 0} {$im<=$ndivm-1} {incr im 1} {
element elasticBeamColumn    [expr $im+$noe]      [expr $im+$noe]       [expr $im+$noe+1]      $Ae   $Econc [expr $Ie+$Ae*pow(($Le+$lm*$im),2)]        1
}
#-------------------------------------
# shear wall elements
#-------------------------------------
#element elasticBeamColumn  $eleTag  $iNode    $jNode   $A     $E   $Iz    $transfTag
element elasticBeamColumn   8003    $midnode   8003    $Awall   $Econc    $Iwall     2
element elasticBeamColumn   8004    8003       8004       $Awall   $Econc     $Iwall     2
element elasticBeamColumn   8005    8004       8005       $Awall   $Econc    $Iwall     2
element elasticBeamColumn   8006    8005       8006       $Awall   $Econc    $Iwall     2
#-------------------------------------
# creating spring elements
#-------------------------------------
#---vertical springs elements---------------------------------------
### Two Extreme End Springs ###
element zeroLength      1001              1              1001              -mat     10    -dir    2
element zeroLength      $endSpring     $endnode     $endSpring     -mat     10    -dir    2
### Other end Springs ###
for {set ix 2} {$ix<=$noe} {incr ix 1} {element zeroLength   [expr 1000+$ix]       [expr $ix]     [expr 1000+$ix]  -mat   11   -dir  2
element zeroLength   [expr 1000+$ix+$noe+$nom-1]   [expr $ix+$noe+$nom-1]   [expr 1000+$ix+$noe+$nom-1] -mat   11   -dir   2
 }
### Mid Springs ###
for {set iy 1} {$iy<=$nom} {incr iy 1} {
 element zeroLength  [expr 1000+$iy+$noe]   [expr $iy+$noe]   [expr 1000+$iy+$noe]     -mat  9  -dir  2
 }
#---horizontal springs elements---------------------------------------
element zeroLength  8001   1   8001  -mat  8  -dir      1
element zeroLength  8002  1  8002  -mat  8  -dir  1
##############################################
## End of Elements.tcl
##############################################

##############################################
```
File Name: ***Recorder.tcl***
```
##############################################
###--recording only mid node and mid element--##
```

```
 set d [concat midnode.dis]
 set f1 [concat midele1.force]
 set f2 [concat midele2.force]
recorder Node -time -file $path/$d -node $midnode -dof 1 2 3 disp
 recorder Element -file $path/$f1 -time -ele  $midele1 localForce
 recorder Element -file $path/$f2 -time -ele  $midele2 localForce

##---recorder for spring elements----------------------
for {set iy 1} {$iy<=$endnode} {incr iy 10} {
 set s [concat spring$iy.force]
 recorder Element [expr $iy+1000] -file $path/$s -time  force
 recorder Node -file $path/node$iy.dis -time -node  $iy -dof 1 2 3 disp
 }
recorder Element 8001 -file $path/element8001.force -time force
recorder Element 8002 -file $path/element8002.force -time force

###---recorder for the shear wall----------------------
for {set ix 8003} {$ix<=8006} {incr ix 1} {
recorder Element -file $path/element$ix.force -time -ele $ix localForce
recorder Node -time -file $path/node$ix.dis -node $ix -dof 1 2 3  disp
 }
recorder Node -file $path/eigen.out  -time -node 8003 8004 8005 8006  -dof 1 "eigen 1"
recorder  Node -time -file $path/acc.acc  -node $midnode 8003 8004 8005 8006  -dof  1 accel

#---recorder for spring elements and nodes (for mean settlement, record all nodes disp)
recorder Element -file $path/spring.force -eleRange 1001  1020  -time  force
recorder Node -time -file $path/spring.dis -node -nodeRange  1  20 -dof  2  disp
##################################################
## End of Recorder.tcl
##################################################

##################################################
## File Name: eigen.tcl
##################################################
set mt 2    ;#---No of modes to be extracted
eigen frequency $mt
set PI 3.1415926
set lambdax [eigen $mt]
for {set i 1} {$i <= $mt} {incr i 1} {
set lambda [lindex $lambdax [expr $i-1]]
set omega [expr pow($lambda,0.5)]
set Tn [expr 2*$PI/$omega]
set fn [expr 1/$Tn]
puts "For mode=$i, Tn=$Tn sec, fn=$fn Hz"
}
##################################################
## End of eigen.tcl
##################################################

##################################################
## File name: Analysis.tcl
##################################################
#-----------------------
# Gravity LOAD PATTERNS
#-----------------------
pattern Plain 1 "Linear" {
    load  $midnode  0.  [expr $Wg]   0.
```

```
   }
#-----------------
# gravity analysis
#-----------------
system UmfPack
constraints Plain
test NormDispIncr 1.0e-8 40 0
algorithm Newton
numberer RCM
integrator LoadControl 0.1
analysis Static
analyze 10

#loadConst
loadConst -time 0.0

###################################
## Define cyclic loads and loadNode
###################################
set np 14000
set loadNode 8006
set dt 10.
set dir 1
set factor 0.001;      #to convert from mm to m
set gdisp "Path -filePath  $inFile  -dt  $dt -factor  $factor"
pattern MultipleSupport 4  {
groundMotion  4  Series  -disp  $gdisp
#imposedMotion      nodeTag?     dirn?   gMotionTag?
imposedSupportMotion  $loadNode     $dir    4
}
#-------------------------------------------
# Create analysis
#-------------------------------------------
system UmfPack
constraints Transformation
test NormDispIncr 1.0e-2  40  0
algorithm KrylovNewton
numberer RCM
set gamma 0.5
set beta 0.25
integrator Newmark $gamma $beta
analysis Transient
#-----------------------------------------------
#Perform analysis
#-----------------------------------------------
puts "np=$np, dt=$dt"
analyze $np $dt
##############################################
## End of Analysis.tcl
##############################################
```

7. TCL Code for OpenSees Simulations of Benchmark Building Using BNWF Model: 4-Story, Motion: b (GM 10/50)

```
#####################################################
# Tcl file for Benchmark building simulations
# Written by: P. Raychowdhury <pri@ucsd.edu>
# Units used: mass [Kg], length [m], time [s], and force [N]
#####################################################

## All the other files are same as cyclic load files (item-6) except the analysis file.

############################################
## File name: Analysis.tcl
############################################
set gmfact 1.0   ;#setting factor for ground motion units
set dir 1
set dt 0.005
set np 7990
set factg [expr $gmfact*$g]
set accelSeries "Series  -dt  $dt  -filePath    $inFile   -factor    $factg"

##UniformExcitation     nodeTag?   dirn?   -acc     $accSeries
pattern UniformExcitation  4       $dir    -accel   $accelSeries

#---------------------------------------------
# Set Rayleigh damping
#---------------------------------------------
set lambdax [eigen 2]
   set w1 [expr sqrt([lindex $lambdax 0])]
   set w2 [expr sqrt([lindex $lambdax 1])]
   set am [expr $damping*2.0*$w1*$w2/($w1+$w2)]
   set bk [expr $damping*2.0/($w1+$w2)]
set bkinit  0.0
set bklast  0.0
rayleigh  $am $bk $bkinit $bklast
puts "$w1 $w2 $am $bk"
#-----------------------------
# Create analysis
#-----------------------------
system UmfPack
constraints Transformation
test NormDispIncr 1.0e-2  40  0
algorithm KrylovNewton
numberer RCM
#Create the integration scheme Newmark with gamma = 0.5 and beta =  0.25
set gamma 0.5
set beta 0.25
#integrator Newmark $gamma $beta $am $bk $bkinit $bklast
integrator Newmark $gamma $beta
analysis Transient
analyze $np $dt
############################################
## End of Analysis.tcl
############################################
```

8. TCL Code for OpenSees Simulations of Shear wall Structures Tested in Centrifuge Using BNWF Model

SSG02_03: Slow Lateral Cyclic Loading

```
#######################################################
# Tcl file for shear wall structures tested in centrifuge (test code: ssg02_03)
# Written by: P. Raychowdhury <pri@ucsd.edu>
# Units used: mass [Kg], length [m], time [s], and force [N]
#######################################################

####################################################
## Name of File: Main.tcl
####################################################
wipe
wipeAnalysis
#-------------------------------
# Create ModelBuilder
#-------------------------------
model BasicBuilder -ndm 2 -ndf 3
geomTransf Linear 1
geomTransf Linear 2
#-------------------------------
# Calling Source Files
#-------------------------------
source Prop.tcl
source Nodes.tcl
source Foundation.tcl
source Materials.tcl
source Elements.tcl
source Recorder.tcl
source Analysis.tcl
####################################################
## End of Main.tcl
####################################################
####################################################
## Name of File: Prop.tcl
####################################################
#-------------------------------
# Soil Properties
#-------------------------------
#soil properties are according to SSG02 report
set g 9.81;         #--m/s^2
set soilType 2;    #---soiltype clay 1, sand 2
set crad 0.05;      #---radiation damping
set cd 0.;             #---ratio of maximum drag to ultimate resistance
set tp 0.1;           #---uplift capacity
set phi 42.;          #---friction abgle
set gamma 16200.;      #---unit wt (N/m^3)
set beta 0.;                   #---angle of load applied
set c 0.;                        #---cohesion
set Esoil [expr 40.*pow(10,6)];    #---Modulus of soil assumed as 40 MPa for dense sand (Dr=80%)
set neu 0.35;
set kunlFact 1.0
#-------------------------------
# Assign Footing Dimensions
#-------------------------------
set footL 2.80;    #----length, width and height of the strip footing in m
```

```
set footB 0.65
set footH 0.66
set Df 0.;          #---depth of embedment
set Lwall 2.5;     #----length, width and height of shear wall in m
set Bwall 0.38
set Hwall 10.1
set AspRatio 1.7;  #--aspect ratio (M/H/L)
set pod  [expr $AspRatio*$footL] ;      #----point of lateral load application
#-------------------------------
# Assign Mass and FSv
#-------------------------------
set Mg 28880.0;              #---mass of structure in prototype scale (kg), provided by Gajan
set FSv 5.2;                 #---vertical factor of safety, provided by Gajan
set Ealum  [expr 68.9*pow(10,9)];       #[N/m^2];
set Wg [expr $Mg*$g]
set Qult [expr $Wg*$FSv]
#-------------------------------
# Mesh Properties
#-------------------------------
set ratioK  2.5;      #----based on Harden, 2003 (or FEMA-356, chapter-10)
set ratioe  12.      ;#----end length ratio (Le/L)
set ndivm  20      ;#----no of divisions at mid region; should always be even
set ratioDIV 4.0 ;#----ratio of mid element length to end element length

####################################
# Define cyclic loads and loadNode
####################################
set inFile input_disp_SSG02_03.txt
set np 13106
set dt 100.
set dir 1
set factor 0.001
##################################################
## End of Prop.tcl
##################################################

##################################################
## Name of File: Nodes.tcl
##################################################
set L $footL
set B $footB
set Le  [expr $ratioe*$L/100.];    #----end length
set Lm  [expr $L-2*$Le];          #---mid length
set lm  [expr $Lm/$ndivm];        #---element length at mid region
set le  [expr $lm/$ratioDIV];      #---element length at end region
set ndive  [expr int($Le/$le)];     #----no of divisions at end region; should always be even
set nom [expr $ndivm-1];                #---no of nodes in mid region
set noe [expr $ndive+1];                #---no of nodes in each end region
set not [expr $nom+2*$noe];             #---total no of nodes in the footing
set elet [expr $not-1] ;              #---total no of elements in the footing
puts "lm=$lm, le=$le, ratioK=$ratioK, not =$not, noe=$noe, nom=$nom, elet =$elet"

#nodes at the footing level starts from 1
#nodes at the spring level starts from 1001

for {set ix 1} {$ix<=$noe} {incr ix 1} {
##--left end portion
```

```
 node    $ix                               [expr $le*($ix-1)]     0.0
 node    [expr 1000+$ix]   [expr $le*($ix-1)]     0.0
 fix [expr 1000+$ix]          1  1  1
##--right end portion
 node    [expr $ix+$noe+$nom]        [expr $L-$Le+$le*($ix-1)]    0.0
 node    [expr 1000+$ix+$noe+$nom]   [expr $L-$Le+$le*($ix-1)]    0.0

fix [expr 1000+$ix+$noe+$nom]   1  1  1
 }
##--mid portion
for {set im 1} {$im<=$nom} {incr im 1} {
 node    [expr $im+$noe]        [expr $Le+$lm*$im]    0.0
 node    [expr 1000+$im+$noe]      [expr $Le+$lm*$im]    0.0

fix [expr 1000+$im+$noe]    1  1  1
 }
#-------------------
# set the midnode
#-------------------
set midnode [expr ($not+1)/2]
set endnode [expr $not]
set midele1 [expr $midnode-1]
set midele2 [expr $midnode]
set endSpring [expr 1000+$endnode]
puts "midnode=$midnode"

#nodes created for horizontal springs
#node IDtag   x             y
#node  8001    0.           0.
node  8002    0.           0.

#fix  IDTag     x  y  rot
#fix   8001          1  1  1
fix   8002           1  1  1

#---shear wall nodes-----
#node IDtag   x     y
node 8003     0.    $pod
node 8004     0.    $Hwall
####################################################
## End of Nodes.tcl
####################################################

####################################################
## Name of File: Foundation.tcl
####################################################
##-------------------
## Bearing Capacity
##-------------------
##---Bearing capacity of the foundation is calculated as Meyerhof, 1963
set PI 3.143
set radphi [expr $PI*$phi/180.]
set theta [expr $PI/4.+$radphi/2.]
set Nphi1 [expr pow(tan($theta),2)]
set Nq [expr $Nphi1*exp($PI*tan($radphi))]
set Nc [expr ($Nq-1.0)/(tan($radphi))]
set Ngamma [expr ($Nq-1.0)*tan(1.4*$radphi)]
```

```
set B $footL
set L $footB
set H $footH

###--ALL BEARING CAPACITY FACTORS ARE CALCULATED AFTER MEYERHOF,1963
##---shape factors---(Meyerholf, 1963)
set Fcs [expr 1+ 0.2*($B/$L)*$Nphi1]
set Fqs [expr 1+ 0.1*($B/$L)*$Nphi1]
set Fgammas [expr $Fqs]

##---depth factors---(Meyerholf, 1963)
set Fcd [expr 1.+ 0.2*($Df/$B)*(pow($Nphi1,0.5))]
set Fqd [expr 1.+ 0.1*($Df/$B)*(pow($Nphi1,0.5))]
set Fgammad [expr $Fqd]

##---inclination factors---
set Fci [expr pow((1-$beta/90),2)];   #--beta in the angle of load application wrt vertical
set Fqi [expr $Fci]
set Fgammai [expr pow((1-$beta/$radphi),2)]

##---ultimate bearing capacity----
set q1 [expr $c*$Nc*$Fcs*$Fcd*$Fci]
set q2 [expr $gamma*$Df*$Nq*$Fqs*$Fqd*$Fqi]
set q3 [expr 0.5*$gamma*$B*$Ngamma*$Fgammas*$Fgammad*$Fgammai]
set qu [expr $q1+$q2+$q3]
set Qult [expr $qu*$L*$B];            #--ultimate load capacity

set qult [expr $Qult/$L];             #---bearing capacity per unit length (N/m)
set q1mid [expr $qult*$lm];           #---capacity of the each mid-spring
set q1end [expr $qult*$le*0.5];       #---capacity of each extreme end spring
set q2end [expr $qult*$le];           #---capacity of other end region springs

##-------------------
## Sliding Capacity
##-------------------
set shearstress [expr $Wg*tan(0.8*$radphi)]
set Qf [expr $shearstress*$B*$L]
##-------------------
## Passive Capacity
##-------------------
set Kp 11.0;  #based on Coulomb (folllowing Das book)
set Pp [expr 0.8*$Kp*$gamma*$Df*$Df]
set Pp [expr $Pp*$L]

#---soil stiffness is calculated as Gazetas, 1991
set G [expr $Esoil/(2.*(1+$neu))];
puts "G= $G"

#---for horizontal soil springs---
set kx0 [expr ($G*$L/(2.-$neu))*(2.+2.5*((pow ($B, 0.85))/(pow ($L,0.85))))]
set ex [expr (1.+0.15*pow((2.*$Df/$B),0.5))*(1+0.52*pow((16.*($Df-0.5*$H)*($L+$B)*$H/($L*$L*$B)),0.4))]
set kxf [expr $kx0*$ex]
set ex_half [expr (1.+0.15*pow((2.*$Df*0.5/$B),0.5))*(1+0.52*pow((16.*($Df*0.5-
0.5*$H)*($L+$B)*$H/($L*$L*$B)),0.4))]
set kxp [expr $ex_half *$kx0]
set KX [expr $kxf]
```

```
###---for vertical soil springs-----
set kv0 [expr ($G*$L/(1.-$neu))*(0.73+1.54*((pow ($B, 0.75))/(pow ($L,0.75))))]
set ez [expr (1.+0.095*($Df/$B)*(1+1.3*$B/$L))*(1+0.2*pow(((2.*$L+2.*$B)*$H/($L*$B)),0.67))]
#set ez 1.0
set kv [expr $kv0*$ez]
###################
#stiffness intensities
set kmid [expr $kz/($Lm+2.*$Le*$ratioK)];             #mid region intensity
set kend [expr $kmid*$ratioK];                         #end region intensity
#component stiffnesses
set kzm [expr $kmid*$lm]                   ;          #stiffness of mid springs
set kze1 [expr $kend*$le*0.5]              ;          #stiffness of extreme end springs
set kze2 [expr $kend*$le]                  ;          #stiffness of other end springs
###################################################
## End of Foundation.tcl
###################################################
```

```
###############################################
## File Name: Materials.tcl
###############################################
##-----------------------------------
## Structural Properties
##-----------------------------------
set Ist [expr $footB*pow($footL,3)/12];      #---I of total footing
set Ifoot [expr $Ist/$elet];                 #---I for each footing element
set Ast [expr $footB*$footH];                #--area of whole footing
set Afoot  $Ast;                             #--area of each element
set Awall [expr $Bwall*$Lwall]
set Iwall [expr $Bwall*pow($Lwall,3)/12.]

##uniaxialMaterial Elastic $matTag $E
uniaxialMaterial Elastic   1      $Ealum
#---------------------------------------------------
# QzSimple1 MATERIAL, PySimple1 and TzSimple1 Material
#---------------------------------------------------
if {$soilType ==1} {
##Qz Properties
     set z1mid [expr 0.525*$q1mid/$kzm]
     set z1end [expr 0.525*$q1end/$kze1]
     set z2end [expr 0.525*$q2end/$kze2]
##Py Properties
#     set y50 [expr 8.0*$Pult/$kx]
##Tz Properties
     set zt50 [expr 0.708*$Qf/$kx]
 }
if {$soilType ==2} {
set z1mid [expr $q1mid*1.39/$kzm]
set z1end  [expr $q1end*1.39/$kze1]
set z2end  [expr $q2end*1.39/$kze2]

##Py Properties
    set y50 [expr 0.542*$Pp/$kxp]
##Tz Properties
          set zt50 [expr 2.05*$Qf/$kxf]
 }
##########################################################################
#--material     QzSimple1   $matTag   $soilType     $qult     $z50    $TP  $crad  <c>
```

```
uniaxialMaterial  QzSimple1   3       $soilType     $q1mid    $z1mid   $tp  $crad    0.0
uniaxialMaterial  QzSimple1   4       $soilType     $q1end    $z1end   $tp  $crad    0.0
uniaxialMaterial  QzSimple1   5       $soilType     $q2end    $z2end   $tp  $crad    0.0

#--material      PySimple1   $matTag   $soilType     $pult     $y50   $Cd
uniaxialMaterial  PySimple1   6      $soilType     $Pp       $y50   $cd

#--material      TzSimple1   $matTag   $soilType     $tult     $zt50   $Cd
uniaxialMaterial  TzSimple1   7      $soilType     $Qf       $zt50   $cd

##--material     Elastic   $matTag    $E
uniaxialMaterial  Elastic      8       $kxf

#--material     ENT       $matTag    $E
uniaxialMaterial  ENT         9       $kxf
################################################
## End of Materials.tcl
################################################
```

```
####################################################
## Name of File: Elements.tcl
####################################################
#----------------------------------
# mass assignment
#----------------------------------
mass  8003  [expr $Mg/2.]   10.  10.
mass  8004  [expr $Mg/2.]   10.  10.
 #-------------------------------------
# Footing elements
#-------------------------------------
for {set iz 1} {$iz<=$elet} {incr iz 1} {
#element elasticBeamColumn   $eleTag   $iNode    $jNode     $A    $E    $I    $transfTag
element elasticBeamColumn    $iz  $iz    [expr $iz+1]     $Afoot    $Ealum     $Ifoot   1
 }
#-------------------------------------
# shear wall elements
#-------------------------------------
#element elasticBeamColumn   $eleTag  $iNode     $jNode   $A    $E   $Iz    $transfTag
element elasticBeamColumn   8003    $midnode   8003     $Awall    $Ealum     $Iwall     2
element elasticBeamColumn   8004    8003       8004     $Awall     $Ealum      $Iwall     2
#-------------------------------------
# Creating spring elements
#-------------------------------------
#---vertical springs elements---------------------------------------
### Two Extreme End Springs ###
element zeroLength      1001           1            1001                   -mat     4   -dir    2
element zeroLength      $endSpring      $endnode      $endSpring   -mat     4   -dir    2
### Other end Springs ###
for {set ix 2} {$ix<$noe-1} {incr ix 1} {
 element zeroLength   [expr 1000+$ix]           [expr $ix]            [expr 1000+$ix]             -mat   5  -dir  2
 element zeroLength   [expr 1000+$ix+$noe+$nom]   [expr $ix+$noe+$nom]    [expr 1000+$ix+$noe+$nom]     -
mat   5  -dir  2
 }
### Mid Springs ###
```

```
for {set iy 1} {$iy<=$nom} {incr iy 1} {
 element  zeroLength  [expr 1000+$iy+$noe]   [expr $iy+$noe]    [expr 1000+$iy+$noe]   -mat  3  -dir  2
 }
#---horizontal springs elements---------------------------------------
#element for earth pressure
element zeroLength  8001   8001  1  -mat  6  -dir  1
#element for sliding
element zeroLength  8002   8002  1  -mat  7  -dir  1

###################################################
## End of Elements.tcl
###################################################

################################################
## File Name: Recorder.tcl
################################################
set path out
for {set iz 1} {$iz<=2} {incr iz 1} {
set d [concat node$iz.dis]
set f [concat ele$iz.force]
 recorder Node -time -file $path/$d -node $iz -dof 1 2 3 disp
 recorder Element -file $path/$f -time -ele $iz localForce
 }
##--recording only mid node and mid element--##
 set d [concat midnode.dis]
 set f1 [concat midele1.force]
 set f2 [concat midele2.force]
 recorder Node -time -file $path/$d -node $midnode -dof 1 2 3 disp
 recorder Element -file $path/$f1 -time -ele  $midele1 localForce
 recorder Element -file $path/$f2 -time -ele  $midele2 localForce

#---recorder for spring elements----------------------
for {set iy 1} {$iy<=2} {incr iy 1} {
 set s [concat spring$iy.force]
 recorder Element [expr $iy+1000] -file $path/$s -time force
 }
recorder Element 8002 -file $path/element8002.force -time force
recorder Element -file $path/element8003.force -time -ele 8003 localForce
recorder Element -file $path/element8004.force -time -ele 8004 localForce
################################################
## End of Recorder.tcl
################################################

################################################
## File Name: Analysis.tcl
################################################
#----------------------
# Gravity LOAD PATTERNS
#----------------------
pattern Plain 1 "Linear" {
    load  $midnode  0.  [expr $Wg*1.3]   0.
   }
#----------------
# gravity analysis
#----------------
system UmfPack
constraints Plain
```

```
test NormDispIncr 1.0e-8 40 0
algorithm Newton
numberer RCM
integrator LoadControl 0.1
analysis Static
analyze 10

#loadConst
loadConst -time 0.0

#-----------------
# cyclic analysis
#------------------
set gdisp1 "Path  -filePath  $inFile  -dt  $dt -factor  $factor"
pattern MultipleSupport 4  {
groundMotion  4  Series  -disp   $gdisp1
##imposedMotion       nodeTag?      dirn?   gMotionTag?
imposedSupportMotion  8003      $dir      4
}
#---------------------------------------------
#Create analysis
#---------------------------------------------
system UmfPack
constraints Transformation
test NormDispIncr 1.0e-1  40  0
algorithm KrylovNewton
numberer RCM
#Create the integration scheme Newmark with gamma = 0.5 and beta =  0.25
integrator Newmark  0.5  0.25
analysis Transient
#------------------------------------------------
#Perform analysis
#------------------------------------------------
puts "np=$np, dt=$dt"
analyze $np $dt
###############################################
## End of File Analysis.tcl
###############################################
```

9. TCL Code for OpenSees Simulations of Shear Wall Structures Tested in Centrifuge Using BNWF Model

SSG04_10: Dynamic Base Shaking

```
#####################################################
# Tcl file for shear wall structures tested in centrifuge (test code: ssg04_10)
# Written by: P. Raychowdhury <pri@ucsd.edu>
# Units used: mass [Kg], length [m], time [s], and force [N]
#####################################################

## All the other files are same as "test code: ssg04_10" (item-8) except the property (Prop.tcl) and analysis file
(Analysis.tcl).

#-------------------------------
# Soil Properties
#-------------------------------
#soil properties are according to Gajan's report
set g 9.81;        #--m/s^2
set soilType 2;   #---soiltype clay 1, sand 2
set crad 0.05;      #---radiation damping
set cd 0.;       #---ratio of maximum drag to ultimate resistance
set tp 0.1;       #---uplift capacity
set phi 42.;      #---friction abgle
set gamma 16200.;  #---unit wt (N/m^3)
set beta 0.;              #---angle of load applied
set c 0.;                 #---cohesion
set Esoil [expr 50.*pow(10,6)];  #---Modulus of soil assumed as 50 MPa for dense sand
set neu 0.35;
set kunlFact 1.0
#-------------------------------
# Assign Footing Dimensions
#-------------------------------
set footL 2.80;   #----length, width and height of the strip footing in m
set footB 0.65
set footH 0.66
set Df 0.;         #---depth of embedment
set Lwall 2.5;     #----length, width and height of shear wall in m
set Bwall 0.38
set Hwall 10.1
set AspRatio 1.8;  #--aspect ratio (M/H/L)
set pod  [expr $AspRatio*$footL] ;     #----point of lateral load application
#-------------------------------
# Assign Mass and FSv
#-------------------------------
set Mg 36000.0;            #---mass of structure in prototype scale (kg), provided by Gajan
set FSv 4.0;               #---vertical factor of safety, provided by Gajan
set Ealum  [expr 68.9*pow(10,9)];       #[N/m^2];
set Wg [expr $Mg*$g]
set Qult [expr $Wg*$FSv]
#-------------------------------
# Mesh Properties
#-------------------------------
set ratioK  2.5                  ;#----based on Harden, 2003 (or FEMA-356, chapter-10)
set ratioe 10.0                         ;#----end length ratio (Le/L)
set ndivm  20                           ;#----no of divisions at mid region; should always be even
set ratioDIV 10.0                       ;#----ratio of mid element length to end element length
```

```
#-----------------------------------------------------
# Define dynamic loads and loadNode
##---------------------------------------------------
set inFile input_acc_SSG04_10.txt
set np 3300
set dt 0.00488
set dir 1
set factor [expr $g*1.3]
set damping 0.05;  #--rayleigh damping


##############################################
## File name: Analysis.tcl
##############################################
#-----------------------
# Gravity LOAD PATTERNS
#-----------------------
pattern Plain 1 "Linear" {
    load  $midnode  0.  [expr -$Wg*1.0]   0.
   }
#-----------------
# gravity analysis
#-----------------
system UmfPack
constraints Plain
test NormDispIncr 1.0e-8 40 0
algorithm Newton
numberer RCM
integrator LoadControl 0.1
analysis Static
analyze 10

#loadConst
loadConst -time 0.0


#-----------------
# Dynamic analysis
#------------------
set accelSeries "Series  -dt   $dt  -filePath    $inFile   -factor    $factor"
pattern UniformExcitation   5       $dir      -accel   $accelSeries

##--------------------------------------------
## Set Rayleigh damping
##--------------------------------------------
set lambdax [eigen 2]
    set w1 [expr sqrt([lindex $lambdax 0])]
    set w2 [expr sqrt([lindex $lambdax 1])]
    set am [expr $damping*2.0*$w1*$w2/($w1+$w2)]
    set bk [expr $damping*2.0/($w1+$w2)]
set bkinit  0.0
set bklast  0.0
rayleigh  $am $bk $bkinit $bklast
puts "$w1 $w2 $am $bk"
#--------------------------------------------
#Create analysis
#--------------------------------------------
```

```
system UmfPack
constraints Transformation
test NormDispIncr 1.0e-3  40  0
algorithm KrylovNewton
numberer RCM
#Create the integration scheme Newmark with gamma = 0.5 and beta =  0.25
integrator Newmark  0.5  0.25
analysis Transient
#------------------------------------------------
#Perform analysis
#------------------------------------------------
puts "np=$np, dt=$dt"
analyze $np $dt

##################################################
## End of File Analysis.tcl
```

10. TCL Code for OpenSees Simulations of Bridge Structures Tested in Centrifuge Using BNWF

<u>JAU_01_05: Dynamic Base Shaking</u>

 # file name: Main

```
##--ISOLATED FOOTING ANALYSIS
##--fall-2005
##--Done by Prishati RC
##--All analysis is done for prototype scale
##--units: SI

wipe
wipeAnalysis

#Create ModelBuilder (with 2-dimensions and 3 DOF/node)
model BasicBuilder -ndm 2 -ndf 3
geomTransf Linear 1
geomTransf Linear 2

set propFile Prop-stationE.tcl

if {$gm==1} {
		set inFile acc-5.txt
		set np  13000
	set path out/shake-5
 }
if {$gm==2} {
		set inFile acc-6.txt
		set np  9350
	set path out/shake-6
 }
if {$gm==3} {
		set inFile acc-8.txt
		set np  9000
	set path out/shake-8
 }

##----------------------------------
## Define cyclic loads and loadNode
##----------------------------------
set g 9.81;   #--m/s^2
set dt 0.002618408
set dir 1
set factor $g
set damping 0.05
set kunlFact 1.0
##----------------------------------
##----------------------------------
source $propFile
source Nodes.tcl
source Foundation.tcl
source Materials.tcl
source Elements.tcl
source eigen.tcl
source Recorder.tcl
source Analysis.tcl
```

```
# file name: Prop-stationE
##--Written by: Prishati RC
##--All analysis is done for prototype scale
##--units: SI


#-------------------------------------
# Mass, Dimension & Inertia
#-------------------------------------
set E [expr 6.9*pow(10,10)]
set I 0.107
set A 0.348

set Hcol 10.1
set Hfoot 1.1

set Mdeck 926e3
set Mfoot 173e3
set Mg [expr $Mdeck+$Mfoot]
set Wg [expr $Mg*$g]
set FSv 17.0
set Qult_exp [expr $Wg*$FSv]

set Ideck [expr 3.34*pow(10,6)]
set Ifoot [expr 8.67*pow(10,5)]

#dimensions of shear wall and strip footing according to SSG test series
set footL 5.4
set footB [expr $footL*1.0]
set Df  1.72;        #---depth of embedment
set Hcgfoot 1.215

set deckL  4.6
set deckB  $deckL
set Hcgdeck 13.47

#-------------------------------
# Soil Properties
#-------------------------------
set soilType 2;                         #---soiltype clay 1, sand 2
set crad 0.05;                    #---radiation damping
set cd 0.1;                             #---ratio of maximum drag to ultimate resistance
set tp 0.1;                       #---uplift capacity
set kunlFact 1.0;           #---reduction factor for unloading stiffness
set beta 0.;                      #---angle of load applied
set c 0.0;                        #---cohesion
set phi 40.;                      #---friction angle
set Esoil [expr  50.*pow(10,6)];     #----modulus of elasticity
set neu 0.35;                     #----Poisson's ratio
set gamma 16.e3;                     #---unit weight (N/m^3)
set N160 25.0

#-------------------------------
# Mesh Properties
#-------------------------------
set ratioK  9.            ;#----based on Harden, 2003 (or FEMA-356, chapter-10)
set ratioe 16.                   ;#----end length ratio (Le/L)
```

```
set ndivm  20                  ;#----no of divisions at mid region; should always be even
set ratioDIV 2.0                ;#----ratio of mid element length to end element length
```

 # file name: Nodes

```
##--ISOLATED FOOTING ANALYSIS
##--fall-2005
##--Done by Prishati RC
##--All analysis is done for prototype scale
##--units: SI (N,m,sec)

set L $footL
set B $footB
set Le  [expr $ratioe*$L/100.];    #----end length
set Lm  [expr $L-2*$Le];           #---mid length
set lm  [expr $Lm/$ndivm];         #---element length at mid region
set le  [expr $lm/$ratioDIV];      #---element length at end region
set ndive  [expr int($Le/$le)];    #----no of divisions at end region; should always be even
set nom [expr $ndivm-1];           #---no of nodes in mid region
set noe [expr $ndive+1];           #---no of nodes in each end region
set not [expr $nom+2*$noe];        #---total no of nodes in the footing
set elet [expr $not-1] ;           #---total no of elements in the footing
puts "lm=$lm, le=$le, ratioK=$ratioK, not =$not, noe=$noe, nom=$nom, elet =$elet"

#nodes at the footing level starts from 1
#nodes at the spring level starts from 1001

for {set ix 1} {$ix<=$noe} {incr ix 1} {
##--left end portion
  node    $ix                       [expr $le*($ix-1)]      $Hcgfoot
  node    [expr 1000+$ix]   [expr $le*($ix-1)]      $Hcgfoot
  fix [expr 1000+$ix]           1  1  1
##--right end portion
  node    [expr $ix+$noe+$nom]        [expr $L-$Le+$le*($ix-1)]     $Hcgfoot
  node    [expr 1000+$ix+$noe+$nom]   [expr $L-$Le+$le*($ix-1)]     $Hcgfoot

fix [expr 1000+$ix+$noe+$nom]    1  1  1
 }
##--mid portion
for {set im 1} {$im<=$nom} {incr im 1} {
  node    [expr $im+$noe]        [expr $Le+$lm*$im]     $Hcgfoot
  node    [expr 1000+$im+$noe]      [expr $Le+$lm*$im]     $Hcgfoot

fix [expr 1000+$im+$noe]     1  1  1
 }

#-------------------
# set the midnode
#-------------------
set midnode [expr ($not+1)/2]
set endnode [expr $not]
set midele1 [expr $midnode-1]
set midele2 [expr $midnode]
set endSpring [expr 1000+$endnode]
puts "midnode=$midnode"

#nodes created for horizontal springs
#node IDtag   x            y
node  8001    0.           $Hcgfoot
```

```
node  8002    0.           $Hcgfoot

#fix  IDTag    x  y  rot
fix   8001             1  1  1
fix   8002             1  1  1

#---shear wall nodes-----
#node IDtag   x     y
node 8003     0.    [expr $Hcgfoot+$Hcol]
node 8004     0.    $Hcgdeck

#fix  $midnode  1  1  1
```

 # file name: Foundation

```
##--ISOLATED FOOTING ANALYSIS
##--fall-2005
##--Done by Prishati RC
##--All analysis is done for prototype scale
##--units: SI

##-------------------
## Bearing Capacity
##-------------------
set Qult Qult_exp
set qult [expr $Qult/$L];            #---bearing capacity per unit length (N/m)
set q1mid [expr $qult*$lm];           #---capacity of the each mid-spring
set q1end [expr $qult*$le*0.5];       #---capacity of each extreme end spring
set q2end [expr $qult*$le];          #---capacity of other end region springs

##-------------------
## Sliding Capacity
##-------------------
set shearstress [expr $gamma*$Df*tan(0.8*$radphi)]
set Qf [expr $shearstress*$B*$L]
##-------------------
## Passive Capacity
##-------------------
set Kp 11.0;  #based on Coulomb (folllowing Das book)
set Pp [expr 0.8*$Kp*$gamma*$Df*$Df]
set Pp [expr $Pp*$L]
puts "Pp=$Pp"

#---soil stiffness is calculated as Gazetas, 1991
#set G [expr $Esoil/(2.*(1+$neu))];
#puts "G= $G"
#Calculate Shear Modulus under foundation (equn 4-5) in FEMA 356
set sv [expr $Wg/($B*$L)];  ### in Pa
set sv [expr $sv/47.88];     ## in Psf
set Go [expr 20000*pow($N160,0.33)*sqrt($sv)]
set G_overGo 1.30
set G [expr $Go*$G_overGo]
set G [expr $G*47.88];  ## in Pa
puts "G=$G"

#---for horizontal soil springs---
set kx0 [expr ($G*$L/(2.-$neu))*(2.+2.5*((pow ($B, 0.85))/(pow ($L,0.85))))]
set ex [expr (1.+0.15*pow((2.*$Df/$B),0.5))*(1+0.52*pow((16.*($Df-
0.5*$Hfoot)*($L+$B)*$Hfoot/($L*$L*$B)),0.4))]
set kxf [expr 0.5*$kx0*$ex]
set ex_half [expr (1.+0.15*pow((2.*$Df*0.5/$B),0.5))*(1+0.52*pow((16.*($Df*0.5-
0.5*$Hfoot)*($L+$B)*$Hfoot/($L*$L*$B)),0.4))]
set kxp [expr 0.5*$kx0*$ex_half]
set KX [expr $kxp+$kxf]
puts "KX=$KX"

#---for vertical soil springs-----
set kv0 [expr ($G*$L/(1.-$neu))*(0.73+1.54*((pow ($B, 0.75))/(pow ($L,0.75))))]
set ez [expr (1.+0.095*($Df/$B)*(1+1.3*$B/$L))*(1+0.2*pow(((2.*$L+2.*$B)*$Hfoot/($L*$B)),0.67))]
```

```
set kz [expr $kv0*$ez]

#stiffness intensities
set kmid [expr $kz/($Lm+2.*$Le*$ratioK)];                    #mid region intensity
set kend [expr $kmid*$ratioK];                               #end region intensity

#component stiffnesses
set kzm [expr $kmid*$lm]                          ;#stiffness of mid springs
set kze1 [expr $kend*$le*0.5]                     ;#stiffness of extreme end springs
set kze2 [expr $kend*$le]                        ;#stiffness of other end springs
```

 # file name: Materials

```
##--ISOLATED FOOTING ANALYSIS
##--fall-2005
##--Done by Prishati RC
##--All analysis is done for prototype scale
##--units: SI

#----------------------------------------------------
# QzSimple1 MATERIAL, PySimple1 and TzSimple1 Material
#----------------------------------------------------
if {$soilType ==1} {
##Qz Properties
     set z1mid [expr 0.525*$q1mid/$kzm]
     set z1end [expr 0.525*$q1end/$kze1]
     set z2end [expr 0.525*$q2end/$kze2]
##Py Properties
     set y50 [expr 8.0*$Pult/$kx]
##Tz Properties
     set zt50 [expr 0.708*$Qf/$kx]
 }
if {$soilType ==2} {
set z1mid [expr $q1mid*1.39/$kzm]
set z1end  [expr $q1end*1.39/$kze1]
set z2end  [expr $q2end*1.39/$kze2]

##Py Properties
    set y50 [expr 0.542*$Pp/$kxp]
#    set y50 0.017
##Tz Properties
     set zt50 [expr 2.05*$Qf/$kxf]
#           set zt50  0.011
 }
puts "z501=$z1end, y50=$y50, zt50= $zt50"
##########################################################################################
##uniaxialMaterial Elastic $matTag $E
uniaxialMaterial Elastic   1      $E

#--material      QzSimple1  $matTag  $soilType     $qult    $z50    $TP  $crad  <c>    $kunlFact
uniaxialMaterial  QzSimple1   3      $soilType     $q1mid   $z1mid  $tp  $crad   0.0   $kunlFact
uniaxialMaterial  QzSimple1   4      $soilType     $q1end   $z1end  $tp  $crad   0.0   $kunlFact
uniaxialMaterial  QzSimple1   5      $soilType     $q2end   $z2end  $tp  $crad   0.0   $kunlFact

#--material      PySimple1  $matTag  $soilType    $pult    $y50   $Cd
uniaxialMaterial  PySimple1   6     $soilType     $Pp      $y50   $cd

#--material      TzSimple1  $matTag  $soilType     $tult    $zt50   $Cd
uniaxialMaterial  TzSimple1   7      $soilType     $Qf      $zt50   $cd

##--material     Elastic   $matTag   $E
uniaxialMaterial  Elastic     8      $kxf

#--material     ENT     $matTag    $E
#uniaxialMaterial   ElasticPP       9      $kxf
```

 # file name: Elements

```
##--ISOLATED FOOTING ANALYSIS
##--fall-2005
##--Done by Prishati RC
##--All analysis is done for prototype scale
##--units: SI

##-----------------
# assign the mass
##-----------------
mass  8004     [expr $Mdeck]    [expr $Mdeck]    [expr $Ideck*1.]
mass $midnode  [expr $Mfoot]    [expr $Mfoot]    [expr $Ifoot*1.]

#-------------------------------------
# isolated footing elements
#-------------------------------------
for {set iz 1} {$iz<=$elet} {incr iz 1} {
 #element elasticBeamColumn   $eleTag   $iNode    $jNode          $A                  $E           $I
$transfTag
 element elasticBeamColumn    $iz     $iz      [expr $iz+1]      [expr $A*4./$elet]   [expr $E*4.]    [expr $I*4.]    1
 }

#-------------------------------------
# shear wall elements
#-------------------------------------
#element elasticBeamColumn   $eleTag    $iNode     $jNode      $A           $E            $Iz           $transfTag
element elasticBeamColumn    8003      $midnode    8003        $A           $E            $I              2
element elasticBeamColumn    8004      8003        8004       [expr $A*4.]   [expr $E*4.]    [expr $I*5.]       2

#-------------------------------------
# creating spring elements
#-------------------------------------
#---vertical springs elements----------------------------------------
### Two Extreme End Springs ###
element zeroLength         1001          1001         1          -mat    4   -dir   2
element zeroLength     $endSpring      $endSpring    $endnode    -mat    4   -dir   2
### Other end Springs ###
for {set ix 1} {$ix<=$noe-1} {incr ix 1} {
 element zeroLength   [expr 1001+$ix]       [expr 1001+$ix]        [expr $ix+1]           -mat   5  -dir   2
 element zeroLength   [expr $endSpring-$ix]  [expr $endSpring-$ix]   [expr $endnode-$ix]     -mat   5  -dir   2
 }
### Mid Springs ###
for {set iy 1} {$iy<=$nom} {incr iy 1} {
 element zeroLength  [expr 1000+$iy+$noe]    [expr 1000+$iy+$noe]    [expr $iy+$noe]    -mat   3   -dir   2
 }

#---horizontal springs elements--------------------------------------
#element for earth pressure
element zeroLength  8001     8001    1    -mat   6   -dir   1
####element for sliding
element zeroLength  8002     8002    1    -mat   7   -dir   1
```

 # file name: eigen

```
##Subroutine to record higher mode properties
##Name of the program: eigen.tcl
##Written by: PRC
##units in SI

set ic stationE
set mt 2    ;#---No of modes to be extracted

eigen frequency $mt

set folder Eigen_Properties
set xic [concat case$ic]
set xfreq [concat $xic-Freq.dat]
set xperiod [concat $xic-Period.dat]

set fileFR [open $folder/$xfreq  w 0600]
set fileTP [open $folder/$xperiod w 0600]

set PI 3.1415926
set lambdax [eigen $mt]
for {set i 1} {$i <= $mt} {incr i 1} {
set lambda [lindex $lambdax [expr $i-1]]
set omega [expr pow($lambda,0.5)]
set Tn [expr 2*$PI/$omega]
set fn [expr 1/$Tn]

puts "For mode=$i, Tn=$Tn sec, fn=$fn Hz"
```

 # file name: Recorder

```
##--ISOLATED FOOTING ANALYSIS
##--fall-2005
##--Done by Prishati RC
##--All analysis is done for prototype scale
##--units: SI

#----------------------------------------------
#--- Recorder
#----------------------------------------------

#----recorder for footings------------------------------
for {set iz 1} {$iz<=2} {incr iz 1} {
set d [concat node$iz.dis]
set f [concat ele$iz.force]
 recorder Node -time -file $path/$d -node $iz -dof 1 2 3 disp
 recorder Element -file $path/$f -time -ele $iz localForce
 }
##--recording only mid node and mid element--##
 recorder Node -time -file $path/midnode.dis -node $midnode -dof 1 2 3 disp
 recorder Element -file $path/midele1.force -time -ele  $midele1 localForce
 recorder Element -file $path/midele2.force -time -ele  $midele2 localForce

##---recorder for column and deck
recorder Element -file $path/element8003.force  -time -ele  8003 localForce
recorder Element -file $path/element8004.force  -time -ele  8004 localForce
recorder Node -time -file $path/acc.acc  -node  $midnode 8003  8004 -dof  1 2  3 accel
recorder Node -file $path/eigen.out  -time  -node  8003  8004  -dof 1 "eigen 1"

#---recorder for spring elements-------------------------
for {set iy 1} {$iy<=2} {incr iy 1} {
 set s [concat spring$iy.force]
 recorder Element [expr $iy+1000] -file $path/$s -time force
 recorder Element  -file  $path/$s  [expr $iy+1000]  -time  force
 }
recorder Element -time -file $path/springPy.force  -element  8001  force
recorder Element -time -file $path/springTz.force  -element  8002  force
```

 # file name: Analysis

```
##--ISOLATED FOOTING ANALYSIS
##--fall-2005
##--Done by Prishati RC
##--All analysis is done for prototype scale
##--units: SI

#-----------------------
# Gravity LOAD PATTERNS
#-----------------------
pattern Plain 1 "Linear" {
   load  $midnode  0.   -$Wg    0.
  }
#-----------------
# gravity analysis
#-----------------
system UmfPack
constraints Plain
test NormDispIncr 1.0e-8 40 0
algorithm Newton
numberer RCM
integrator LoadControl 0.1
analysis Static
analyze 10

##loadConst
loadConst -time 0.0

#######################################
# Dynamic
#######################################
set accelSeries "Series  -dt   $dt  -filePath    $inFile   -factor    $factor"

#UniformExcitation     loadTag    direction  -acc     $accSeries
pattern UniformExcitation   5       $dir      -accel   $accelSeries
###################################
#set gdisp "Path  -filePath  $inFile  -dt  $dt -factor  $factor"
#puts "input file= $inFile"
#
#pattern MultipleSupport 4  {
#groundMotion  4  Series  -disp  $gdisp
###imposedMotion      nodeTag?    dirn?   gMotionTag?
#imposedSupportMotion  8004        1        4
##imposedSupportMotion    $midnode    3       4
#}
##--------------------------------------------
##Set Rayleigh damping
##--------------------------------------------
source DampingMKProp.tcl

##--------------------------------------------
##Create analysis
##--------------------------------------------
system UmfPack
constraints Transformation
```

```
test NormDispIncr  1.0e-8  40  0
algorithm KrylovNewton
numberer RCM
#Create the integration scheme Newmark with gamma = 0.5 and beta =  0.25
integrator Newmark   0.5   0.25
analysis Transient
###------------------------------------------------
###Perform analysis
###------------------------------------------------
puts "np=$np, dt=$dt"
analyze $np $dt
```

 # file name: DampingMKProp

```
# set the rayleigh damping factors for nodes & elements
#mass and stiffness proportional damping
##################################################
#  get damping coefficient
##----------------------------------------------------
set lambdax [eigen 2]
    set w1 [expr sqrt([lindex $lambdax 0])]
    set w2 [expr sqrt([lindex $lambdax 1])]
    set am [expr $damping*2.0*$w1*$w2/($w1+$w2)]
    set bk [expr $damping*2.0/($w1+$w2)]
set bkinit  0.0
set bklast  0.0
rayleigh  $am $bk $bkinit $bklast
puts "$w1 $w2 $am $bk"
###--------------------------------------------------
#mass proportional damping
# set w1 [expr sqrt([lindex $lambdax 0])]
# set am [expr $damping*2.0*$w1]
# set bk     0.0
# set bkinit 0.0
# set bklast 0.0
# rayleigh  $am $bk $bkinit $bklast
#----------------------------------------------------
```

PEER REPORTS

PEER reports are available from the National Information Service for Earthquake Engineering (NISEE). To order PEER reports, please contact the Pacific Earthquake Engineering Research Center, 1301 South 46th Street, Richmond, California 94804-4698. Tel.: (510) 665-3405; Fax: (510) 665-3420.

PEER 2007/11 *Bar Buckling in Reinforced Concrete Bridge Columns.* Wayne A. Brown, Dawn E. Lehman, and John F. Stanton. February 2008.

PEER 2007/10 *Computational Modeling of Progressive Collapse in Reinforced Concrete Frame Structures.* Mohamed M. Talaat and Khalid M. Mosalam. May 2008.

PEER 2007/09 *Integrated Probabilistic Performance-Based Evaluation of Benchmark Reinforced Concrete Bridges.* Kevin R. Mackie, John-Michael Wong, and Božidar Stojadinović. January 2008.

PEER 2007/08 *Assessing Seismic Collapse Safety of Modern Reinforced Concrete Moment-Frame Buildings.* Curt B. Haselton and Gregory G. Deierlein. February 2008.

PEER 2007/07 *Performance Modeling Strategies for Modern Reinforced Concrete Bridge Columns.* Michael P. Berry and Marc O. Eberhard. April 2008.

PEER 2007/06 *Development of Improved Procedures for Seismic Design of Buried and Partially Buried Structures.* Linda Al Atik and Nicholas Sitar. June 2007.

PEER 2007/05 *Uncertainty and Correlation in Seismic Risk Assessment of Transportation Systems.* Renee G. Lee and Anne S. Kiremidjian. July 2007.

PEER 2007/04 *Numerical Models for Analysis and Performance-Based Design of Shallow Foundations Subjected to Seismic Loading.* Sivapalan Gajan, Tara C. Hutchinson, Bruce L. Kutter, Prishati Raychowdhury, José A. Ugalde, and Jonathan P. Stewart. May 2008.

PEER 2007/03 *Beam-Column Element Model Calibrated for Predicting Flexural Response Leading to Global Collapse of RC Frame Buildings.* Curt B. Haselton, Abbie B. Liel, Sarah Taylor Lange, and Gregory g. Deierlein. May 2008.

PEER 2007/02 *Campbell-Bozorgnia NGA Ground Motion Relations for the Geometric Mean Horizontal Component of Peak and Spectral Ground Motion Parameters.* Kenneth W. Campbell and Yousef Bozorgnia. May 2007.

PEER 2007/01 *Boore-Atkinson NGA Ground Motion Relations for the Geometric Mean Horizontal Component of Peak and Spectral Ground Motion Parameters.* David M. Boore and Gail M. Atkinson. May. May 2007.

PEER 2006/12 *Societal Implications of Performance-Based Earthquake Engineering.* Peter J. May. May 2007.

PEER 2006/11 *Probabilistic Seismic Demand Analysis Using Advanced Ground Motion Intensity Measures, Attenuation Relationships, and Near-Fault Effects.* Polsak Tothong and C. Allin Cornell. March 2007.

PEER 2006/10 *Application of the PEER PBEE Methodology to the I-880 Viaduct.* Sashi Kunnath. February 2007.

PEER 2006/09 *Quantifying Economic Losses from Travel Forgone Following a Large Metropolitan Earthquake.* James Moore, Sungbin Cho, Yue Yue Fan, and Stuart Werner. November 2006.

PEER 2006/08 *Vector-Valued Ground Motion Intensity Measures for Probabilistic Seismic Demand Analysis*. Jack W. Baker and C. Allin Cornell. October 2006.

PEER 2006/07 *Analytical Modeling of Reinforced Concrete Walls for Predicting Flexural and Coupled–Shear-Flexural Responses*. Kutay Orakcal, Loenardo M. Massone, and John W. Wallace. October 2006.

PEER 2006/06 *Nonlinear Analysis of a Soil-Drilled Pier System under Static and Dynamic Axial Loading.* Gang Wang and Nicholas Sitar. November 2006.

PEER 2006/05 *Advanced Seismic Assessment Guidelines.* Paolo Bazzurro, C. Allin Cornell, Charles Menun, Maziar Motahari, and Nicolas Luco. September 2006.

PEER 2006/04 *Probabilistic Seismic Evaluation of Reinforced Concrete Structural Components and Systems.* Tae Hyung Lee and Khalid M. Mosalam. August 2006.

PEER 2006/03 *Performance of Lifelines Subjected to Lateral Spreading.* Scott A. Ashford and Teerawut Juirnarongrit. July 2006.

PEER 2006/02 *Pacific Earthquake Engineering Research Center Highway Demonstration Project.* Anne Kiremidjian, James Moore, Yue Yue Fan, Nesrin Basoz, Ozgur Yazali, and Meredith Williams. April 2006.

PEER 2006/01 *Bracing Berkeley. A Guide to Seismic Safety on the UC Berkeley Campus.* Mary C. Comerio, Stephen Tobriner, and Ariane Fehrenkamp. January 2006.

PEER 2005/16 *Seismic Response and Reliability of Electrical Substation Equipment and Systems.* Junho Song, Armen Der Kiureghian, and Jerome L. Sackman. April 2006.

PEER 2005/15 *CPT-Based Probabilistic Assessment of Seismic Soil Liquefaction Initiation.* R. E. S. Moss, R. B. Seed, R. E. Kayen, J. P. Stewart, and A. Der Kiureghian. April 2006.

PEER 2005/14 *Workshop on Modeling of Nonlinear Cyclic Load-Deformation Behavior of Shallow Foundations.* Bruce L. Kutter, Geoffrey Martin, Tara Hutchinson, Chad Harden, Sivapalan Gajan, and Justin Phalen. March 2006.

PEER 2005/13 *Stochastic Characterization and Decision Bases under Time-Dependent Aftershock Risk in Performance-Based Earthquake Engineering.* Gee Liek Yeo and C. Allin Cornell. July 2005.

PEER 2005/12 *PEER Testbed Study on a Laboratory Building: Exercising Seismic Performance Assessment.* Mary C. Comerio, editor. November 2005.

PEER 2005/11 *Van Nuys Hotel Building Testbed Report: Exercising Seismic Performance Assessment.* Helmut Krawinkler, editor. October 2005.

PEER 2005/10 *First NEES/E-Defense Workshop on Collapse Simulation of Reinforced Concrete Building Structures.* September 2005.

PEER 2005/09 *Test Applications of Advanced Seismic Assessment Guidelines.* Joe Maffei, Karl Telleen, Danya Mohr, William Holmes, and Yuki Nakayama. August 2006.

PEER 2005/08 *Damage Accumulation in Lightly Confined Reinforced Concrete Bridge Columns.* R. Tyler Ranf, Jared M. Nelson, Zach Price, Marc O. Eberhard, and John F. Stanton. April 2006.

PEER 2005/07 *Experimental and Analytical Studies on the Seismic Response of Freestanding and Anchored Laboratory Equipment.* Dimitrios Konstantinidis and Nicos Makris. January 2005.

PEER 2005/06 *Global Collapse of Frame Structures under Seismic Excitations*. Luis F. Ibarra and Helmut Krawinkler. September 2005.

PEER 2005//05 *Performance Characterization of Bench- and Shelf-Mounted Equipment.* Samit Ray Chaudhuri and Tara C. Hutchinson. May 2006.

PEER 2005/04 *Numerical Modeling of the Nonlinear Cyclic Response of Shallow Foundations.* Chad Harden, Tara Hutchinson, Geoffrey R. Martin, and Bruce L. Kutter. August 2005.

PEER 2005/03 *A Taxonomy of Building Components for Performance-Based Earthquake Engineering.* Keith A. Porter. September 2005.

PEER 2005/02 *Fragility Basis for California Highway Overpass Bridge Seismic Decision Making*. Kevin R. Mackie and Božidar Stojadinović. June 2005.

PEER 2005/01 *Empirical Characterization of Site Conditions on Strong Ground Motion.* Jonathan P. Stewart, Yoojoong Choi, and Robert W. Graves. June 2005.

PEER 2004/09 *Electrical Substation Equipment Interaction: Experimental Rigid Conductor Studies.* Christopher Stearns and André Filiatrault. February 2005.

PEER 2004/08 *Seismic Qualification and Fragility Testing of Line Break 550-kV Disconnect Switches.* Shakhzod M. Takhirov, Gregory L. Fenves, and Eric Fujisaki. January 2005.

PEER 2004/07 *Ground Motions for Earthquake Simulator Qualification of Electrical Substation Equipment.* Shakhzod M. Takhirov, Gregory L. Fenves, Eric Fujisaki, and Don Clyde. January 2005.

PEER 2004/06 *Performance-Based Regulation and Regulatory Regimes.* Peter J. May and Chris Koski. September 2004.

PEER 2004/05 *Performance-Based Seismic Design Concepts and Implementation: Proceedings of an International Workshop.* Peter Fajfar and Helmut Krawinkler, editors. September 2004.

PEER 2004/04 *Seismic Performance of an Instrumented Tilt-up Wall Building.* James C. Anderson and Vitelmo V. Bertero. July 2004.

PEER 2004/03 *Evaluation and Application of Concrete Tilt-up Assessment Methodologies.* Timothy Graf and James O. Malley. October 2004.

PEER 2004/02 *Analytical Investigations of New Methods for Reducing Residual Displacements of Reinforced Concrete Bridge Columns.* Junichi Sakai and Stephen A. Mahin. August 2004.

PEER 2004/01 *Seismic Performance of Masonry Buildings and Design Implications.* Kerri Anne Taeko Tokoro, James C. Anderson, and Vitelmo V. Bertero. February 2004.

PEER 2003/18 *Performance Models for Flexural Damage in Reinforced Concrete Columns.* Michael Berry and Marc Eberhard. August 2003.

PEER 2003/17 *Predicting Earthquake Damage in Older Reinforced Concrete Beam-Column Joints.* Catherine Pagni and Laura Lowes. October 2004.

PEER 2003/16 *Seismic Demands for Performance-Based Design of Bridges.* Kevin Mackie and Božidar Stojadinović. August 2003.

PEER 2003/15 *Seismic Demands for Nondeteriorating Frame Structures and Their Dependence on Ground Motions.* Ricardo Antonio Medina and Helmut Krawinkler. May 2004.

PEER 2003/14 *Finite Element Reliability and Sensitivity Methods for Performance-Based Earthquake Engineering.* Terje Haukaas and Armen Der Kiureghian. April 2004.

PEER 2003/13 *Effects of Connection Hysteretic Degradation on the Seismic Behavior of Steel Moment-Resisting Frames.* Janise E. Rodgers and Stephen A. Mahin. March 2004.

PEER 2003/12 *Implementation Manual for the Seismic Protection of Laboratory Contents: Format and Case Studies.* William T. Holmes and Mary C. Comerio. October 2003.

PEER 2003/11 *Fifth U.S.-Japan Workshop on Performance-Based Earthquake Engineering Methodology for Reinforced Concrete Building Structures.* February 2004.

PEER 2003/10 *A Beam-Column Joint Model for Simulating the Earthquake Response of Reinforced Concrete Frames.* Laura N. Lowes, Nilanjan Mitra, and Arash Altoontash. February 2004.

PEER 2003/09 *Sequencing Repairs after an Earthquake: An Economic Approach.* Marco Casari and Simon J. Wilkie. April 2004.

PEER 2003/08 *A Technical Framework for Probability-Based Demand and Capacity Factor Design (DCFD) Seismic Formats.* Fatemeh Jalayer and C. Allin Cornell. November 2003.

PEER 2003/07 *Uncertainty Specification and Propagation for Loss Estimation Using FOSM Methods.* Jack W. Baker and C. Allin Cornell. September 2003.

PEER 2003/06 *Performance of Circular Reinforced Concrete Bridge Columns under Bidirectional Earthquake Loading.* Mahmoud M. Hachem, Stephen A. Mahin, and Jack P. Moehle. February 2003.

PEER 2003/05 *Response Assessment for Building-Specific Loss Estimation.* Eduardo Miranda and Shahram Taghavi. September 2003.

PEER 2003/04 *Experimental Assessment of Columns with Short Lap Splices Subjected to Cyclic Loads*. Murat Melek, John W. Wallace, and Joel Conte. April 2003.

PEER 2003/03 *Probabilistic Response Assessment for Building-Specific Loss Estimation.* Eduardo Miranda and Hesameddin Aslani. September 2003.

PEER 2003/02 *Software Framework for Collaborative Development of Nonlinear Dynamic Analysis Program.* Jun Peng and Kincho H. Law. September 2003.

PEER 2003/01 *Shake Table Tests and Analytical Studies on the Gravity Load Collapse of Reinforced Concrete Frames.* Kenneth John Elwood and Jack P. Moehle. November 2003.

PEER 2002/24 *Performance of Beam to Column Bridge Joints Subjected to a Large Velocity Pulse.* Natalie Gibson, André Filiatrault, and Scott A. Ashford. April 2002.

PEER 2002/23 *Effects of Large Velocity Pulses on Reinforced Concrete Bridge Columns.* Greg L. Orozco and Scott A. Ashford. April 2002.

PEER 2002/22 *Characterization of Large Velocity Pulses for Laboratory Testing.* Kenneth E. Cox and Scott A. Ashford. April 2002.

PEER 2002/21 *Fourth U.S.-Japan Workshop on Performance-Based Earthquake Engineering Methodology for Reinforced Concrete Building Structures*. December 2002.

PEER 2002/20 *Barriers to Adoption and Implementation of PBEE Innovations.* Peter J. May. August 2002.

PEER 2002/19 *Economic-Engineered Integrated Models for Earthquakes: Socioeconomic Impacts.* Peter Gordon, James E. Moore II, and Harry W. Richardson. July 2002.

PEER 2002/18 *Assessment of Reinforced Concrete Building Exterior Joints with Substandard Details.* Chris P. Pantelides, Jon Hansen, Justin Nadauld, and Lawrence D. Reaveley. May 2002.

PEER 2002/17 *Structural Characterization and Seismic Response Analysis of a Highway Overcrossing Equipped with Elastomeric Bearings and Fluid Dampers: A Case Study.* Nicos Makris and Jian Zhang. November 2002.

PEER 2002/16 *Estimation of Uncertainty in Geotechnical Properties for Performance-Based Earthquake Engineering.* Allen L. Jones, Steven L. Kramer, and Pedro Arduino. December 2002.

PEER 2002/15 *Seismic Behavior of Bridge Columns Subjected to Various Loading Patterns.* Asadollah Esmaeily-Gh. and Yan Xiao. December 2002.

PEER 2002/14 *Inelastic Seismic Response of Extended Pile Shaft Supported Bridge Structures.* T.C. Hutchinson, R.W. Boulanger, Y.H. Chai, and I.M. Idriss. December 2002.

PEER 2002/13 *Probabilistic Models and Fragility Estimates for Bridge Components and Systems.* Paolo Gardoni, Armen Der Kiureghian, and Khalid M. Mosalam. June 2002.

PEER 2002/12 *Effects of Fault Dip and Slip Rake on Near-Source Ground Motions: Why Chi-Chi Was a Relatively Mild M7.6 Earthquake.* Brad T. Aagaard, John F. Hall, and Thomas H. Heaton. December 2002.

PEER 2002/11 *Analytical and Experimental Study of Fiber-Reinforced Strip Isolators*. James M. Kelly and Shakhzod M. Takhirov. September 2002.

PEER 2002/10 *Centrifuge Modeling of Settlement and Lateral Spreading with Comparisons to Numerical Analyses***.** Sivapalan Gajan and Bruce L. Kutter. January 2003.

PEER 2002/09 *Documentation and Analysis of Field Case Histories of Seismic Compression during the 1994 Northridge, California, Earthquake.* Jonathan P. Stewart, Patrick M. Smith, Daniel H. Whang, and Jonathan D. Bray. October 2002.

PEER 2002/08 *Component Testing, Stability Analysis and Characterization of Buckling-Restrained Unbonded Braces™.* Cameron Black, Nicos Makris, and Ian Aiken. September 2002.

PEER 2002/07 *Seismic Performance of Pile-Wharf Connections.* Charles W. Roeder, Robert Graff, Jennifer Soderstrom, and Jun Han Yoo. December 2001.

PEER 2002/06 *The Use of Benefit-Cost Analysis for Evaluation of Performance-Based Earthquake Engineering Decisions.* Richard O. Zerbe and Anthony Falit-Baiamonte. September 2001.

PEER 2002/05 *Guidelines, Specifications, and Seismic Performance Characterization of Nonstructural Building Components and Equipment*. André Filiatrault, Constantin Christopoulos, and Christopher Stearns. September 2001.

PEER 2002/04 *Consortium of Organizations for Strong-Motion Observation Systems and the Pacific Earthquake Engineering Research Center Lifelines Program: Invited Workshop on Archiving and Web Dissemination of Geotechnical Data, 4–5 October 2001*. September 2002.

PEER 2002/03 *Investigation of Sensitivity of Building Loss Estimates to Major Uncertain Variables for the Van Nuys Testbed.* Keith A. Porter, James L. Beck, and Rustem V. Shaikhutdinov. August 2002.

PEER 2002/02 *The Third U.S.-Japan Workshop on Performance-Based Earthquake Engineering Methodology for Reinforced Concrete Building Structures*. July 2002.

PEER 2002/01 *Nonstructural Loss Estimation: The UC Berkeley Case Study.* Mary C. Comerio and John C. Stallmeyer. December 2001.

PEER 2001/16 *Statistics of SDF-System Estimate of Roof Displacement for Pushover Analysis of Buildings.* Anil K. Chopra, Rakesh K. Goel, and Chatpan Chintanapakdee. December 2001.

PEER 2001/15 *Damage to Bridges during the 2001 Nisqually Earthquake.* R. Tyler Ranf, Marc O. Eberhard, and Michael P. Berry. November 2001.

PEER 2001/14 *Rocking Response of Equipment Anchored to a Base Foundation.* Nicos Makris and Cameron J. Black. September 2001.

PEER 2001/13 *Modeling Soil Liquefaction Hazards for Performance-Based Earthquake Engineering.* Steven L. Kramer and Ahmed-W. Elgamal. February 2001.

PEER 2001/12 *Development of Geotechnical Capabilities in OpenSees.* Boris Jeremi . September 2001.

PEER 2001/11 *Analytical and Experimental Study of Fiber-Reinforced Elastomeric Isolators*. James M. Kelly and Shakhzod M. Takhirov. September 2001.

PEER 2001/10 *Amplification Factors for Spectral Acceleration in Active Regions.* Jonathan P. Stewart, Andrew H. Liu, Yoojoong Choi, and Mehmet B. Baturay. December 2001.

PEER 2001/09 *Ground Motion Evaluation Procedures for Performance-Based Design.* Jonathan P. Stewart, Shyh-Jeng Chiou, Jonathan D. Bray, Robert W. Graves, Paul G. Somerville, and Norman A. Abrahamson. September 2001.

PEER 2001/08 *Experimental and Computational Evaluation of Reinforced Concrete Bridge Beam-Column Connections for Seismic Performance*. Clay J. Naito, Jack P. Moehle, and Khalid M. Mosalam. November 2001.

PEER 2001/07 *The Rocking Spectrum and the Shortcomings of Design Guidelines.* Nicos Makris and Dimitrios Konstantinidis. August 2001.

PEER 2001/06 *Development of an Electrical Substation Equipment Performance Database for Evaluation of Equipment Fragilities*. Thalia Agnanos. April 1999.

PEER 2001/05 *Stiffness Analysis of Fiber-Reinforced Elastomeric Isolators.* Hsiang-Chuan Tsai and James M. Kelly. May 2001.

PEER 2001/04 *Organizational and Societal Considerations for Performance-Based Earthquake Engineering.* Peter J. May. April 2001.

PEER 2001/03 *A Modal Pushover Analysis Procedure to Estimate Seismic Demands for Buildings: Theory and Preliminary Evaluation.* Anil K. Chopra and Rakesh K. Goel. January 2001.

PEER 2001/02 *Seismic Response Analysis of Highway Overcrossings Including Soil-Structure Interaction.* Jian Zhang and Nicos Makris. March 2001.

PEER 2001/01 *Experimental Study of Large Seismic Steel Beam-to-Column Connections.* Egor P. Popov and Shakhzod M. Takhirov. November 2000.

PEER 2000/10 *The Second U.S.-Japan Workshop on Performance-Based Earthquake Engineering Methodology for Reinforced Concrete Building Structures.* March 2000.

PEER 2000/09 *Structural Engineering Reconnaissance of the August 17, 1999 Earthquake: Kocaeli (Izmit), Turkey.* Halil Sezen, Kenneth J. Elwood, Andrew S. Whittaker, Khalid Mosalam, John J. Wallace, and John F. Stanton. December 2000.

PEER 2000/08 *Behavior of Reinforced Concrete Bridge Columns Having Varying Aspect Ratios and Varying Lengths of Confinement.* Anthony J. Calderone, Dawn E. Lehman, and Jack P. Moehle. January 2001.

PEER 2000/07 *Cover-Plate and Flange-Plate Reinforced Steel Moment-Resisting Connections.* Taejin Kim, Andrew S. Whittaker, Amir S. Gilani, Vitelmo V. Bertero, and Shakhzod M. Takhirov. September 2000.

PEER 2000/06 *Seismic Evaluation and Analysis of 230-kV Disconnect Switches.* Amir S. J. Gilani, Andrew S. Whittaker, Gregory L. Fenves, Chun-Hao Chen, Henry Ho, and Eric Fujisaki. July 2000.

PEER 2000/05 *Performance-Based Evaluation of Exterior Reinforced Concrete Building Joints for Seismic Excitation.* Chandra Clyde, Chris P. Pantelides, and Lawrence D. Reaveley. July 2000.

PEER 2000/04 *An Evaluation of Seismic Energy Demand: An Attenuation Approach.* Chung-Che Chou and Chia-Ming Uang. July 1999.

PEER 2000/03 *Framing Earthquake Retrofitting Decisions: The Case of Hillside Homes in Los Angeles.* Detlof von Winterfeldt, Nels Roselund, and Alicia Kitsuse. March 2000.

PEER 2000/02 *U.S.-Japan Workshop on the Effects of Near-Field Earthquake Shaking.* Andrew Whittaker, ed. July 2000.

PEER 2000/01 *Further Studies on Seismic Interaction in Interconnected Electrical Substation Equipment.* Armen Der Kiureghian, Kee-Jeung Hong, and Jerome L. Sackman. November 1999.

PEER 1999/14 *Seismic Evaluation and Retrofit of 230-kV Porcelain Transformer Bushings*. Amir S. Gilani, Andrew S. Whittaker, Gregory L. Fenves, and Eric Fujisaki. December 1999.

PEER 1999/13 *Building Vulnerability Studies: Modeling and Evaluation of Tilt-up and Steel Reinforced Concrete Buildings.* John W. Wallace, Jonathan P. Stewart, and Andrew S. Whittaker, editors. December 1999.

PEER 1999/12 *Rehabilitation of Nonductile RC Frame Building Using Encasement Plates and Energy-Dissipating Devices.* Mehrdad Sasani, Vitelmo V. Bertero, James C. Anderson. December 1999.

PEER 1999/11 *Performance Evaluation Database for Concrete Bridge Components and Systems under Simulated Seismic Loads.* Yael D. Hose and Frieder Seible. November 1999.

PEER 1999/10 *U.S.-Japan Workshop on Performance-Based Earthquake Engineering Methodology for Reinforced Concrete Building Structures.* December 1999.

PEER 1999/09 *Performance Improvement of Long Period Building Structures Subjected to Severe Pulse-Type Ground Motions*. James C. Anderson, Vitelmo V. Bertero, and Raul Bertero. October 1999.

PEER 1999/08 *Envelopes for Seismic Response Vectors.* Charles Menun and Armen Der Kiureghian. July 1999.

PEER 1999/07 *Documentation of Strengths and Weaknesses of Current Computer Analysis Methods for Seismic Performance of Reinforced Concrete Members.* William F. Cofer. November 1999.

PEER 1999/06 *Rocking Response and Overturning of Anchored Equipment under Seismic Excitations.* Nicos Makris and Jian Zhang. November 1999.

PEER 1999/05 *Seismic Evaluation of 550 kV Porcelain Transformer Bushings.* Amir S. Gilani, Andrew S. Whittaker, Gregory L. Fenves, and Eric Fujisaki. October 1999.

PEER 1999/04 *Adoption and Enforcement of Earthquake Risk-Reduction Measures.* Peter J. May, Raymond J. Burby, T. Jens Feeley, and Robert Wood.

PEER 1999/03 *Task 3 Characterization of Site Response General Site Categories*. Adrian Rodriguez-Marek, Jonathan D. Bray, and Norman Abrahamson. February 1999.

PEER 1999/02 *Capacity-Demand-Diagram Methods for Estimating Seismic Deformation of Inelastic Structures: SDF Systems.* Anil K. Chopra and Rakesh Goel. April 1999.

PEER 1999/01 *Interaction in Interconnected Electrical Substation Equipment Subjected to Earthquake Ground Motions.* Armen Der Kiureghian, Jerome L. Sackman, and Kee-Jeung Hong. February 1999.

PEER 1998/08 *Behavior and Failure Analysis of a Multiple-Frame Highway Bridge in the 1994 Northridge Earthquake.* Gregory L. Fenves and Michael Ellery. December 1998.

PEER 1998/07 *Empirical Evaluation of Inertial Soil-Structure Interaction Effects.* Jonathan P. Stewart, Raymond B. Seed, and Gregory L. Fenves. November 1998.

PEER 1998/06 *Effect of Damping Mechanisms on the Response of Seismic Isolated Structures.* Nicos Makris and Shih-Po Chang. November 1998.

PEER 1998/05 *Rocking Response and Overturning of Equipment under Horizontal Pulse-Type Motions.* Nicos Makris and Yiannis Roussos. October 1998.

PEER 1998/04 *Pacific Earthquake Engineering Research Invitational Workshop Proceedings, May 14–15, 1998: Defining the Links between Planning, Policy Analysis, Economics and Earthquake Engineering.* Mary Comerio and Peter Gordon. September 1998.

PEER 1998/03 *Repair/Upgrade Procedures for Welded Beam to Column Connections.* James C. Anderson and Xiaojing Duan. May 1998.

PEER 1998/02 *Seismic Evaluation of 196 kV Porcelain Transformer Bushings.* Amir S. Gilani, Juan W. Chavez, Gregory L. Fenves, and Andrew S. Whittaker. May 1998.

PEER 1998/01 *Seismic Performance of Well-Confined Concrete Bridge Columns.* Dawn E. Lehman and Jack P. Moehle. December 2000.

ONLINE REPORTS

The following PEER reports are available by Internet only at http://peer.berkeley.edu/publications/peer_reports.html

PEER 2007/101 *Generalized Hybrid Simulation Framework for Structural Systems Subjected to Seismic Loading.* Tarek Elkhoraibi and Khalid M. Mosalam. July 2007.

PEER 2007/100 *Seismic Evaluation of Reinforced Concrete Buildings Including Effects of Masonry Infill Walls.* Alidad Hashemi and Khalid M. Mosalam. July 2007.